Universidad de Navarra

# IMPLICATIONS OF GHRELIN ISOFORMS IN THE IMPROVEMENT OF NONALCOHOLIC FATTY LIVER DISEASE AFTER BARIATRIC SURGERY

**Silvia Ezquerro Ezquerro**

Universidad de Navarra

**SCHOOL OF SCIENCES**

# IMPLICATIONS OF GHRELIN ISOFORMS IN THE IMPROVEMENT OF NONALCOHOLIC FATTY LIVER DISEASE AFTER BARIATRIC SURGERY

Submitted by **Silvia Ezquerro Ezquerro** in fulfillment of the requirements for the Doctoral Degree by the University of Navarra

This dissertation has been written under our supervision at the Metabolic Research Laboratory of the University of Navarra and we approved its submission to the Defense Committee.

Signed on June, 2019

**Dr. Amaia Rodríguez Murueta-Goyena** **Prof. Gema Frühbeck Martínez**

*A mis padres*

*A Jorge*

# AGRADECIMIENTOS

Quisiera agradecer a la Universidad de Navarra, al CIBER Fisiopatología de la Obesidad y Nutrición del Instituto de Salud Carlos III y al Ministerio de Educación, Cultura y Deporte (FPU15/02599) por las ayudas predoctorales y becas para la realización de la estancia internacional. La presente tesis doctoral ha sido realizada gracias a la financiación concedida por el Fondo de Investigación Sanitaria-FEDER (PI12/00515, PI13/01430, PI16/00221 y PI16/01217) del Instituto de Salud Carlos III, al Departamento de Salud del Gobierno de Navarra (61/2014) y al Plan de Investigación de la Universidad de Navarra (PIUNA 2011-14).

En primer lugar, me gustaría expresar mi gratitud hacia mis directoras de tesis. Prof. Gema Frühbeck, muchas gracias por darme la oportunidad de poder formarme en tu laboratorio, por confiar en mí desde el primer momento y por transmitirme esa pasión por la ciencia y por intentar superarme día a día. Ha sido un auténtico placer poder aprender de ti. A la Dra. Amaia Rodríguez, gracias por tu paciencia, tu comprensión y por estar en todo momento disponible para resolver mis dudas. Has sido fuente de motivación cuando no salían bien las cosas y gracias al esfuerzo que has dedicado en mi formación y a tus consejos has conseguido hacer que esta etapa haya sido muy estimulante y productiva. Trabajar día a día a tu lado ha sido un gran privilegio y me siento muy afortunada de haberte tenido como directora. Os estoy profundamente agradecida a las dos por hacer posible la realización de esta tesis y mi desarrollo profesional durante estos años.

A mis compañeros del Laboratorio de Investigación Metabólica: Javier, Victoria, Sara, Bea, Xavi y Leire ha sido una suerte haberos conocido y poder aprender personal y profesionalmente de cada uno de vosotros. Gracias por vuestros consejos, por ayudarme siempre que lo he necesitado y por la fantástica compañía, haciendo que los días en el laboratorio hayan sido tan amenos. Por todos los almuerzos, las comidas y las cenas con villancicos, por las sesiones de coach y los buenos momentos de los congresos, muchísimas gracias. Me siento muy afortunada porque no imagino unos compañeros mejores. También ha sido un placer conocer a los alumnos de Medicina y Bioquímica que han pasado por el laboratorio.

Gracias a todos los miembros del Departamento de Endocrinología y Nutrición de la Clínica Universidad de Navarra, particularmente al Dr. Javier Salvador por su trato, siempre tan amable y por su preocupación por nuestro trabajo.

También agradecer a todo el personal del animalario del CIFA de la Universidad de Navarra por su inestimable ayuda con los experimentos con animales.

También me gustaría agradecer a la División de Diabetes, Endocrinología y Gastroenterología de la Universidad de Mánchester por ayudarme y hacerme sentir como en casa durante mi estancia. Especialmente, me gustaría agradecer a la Prof. Karen Piper Hanley por darme la oportunidad de poder aprender en su laboratorio y por su amabilidad y generosidad en todo momento.

A toda la gente que me ha ido acompañando durante todos estos años, a mis amigos bioquímicos, que aunque cada uno estemos en una punta del mundo, siempre que nos encontramos es como si el tiempo no hubiera pasado. A la gente que he conocido en Pamplona, muy especialmente a mis Martis. Ha sido una gran suerte conoceros, sois de lo mejor que me llevo. Mil gracias por estar siempre ahí, por nuestras conversaciones de sobremesa y por llenar de buenos momentos estos 4 años en el piso. Por supuesto, agradecer a mis amigas de toda la vida por interesarse y apoyarme en esta etapa, por haber crecido juntas y estar siempre presentes en los mejores y en los peores momentos. Sois muy importantes para mí, os quiero. También agradecer a todas las personas y amigos que de un modo u otro han estado presentes y se alegran por esta tesis.

A toda mi familia, por preocuparse y animarme en todo momento y en especial a mis primillos pequeños, por alegrarme tanto y porque un beso y un abrazo suyo arregla cualquier mal día.

Finalmente, me gustaría agradecer a las tres personas que son los pilares fundamentales de mi vida. A mis padres, por todo su cariño, por todo lo que hacen día a día por mí, por ser el mejor ejemplo que se puede tener y un apoyo incondicional. Todo lo que soy y lo que he conseguido es gracias a vosotros. A Jorge, por confiar tanto en mí, por la paciencia que has tenido, sobre todo en esta última etapa, por ayudarme a relativizar los problemas y por sacarme siempre una sonrisa. En definitiva, gracias por ser el mejor compañero de viaje que se puede tener. Millones de gracias a los tres, os quiero muchísimo.

# ABBREVIATIONS

ACC: acetyl-CoA carboxylase

AGPAT: acylglycerol-3-phosphate acyltransferase

AgRP: agouti-related peptide

ALT: alanine aminotransferase

AMPK: AMP-activated protein kinase

AST: aspartate aminotransferase

ATF: activating transcription factor

ATG: autophagy-related

BAT: brown adipose tissue

BChE: butyrylcholinesterase

BMI: body mass index

CD36: fatty acid translocase

CHOP: C/EBP homologous protein

ChREBP: carbohydrate response element-binding protein

CPT: carnitine acyltransferase

CRP: C reactive protein

CT: computed tomography

DAMP: damage-associated molecular pattern molecule

DGAT: diacylglycerol acyltransferase

DR: death receptor

eiF2α: eukaryotic translation initiation factor 2α

ER: endoplasmic reticulum

ERAD: ER-associated degradation

FABP: fatty acid binding protein

FAS: fatty acid synthase

FATP: fatty acid transporter protein

FFA: free fatty acids

GADD34: growth arrest and DNA damage-inducible protein

GHS-R: growth hormone secretagogue receptor

GOAT: ghrelin *O*-acyltransferase

GRP78: 78-kDa glucose-regulated protein

GWAS: genome-wide association studies

HFD: high-fat diet

HMGB1: high mobility group box1

IL: interleukin

IRE1: inositol-requiring enzyme-1

JNK: c-Jun N-terminal kinase

LC3: light chain 3

LEAP: liver-expressed antimicrobial peptide 2

LPS: lipopolysaccharide

MMP: matrix metallopeptidases

MOGAT: monoacylglycerol acyltransferase

MSH: melanocyte-stimulating hormone

mtDNA: mitochondrial DNA

mTOR: mechanistic target of rapamycin

NAFLD: nonalcoholic fatty liver disease

NASH: nonalcoholic steatohepatitis

NF-κB: nuclear factor κB

NPY: neuropeptide Y

OXPHOS: oxidative phosphorylation

PERK: protein kinase R-like ER kinase

PI3K: phosphatidylinositol 3-kinase

PNPLA3: patatin-like phospholipase domain-containing 3

POMC: proopiomelanocortin

PPAR: peroxisome proliferator-activated-receptor

RAGE: receptor for advanced glycation end products

ROS: reactive oxygen species

RYGB: Roux-en-Y gastric bypass

SOS: Swedish obese subjects

SQSTM1: sequestosome-1

SREBP1c: sterol response element-binding protein 1c

TCA: tricarboxylic acid

TG: triacylglycerol

TGF-β: transforming growth factor β

TIMP: tissue inhibitors of metalloproteinases

TLR: toll-like receptor

TNF: tumor necrosis factor

TNFR1: TNF receptor 1

TRAIL: TNF-related apoptosis-inducing ligand

T2D: type 2 diabetes

UCP1: uncoupling protein 1

ULK1: unc51-like kinase 1

UPR: unfolded protein response

VLDL: very-low density lipoproteins

WAT: white adipose tissue

WHO: World Health Organization

XBP1: X-box binding protein 1

# Index

# Introduction

# 1. NONALCOHOLIC FATTY LIVER DISEASE

## 1.1. Definition and prevalence of NAFLD and NASH

Nonalcoholic fatty liver disease (NAFLD) encompasses a variety of clinical conditions from simple steatosis to nonalcoholic steatohepatitis (NASH), in the absence of competing etiologies, including excess alcohol consumption, certain steatogenic medications, such as valproate or anti-retrovirals, and other medical conditions (Chalasani *et al*, 2012, European Association for the Study of the Liver (EASL) *et al*, 2016). A subset of patients with NASH progresses to fibrosis, which can ultimately lead to cirrhosis, hepatocellular carcinoma and/or liver transplantation (Younossi *et al*, 2016). The underlying mechanisms for the development and progression of NAFLD are complex and multifactorial. Within the last years, multiple genome-wide association studies (GWAS) have contributed to the identification of genetic contributors to NAFLD (Anstee and Day, 2013, Eslam *et al*, 2018). Among them, the variant rs738409 (c.444 C>G, Ile148Met) of the human gene patatin-like phospholipase domain-containing 3 (*PNPLA3*) encoding the adiponutrin protein, has consistently shown the most robust association with NAFLD (**Figure 1**) (Romeo *et al*, 2008). Variants in the *TM6SF2*, *MBOAT7* and *GCKR* genes also exhibit a moderate, but significant, contribution in the susceptibility to NAFLD (Eslam *et al*, 2018). The "multiple-hit" hypothesis considers multiple insults, including insulin resistance, visceral obesity, nutritional factors or gut microbiota, acting together on genetically predisposed subjects to develop NAFLD (Buzzetti *et al*, 2016).

The global prevalence of NAFLD and NASH has been estimated to be 24% and 3-5%, respectively (**Figure 1**) (Younossi *et al*, 2016, Younossi *et al*, 2018). The prevalence of NAFLD increases with age (Younossi *et al*, 2016), and NAFLD more often affects men (Ballestri *et al*, 2017). The highest prevalence rates worldwide are reported from South America (31%) and the Middle East (32%), whereas Africa shows the lowest prevalence of NAFLD (14%). A meta-analysis published in 2016 indicated that the average prevalence of NAFLD in Europe is 23.7%, varying from 5% to 44% in different countries (Younossi *et al*, 2016). Epidemiological data from Spain describe a prevalence of 25.8% in the adult population (Caballería *et al*, 2010).

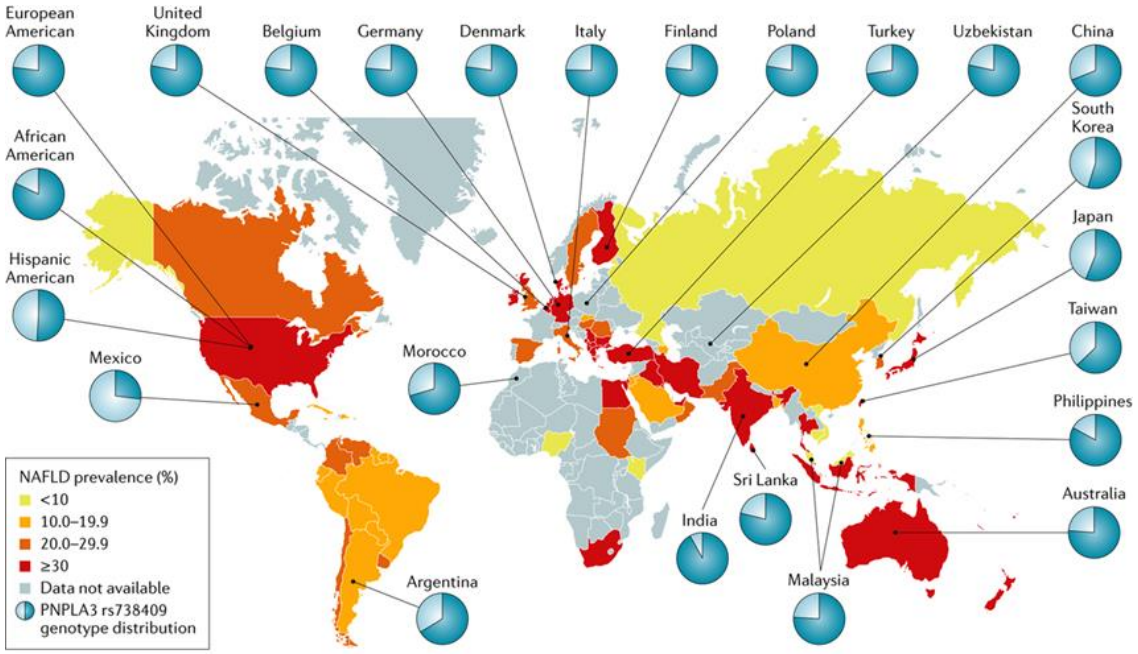


**Figure 1.** Global prevalence of NAFLD and distribution of PNPLA3 genotypes. PNPLA3 is shown as minor allele frequency (light blue section of the pie chart) (modified from Younossi *et al*, 2018).

The incidence of NAFLD in adults and children is rising due to the global epidemics of obesity, type 2 diabetes (T2D) and the metabolic syndrome (Frühbeck *et al*, 2013, Lonardo *et al*, 2017). Although NAFLD is common in obese children, NAFLD and obesity are not concomitant during childhood (Yu *et al*, 2018). Nonetheless, children and adolescents with overweight exhibit increased risk of NAFLD during adulthood, and consequently, the threshold of liver disease-associated morbidity and mortality is reached early in life (Younossi *et al*, 2018). The prevalence of NAFLD and NASH in obese patients is 75% and 25% to 70%, respectively, (Machado *et al*, 2006, Younossi *et al*, 2016) and 58% and 65% in patients with T2D (Younossi, 2018b). The severity of steatosis is closely associated with visceral obesity, while it is weakly associated with the amount of subcutaneous fat (Camhi *et al*, 2011). Furthermore, the presence of T2D seems to accelerate the course of NAFLD and is a predictor of advanced fibrosis and mortality (Younossi *et al*, 2018). Although NAFLD is usually associated with obesity, non-obese patients can also present NAFLD, the so-called "lean NAFLD" (Younossi *et al*, 2012, Wei *et al*, 2015). Increased visceral obesity, high- fructose and/or high-fat diet and genetic risk factors, including congenital lipodystrophies and defects of metabolism (familiar hypobetalipoproteinaemia or lysosomal acid lipase deficiency), might be associated with lean NAFLD (Younossi *et al*, 2018).

### 1.2. Diagnosis of NAFLD and NASH

NAFLD is usually asymptomatic, although fatigue, malaise, and vague right upper quadrant pain may occur. Its diagnosis usually follows the incidental finding of abnormal liver enzymes or steatosis on imaging (Pereira *et al*, 2015). Patients with NAFLD commonly exhibit central obesity and hepatomegaly (Rinella, 2015). The presence of *acanthosis nigricans* correlates with insulin resistance and advanced NAFLD, and the presence of a dorsocervical hump is specifically associated with NASH. Other clinical manifestations, such as palmar erythema, spider angiomata, gynecomastia (in men) or prominent upper abdominal veins may appear following the onset of cirrhosis. The diagnosis of NAFLD and NASH requires: a) the confirmation by biochemical analyses, imaging methods and/or liver biopsy; b) that there are not secondary causes for hepatic steatosis, such as significant alcohol consumption, use of steatogenic medication or hereditary disorders (Kleiner *et al*, 2005, Kleiner and Brunt, 2012). Alcohol abuse is considered as a daily consumption ≥30 g in men and ≥20 g in women (Fazel *et al*, 2016, Younossi, 2018a). Common alternative causes of hepatic steatosis are the presence of hepatitis B virus surface antigen or hepatitis C virus antibodies in absence of a history of vaccination, use of steatogenic medications like amiodarone, valproate, tamoxifen, methotrexate, antiretrovirals or corticosteroids and other chronic liver diseases, including hemochromatosis, Wilson´s disease, autoimmune liver disease or α1-antitrypsin deficiency (Kowdley, 2010, Chalasani *et al*, 2012).

#### 1.2.1. Biochemical analysis

Elevated serum alanine (ALT) and aspartate (AST) aminotransferases are surrogate markers of NAFLD. The specificity and sensitivity of ALT for the diagnosis of NASH are 85% and 45%, respectively (Rinella, 2015). Based on currently accepted gender-specific threshold values (males <40 IU/L and females <31 IU/L), ALT levels 1.5 times over normal values has been used to identify those patients with a higher likelihood of NASH (Rinella, 2015, Fazel *et al*, 2016). However, ~80% of patients have normal-range ALT levels, and even if elevated, the ALT typically falls (and AST may rise) as fibrosis progresses to cirrhosis (Fazel *et al*, 2016, Younossi, 2018a). Patients with persistent elevation (>6 months) in AST and ALT levels and with a concomitant pathology (autoimmune, hemochromatosis) or any evidence suggestive of progressive liver disease (ratio AST/ALT>1, thrombocytopenia, hyperbilirubinemia, coagulopathy) should prompt a liver biopsy for further evaluation (Rinella, 2015).

Even though elevated AST and ALT levels have moderate specificity in the appropriate clinical setting, their sensitivity makes them unreliable to identify those with NASH (Rinella, 2015). Current serum biomarkers for the diagnosis of NASH include predictive models for staging fibrosis (i.e., NAFLD Fibrosis Score), direct measures of hepatocellular damage (i.e., circulating cytokeratin-18) or fibrosis (i.e., N-terminal propeptide of type III collagen) (Castera *et al*, 2019). However, the most promising biomarkers are limited to the clinical research due to the insufficient accuracy to replace liver biopsy to diagnose NASH (Musso *et al*, 2011, Fazel *et al*, 2016).

### 1.2.2. Imaging techniques

Non-invasive imaging techniques, such as ultrasonography, computed tomography (CT), magnetic resonance imaging and elastography, have demonstrated their values for NAFLD risk stratification and management (Pereira *et al*, 2015, Li *et al*, 2018, Tapper and Loomba, 2018). However, they are relatively limited in the detection of NASH and its associated risk for fibrosis, cirrhosis and hepatocellular carcinoma.

*Ultrasonography.* Ultrasonography is a well-established, cost-effective, non-radiant imaging technique for the screening of suspected NAFLD based on the echogenicity of the liver (Lee and Park, 2014). The echotexture of normal liver is homogeneous and similar to the right kidney´s cortex and the spleen´s parenchyma, whereas hepatic steatosis is associated with increased echogenicity, hepatomegaly and intrahepatic vascular blurring (Hannah and Harrison, 2016, Kinner *et al*, 2016, Li *et al*, 2018). Depending on echogenicity features, the degree of steatosis can be scored as: 1) mild, increased echogenicity and hepatomegaly; 2) moderate, enhanced hepatic parenchyma echogenicity and walls of portal vein branches slightly obscured; and 3) severe, diaphragmatic outline and portal vein branches strongly obscured by liver echogenicity and attenuation of sound waves. (Joseph *et al*, 1991, Saadeh *et al*, 2002, Lăpădat *et al*, 2017). The limitations of ultrasonography include its limited sensitivity (<20%) for detecting mild steatosis (Castera *et al*, 2019), the difficulty to detect NASH (Dasarathy *et al*, 2009, Hannah and Harrison, 2016), high inaccuracies in subjects with morbid obesity (Mottin *et al*, 2004) and poor inter-rater reliability (Lăpădat *et al*, 2017).

*Computed tomography.* Unenhanced CT is used for the estimation of liver fat by simple measurement of liver attenuation in Hounsfield units (HU) (Lee and Park, 2014). Liver attenuation values diminish by about 1.6 HU for every milligram of triglyceride deposited per gram of liver tissue. A normal liver has higher attenuation than a normal

spleen. Therefore, decreased liver attenuation levels may be considered a possible diagnosis of hepatic steatosis (Park *et al*, 2011, Pereira *et al*, 2015). Although CT is accurate for the diagnosis of moderate-to-severe steatosis, the accuracy in the detection of mild steatosis is limited. Moreover, the potential radiation hazard makes CT unsuitable for longitudinal follow-up or use in children (Li *et al*, 2018). By contrast, CT is useful to identify complications of cirrhosis as well as moderate-to-severe hepatic steatosis in donor candidates for liver transplantation (Lee *et al*, 2007).

*Magnetic resonance.* Magnetic resonance spectroscopy is considered the most sensitive, accurate and reproducible imaging technique due to its capacity to detect small amounts of fat in the liver without radiation exposure (Pereira *et al*, 2015). Magnetic resonance measures proton density fat fraction, defined as the amount of protons bound to fat divided by the amount of all protons in the liver, including those bound to fat and water (Qayyum *et al*, 2005, Lee and Park, 2014). The protons in fat and water oscillate regularly and are positioned in-phase (IP) or in opposed phase (OP) (Reeder *et al*, 2011, Lee and Park, 2014). In a normal liver, the IP and OP signals exhibit similar intensities, while in the fatty liver, OP images show relative signal loss to IP, allowing a reliable and reproducible detection of liver fat (Li *et al*, 2018).

*Elastography.* Liver stiffness is evaluated by elastography, which measures the velocity of wave propagation (Asrani, 2015, Hannah and Harrison, 2016). Four devices are used to diagnose liver fibrosis: ultrasound-based vibration controlled transient elastography, shear-wave elastography, acoustic radiation force impulse imaging and magnetic resonance elastography (Tapper and Loomba, 2018). Elastography is non-invasive, reproducible and provides information from larger portions of the liver than the biopsy. However, it is unsuccessful in severe obesity (Martínez *et al*, 2011).

### 1.2.3. Liver biopsy

Liver biopsy is the gold standard for the detection of NASH, but this invasive method is limited by sampling error, poor inter-rater reliability, cost and procedure-related morbidity and mortality (Hannah and Harrison, 2016). The evaluation of NAFLD and NASH by liver biopsy is based on the Kleiner and Brunt criteria (Kleiner and Brunt, 2012, European Association for the Study of the Liver (EASL) *et al*, 2016) and only requires hematoxylin and eosin (H&E) and Masson's trichrome stains. The histological features evaluated are steatosis, inflammation, hepatocellular injury, fibrosis and miscellaneous features (**Table 1**).

**Table 1**. Kleiner and Brunt criteria for staging and grading NAFLD by liver biopsy.

| Item | Definition | Score |
|---|---|---|
| **Steatosis** | | |
| Grade | <5% | 0 |
| | 5-33% | 1 |
| | >33-66% | 2 |
| | >66% | 3 |
| Location | Zone 3 | 0 |
| | Zone 1 | 1 |
| | Azonal | 2 |
| | Panacinar | 3 |
| Microvesicular steatosis | Absent | 0 |
| | Present | 1 |
| **Fibrosis** | | |
| Stage | None | 0 |
| | Perisinusoidal or periportal/portal | 1 |
| | Perisinusoidal and portal/periportal | 2 |
| | Bridging fibrosis | 3 |
| | Cirrhosis | 4 |
| **Inflammation** | | |
| Lobular inflammation | No foci | 0 |
| | <2 foci, per 200X field | 1 |
| | 2-4 foci, per 200X field | 2 |
| | >4 foci, per 200X field | 3 |
| Portal inflammation | None to minimal | 0 |
| | Greater than minimal | 1 |
| Microgranulomas | Absent | 0 |
| | Present | 1 |
| Large lipogranulomas | Absent | 0 |
| | Present | 1 |
| **Liver cell injury** | | |
| Hepatocyte ballooning | None | 0 |
| | Few balloon cells | 1 |
| | Many/prominent balloon cells | 2 |
| Acidophil bodies | None to rare | 0 |
| | Many | 1 |
| Pigmented macrophages | None to rare | 0 |
| | Many | 1 |
| Megamitochondria | None to rare | 0 |
| | Many | 1 |
| **Other findings** | | |
| Mallory's hyaline | None to rare | 0 |
| | Many | 1 |
| Glycogenated nuclei | None to rare | 0 |
| | Many | 1 |

The diagnosis of NASH by liver biopsy is established by the presence of steatosis, hepatocyte ballooning and lobular inflammation (European Association for the Study of the Liver (EASL) *et al*, 2016). The NAFLD Activity Score (NAS) was developed and validated by the NIDDK sponsored Nonalcoholic Steatohepatitis Clinical Research Network (NASH CRN) Pathology Committee and is used to evaluate disease severity, once the diagnosis has been established by the pathological assessment or in clinical trials (Brunt *et al*, 2011, Kleiner and Brunt, 2012, Kleiner and Makhlouf, 2016).

# 2. OBESITY

## 2.1. Classification and prevalence of obesity

Obesity is a complex multifactorial disorder characterized by excess adiposity due to a chronic imbalance between energy intake and energy expenditure (Kopelman, 2000), which was declared as a disease by the American Medical Association in 2013 (Atkinson, 2014). Obesity is one of the leading causes of morbidity and mortality in the last decades, since it represents a major risk factor for the development of T2D, cardiovascular diseases, certain types of cancer and NAFLD, among others (Atkinson, 2014, Targher and Byrne, 2016). The most widely used tool to determine the ponderal categories in clinical practice is the body mass index (BMI), which was firstly described by Quetelet in 1869, and its formula is weight in kilograms divided by the square of the height in meters. The World Health Organization (WHO) establishes several cut-off points in order to categorize the weight status: underweight (<18.5 $kg/m^2$), normal weight (18.5 to 24.9 $kg/m^2$), overweight (25.0 to 29.9 $kg/m^2$) and obesity ( ≥ 30.0 $kg/m^2$) (**Table 2**).

Increasing evidence suggests that BMI is an imprecise measure of body composition due to its inability to distinguish between lean and fat mass and identify fat distribution (Blundell *et al*, 2014), leading to a high rate of misclassification of obesity (Gómez-Ambrosi *et al*, 2012). In this context, other methods focus on measuring body fat, such as dual-energy X-ray absorptiometry (DEXA), air-displacement plethysmography or bioimpedance (Gallagher *et al*, 2000). According to the cut-off points established for the percentage of body fat, overweight is defined as a percentage of body fat ranging from 20.1% to 24.9% for men and 30.1% to 34.9% for women, whereas obesity corresponds to a percentage of body fat ≥25.0% in men and ≥35.0% in women (Gómez-Ambrosi *et al*, 2012).

**Table 2**. Classification of ponderal categories according to BMI cut-off points.

| Classification | BMI (kg/m$^2$) | |
|---|---|---|
| | **Principal cut-off points** | **Additional cut-off points** |
| **Underweight** | **<18.5** | **<18.5** |
| Severe thinness | <16.0 | <16.0 |
| Moderate thinness | 16.0-16.9 | 16.0-16.9 |
| Mild thinness | 17.0-18.4 | 17.0-18.4 |
| **Normal range** | **18.5-24.9** | **18.5-22.9** |
| | | **23.0-24.9** |
| **Overweight** | **≥25.0** | **≥25.0** |
| Pre-obese | 25.0-29.9 | 25.0-27.4 |
| | | 27.5-29.9 |
| **Obese** | **≥30.0** | **≥30.0** |
| Obese class I | 30.0-34.9 | 30.0-32.4 |
| | | 32.5-34.9 |
| Obese class II | 35.0-39.9 | 35.0-37.4 |
| | | 37.5-39.9 |
| Obese class III | **≥40.0** | **≥40.0** |

During the last decades, the substantial increase in the prevalence of obesity and overweight has become a major worldwide health and economic burden in both developing and developed countries (Ng *et al*, 2014, Scully, 2014). According to WHO data, more than 1.9 billion adults aged 18 years and older were overweight, over 650 million of them being obese in 2016. The prevalence of childhood obesity is also rising with an estimated 41 million children under the age of 5 being overweight. The rise in childhood obesity has plateaued in high-income countries, but continues in low and middle-income countries (NCD Risk Factor Collaboration (NCD-RisC), 2017). The prevalence of overweight and obesity affects more than 50% of the European population (Frühbeck *et al*, 2013). In Spain, the prevalence of overweight and obesity in the adult population is estimated to be 39.4% (46.4% in men and 32.5% in women) and 22.9% (22.4% men and 21.4% women), respectively, according to the data of the ENRICA study (Gutiérrez-Fisac *et al*, 2012).

### 2.2. Pathophysiology of obesity-associated NAFLD and NASH

During the development of obesity-associated NAFLD several functional changes take place in the different hepatic cell populations leading to the histological phenotypic alterations characteristics of NAFLD (**Figure 2**). Putative mechanisms for the role of

visceral adipose tissue in the onset of obesity-associated NAFLD include an increased portal release of free fatty acids (FFA), which leads to hepatic fat accumulation, together with an abnormal secretion of proinflammatory adipokines that triggers hepatocellular injury (Rodríguez *et al*, 2007). Obesity-associated changes in gut microbiota or dysbiosis can increase gut permeability to bacterial products that trigger hepatic inflammation and fibrosis (Leung *et al*, 2016). The inability to quell injurious processes, such as lipotoxicity, mitochondrial dysfunction, oxidative stress, endoplasmic reticulum (ER) stress and apoptotic pathways, contribute to the progression of NAFLD to NASH, progressive fibrosis that can lead to cirrhosis and hepatocellular carcinoma in some patients (Rinella, 2015).

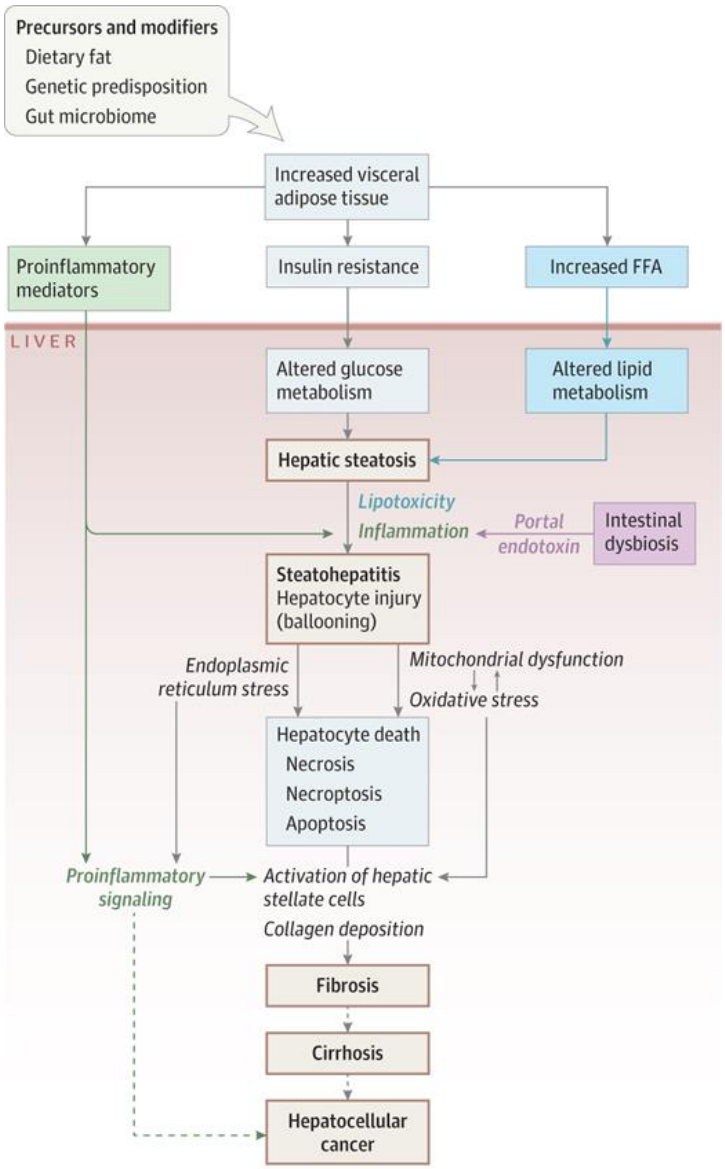


**Figure 2**. Mechanisms involved in obesity-associated NAFLD (modified from Rinella, 2015).

### 2.2.1. Alterations in lipogenesis and β-oxidation

Hepatic triacylglycerol (TG) content is regulated by FFA uptake, *de novo* lipogenesis, β-oxidation of FFA and secretion of lipids in the form of very-low density lipoprotein (VLDL) particles, with alterations in these pathways leading to the development of NAFLD (Kawano and Cohen, 2013, Ipsen *et al*, 2018) (**Figure 3**).

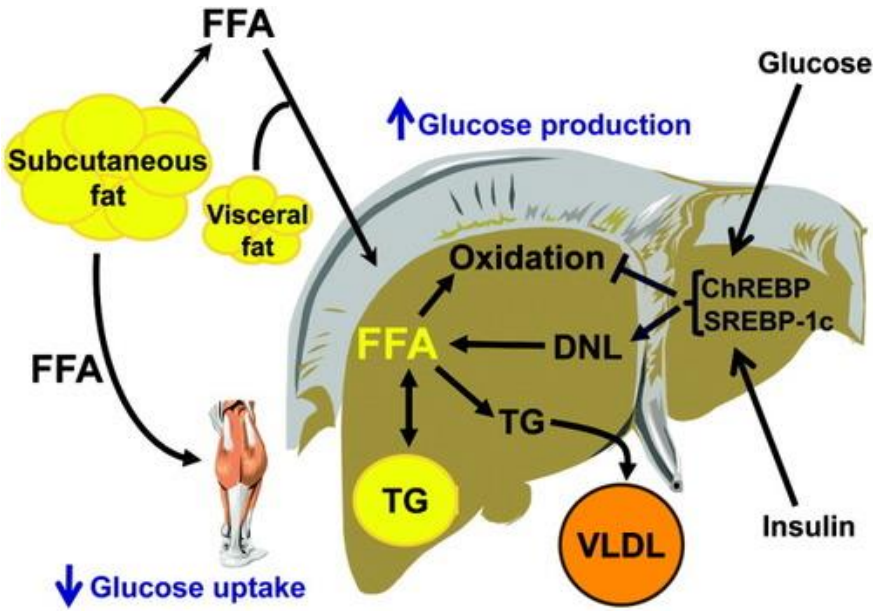


**Figure 3.** Changes in hepatic lipid metabolism in NAFLD (modified from Fabbrini *et al*, 2010). DNL, *de novo* lipogenesis.

Obesity is associated with increased circulating FFA, which derive from different sources: excess dietary fat, which is packaged into chylomicrons and VLDL particles and released to the bloodstream, together with higher FFA release from adipocytes via lipolysis (Donnelly *et al*, 2005, Frühbeck *et al*, 2014, Zhang *et al*, 2014). Lipoprotein lipase (LPL), located on the surface of hepatocytes, removes FFA from chylomicrons and VLDL. FFA transport is mediated by fatty acid binding protein (FABP), fatty acid transporter protein (FATP) and fatty acid translocase (CD36) (Koo, 2013). In addition, caveolins also contribute to FFA uptake in an indirect manner, since caveolin-1 is necessary to target CD36 toward the plasma membrane and, hence, regulate the surface availability of CD36 (Ring *et al*, 2006, Méndez-Giménez *et al*, 2014). These transporters are upregulated in obesity-associated NAFLD, contributing to hepatosteatosis (Fabbrini *et al*, 2010, Kawano and Cohen, 2013).

FFA can be also synthesized from the excess glucose flux in the liver in a process called *de novo* lipogenesis (Rodríguez *et al*, 2013). Piruvate resulting from glycolysis is transported to the mitochondria, where it is converted into acetyl-CoA to be used in the

tricarboxylic acid (TCA) cycle, which produces the accumulation of the intermediate citrate. Citrate is transported back into the cytosol and converted to acetyl-CoA by the action of ATP citrate lyase. Acetyl-CoA carboxylase (ACC) converts acetyl-CoA into malonyl-CoA, which can be used by the fatty acid synthase (FAS) for the synthesis of long-chain fatty acyl-CoA (Ducheix *et al*, 2016, Softic *et al*, 2016).

FFA derived from diet, lipolysis or *de novo* lipogenesis are metabolized by two main pathways: i) the esterification of FFA to glycerol-3 phosphate to produce TG, which can be either stored within the hepatocytes or incorporated into VLDL particles; and ii) the mitochondrial β-oxidation to generate ATP (Rodríguez *et al*, 2013) (**Figure 3**). AMP-activated protein kinase (AMPK) is a key regulatory element that controls the activity of enzymes involved in lipid metabolism and regulates the partitioning of FFA both in oxidative and biosynthetic pathways, with defects in these pathways promoting the onset of NAFLD (Kahn *et al*, 2005, Rodríguez *et al*, 2008, Yin *et al*, 2009). During fasting, the decrease in the ATP/AMP ratio activates AMPK, which phosphorylates and inactivates ACC, an enzyme that catalyzes the rate-limiting reaction for FFA synthesis (Long and Zierath, 2006). The inhibition of ACC reduces the production of malonyl-CoA, an allosteric inhibitor of carnitine acyltransferase 1 (CPT1), a key regulator of mitochondrial FFA uptake (Munday, 2002).

TG synthesis is catalysed by 1-acylglycerol-3-phosphate acyltransferase (AGPAT), monoacylglycerol acyltransferase (MOGAT) and diacylglycerol acyltransferase (DGAT) enzymes (Hall *et al*, 2012, Ducheix *et al*, 2016). Hyperglycemia and hyperinsulinemia upregulate lipogenic enzymes (ACC, FAS, MOGAT2 and DGAT1) through the stimulation of the carbohydrate response element-binding protein (ChREBP) and the sterol response element-binding protein 1c (SREBP1c) transcription factors, respectively (Fabbrini *et al*, 2010, Ipsen *et al*, 2018) (**Figure 3**). TG can be released from the liver to peripheral tissues in form of VLDL particles, which consist of an hydrophobic core of lipids that contains TG and cholesterol esters covered with an hydrophilic envelop of phospholipids and apolipoprotein B (ApoB) 100 (Koo, 2013). Insulin signalling inhibits hepatic VLDL secretion (Chirieac *et al*, 2002), whereas glucagon, cortisol, growth hormone and insulin resistance stimulate its secretion (Elam *et al*, 1992, Bjornsson *et al*, 1994). NAFLD is characterized by enhanced VLDL production and release, which contributes to obesity-associated dyslipemia (Fujita *et al*, 2009, Geisler and Renquist, 2017). However, in a long term, VLDL particles seem to be

larger and present difficulties to be secreted by the liver, ultimately leading to lipid accumulation and worsening hepatic steatosis (Horton *et al*, 1999, Ipsen *et al*, 2018).

The β-oxidation of FFA takes place primarily in the mitochondria and, to a lesser extent, in peroxisomes and microsomes. This process converts FFA into acetyl-CoA, which is incorporated into the TCA cycle to produce ATP. FFA must be activated by acyl-CoA synthetase before they can enter into the mitochondria. Then, CPT1 and CPT2 which are located in the inner and the outer membrane of the mitochondria, respectively, are required for entry of the long chain fatty acid-acyl-CoA molecules into the mitochondria matrix for β-oxidation (Eaton *et al*, 1996, Fabbrini *et al*, 2010). In addition, activation of peroxisome proliferator-activated receptor α (PPARα) induces the expression of molecules related to β-oxidation pathway (Desvergne and Wahli, 1999). Although the current data on FFA β-oxidation in NAFLD are controversial (Kotronen *et al*, 2009, Dasarathy *et al*, 2011, Croci *et al*, 2013), this pathology is associated with impaired β-oxidation. Even in studies suggesting enhanced FFA β-oxidation, this increase seems to be inadequate in hepatic lipid clearance and could promote excessive reactive oxygen species (ROS) production, that ultimately favours the disease progression by inducing oxidative stress and inflammation (Sanyal *et al*, 2001, Ipsen *et al*, 2018).

### 2.2.2. Impaired lipophagy

Autophagy is an intracellular pathway whereby lysosomes degrade and recycle long-lived proteins and cellular organelles. Although three distinct types of autophagy have been described (macroautophagy, chaperone-mediated autophagy and microautophagy), most studies have been focused on macroautophagy (hereafter refered to as autophagy). In autophagy, a portion of cytosol is engulfed by double-membrane vesicles, termed autophagosomes, which fuses with lysosomes for content degradation (Farah *et al*, 2016). Autophagy is activated in order to provide an alternative source of energy during starvation or maintain the cellular quality control. The depletion of nutrients activates AMPK, which inhibits the action of mechanistic target of rapamycin (mTOR) (the best-characterized negative regulator of autophagy) and further activates and phosphorylates the unc51-like kinase 1 (ULK1) at Ser555 and Ser777, among others. Active ULK1 induces autophagy by the phosphorylation of beclin-1, a protein that recruits several regulatory proteins to the VPS34 complex that together constitute the class III phosphatidylinositol 3-kinase (PI3K) activity, which is essential for the formation of the limiting membrane (Martínez-López and Singh, 2015, Park *et al*, 2016).

During the elongation of the phagophore or limiting membrane, autophagy-related 7 (ATG7) induces the conjugation of ATG12 to ATG5 as well as the conjugation of cytosolic light chain 3 (LC3)-I to phosphatidylethanolamine to generate LC3-II, one of the best characterized components of the autophagosomes (Martínez-López and Singh, 2015). The LC3-II-positive autophagosomes recognize and capture cargo due to the interaction between LC3 and p62/sequestosome-1 (SQSTM1) (Pankiv *et al*, 2007), which is a cargo adaptor protein that is bound to polyubiquitinated cargo to enable their degradation in the lysosome. When autophagy is inhibited, p62 is accumulated, while decreased levels of the protein are observed when autophagy is induced. Therefore, p62 may be used as a marker to study autophagic flux (Katsuragi *et al*, 2015).

Autophagy plays a key role in the regulation of hepatic lipid metabolism by mediating the breakdown of lipid stores and its mobilization to lysosomes in a process called lipophagy (Singh *et al*, 2009). Under basal conditions, a certain percentage of lysosomal degradation of lipid droplets occurs continuously in hepatocytes. The inhibition of autophagy through knockdown of the autophagy-related proteins ATG5 and ATG7 in hepatocytes leads to a significant increase in the number of lipid droplets (Madrigal-Matute and Cuervo, 2016). Long-term starvation triggers lipophagy, resulting in FFA release that are oxidized by the mitochondria in order to produce ATP to supply the energy needs (Zhang *et al*, 2015, Madrigal-Matute and Cuervo, 2016) (**Figure 4**).

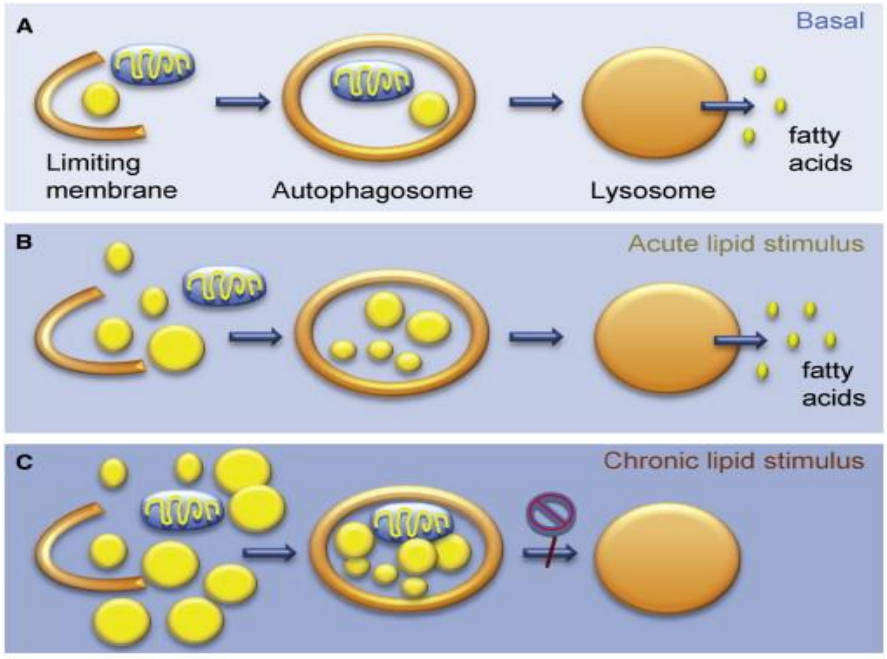


**Figure 4.** Lipophagy under physiological conditions (A), long-term starvation (B), and chronic lipid stimulus (C) (modified from Singh and Cuervo, 2011).

Under lipogenic conditions such as obesity, the excessive lipid influx in the liver leads to a marked increase in the biogenesis of lipid droplets, as a mechanism of defence against lipotoxicity. An altered lipophagy promotes lipid accumulation and impairs hepatic function leading to the development of obesity-associated NAFLD (**Figure 4**). In this sense, decreased levels of autophagy have been found in the liver of severely obese leptin-deficient *ob/ob* mice, obese, diabetic OLETF rats as well as in high-fat diet (HFD)-induced obese rats (Chang *et al*, 2015, Song *et al*, 2015).

### 2.2.3. Inflammation and cell death

The mechanisms underlying the progression from NAFLD to NASH in obesity are poorly understood, but involve several extrahepatic drivers, such as lipotoxins, adipose-tissue derived proinflammatory adipokines (explained in section 2.2.6) and changes in gut microbiota (Leung *et al*, 2016). Increased accumulation of FFA, ceramides, free cholesterol and lysophosphatidylcholine in the hepatocytes triggers hepatic inflammation through nuclear factor κB (NF-κB) and c-Jun N-terminal kinase (JNK) activation and downstream cytokine production (Ertunc and Hotamisligil, 2016, Marra and Svegliati-Baroni, 2018). In addition, harmful lipids dysregulate the function of intracellular organelles, including ER and mitochondria, contributing to the inflammatory signals (Fu *et al*, 2012). Interestingly, gut microbiota also produces lipotoxins that contribute to the pathogenesis of obesity-associated NAFLD (Caesar *et al*, 2015). The heterogeneous gut microbiota contains at least 100 trillion of microorganisms, mainly belonging to four bacterial phyla: *Firmicutes*, *Bacteroidetes*, *Actinobacteria* and *Proteobacteria*, being *Bacteroidetes* and *Firmicutes* the 90% of all microbial cells (Neish, 2009). Microbial populations are altered in patients with NAFLD (Chan *et al*, 2013). This dysbiosis can induce permeability changes leading to the translocation of bacteria, lipopolysaccharide (LPS) and endotoxins to the liver through the portal vein (Federico *et al*, 2016). Toll-like receptors (TLR), that recognize specially LPS, are activated on hepatic Kupffer cells and stellate cells to induce inflammatory and profibrotic pathways by increasing interleukin (IL)-1β, IL-6 and tumor necrosis factor α (TNF-α) levels (Mencin *et al*, 2009, Leung *et al*, 2016).

Intense inflammatory responses that fail to resolve cell damage trigger hepatocyte cell death, which plays a main role in the pathology of NAFLD, NASH and in the development of hepatic fibrosis (Canbay *et al*, 2004) (**Figure 5**).

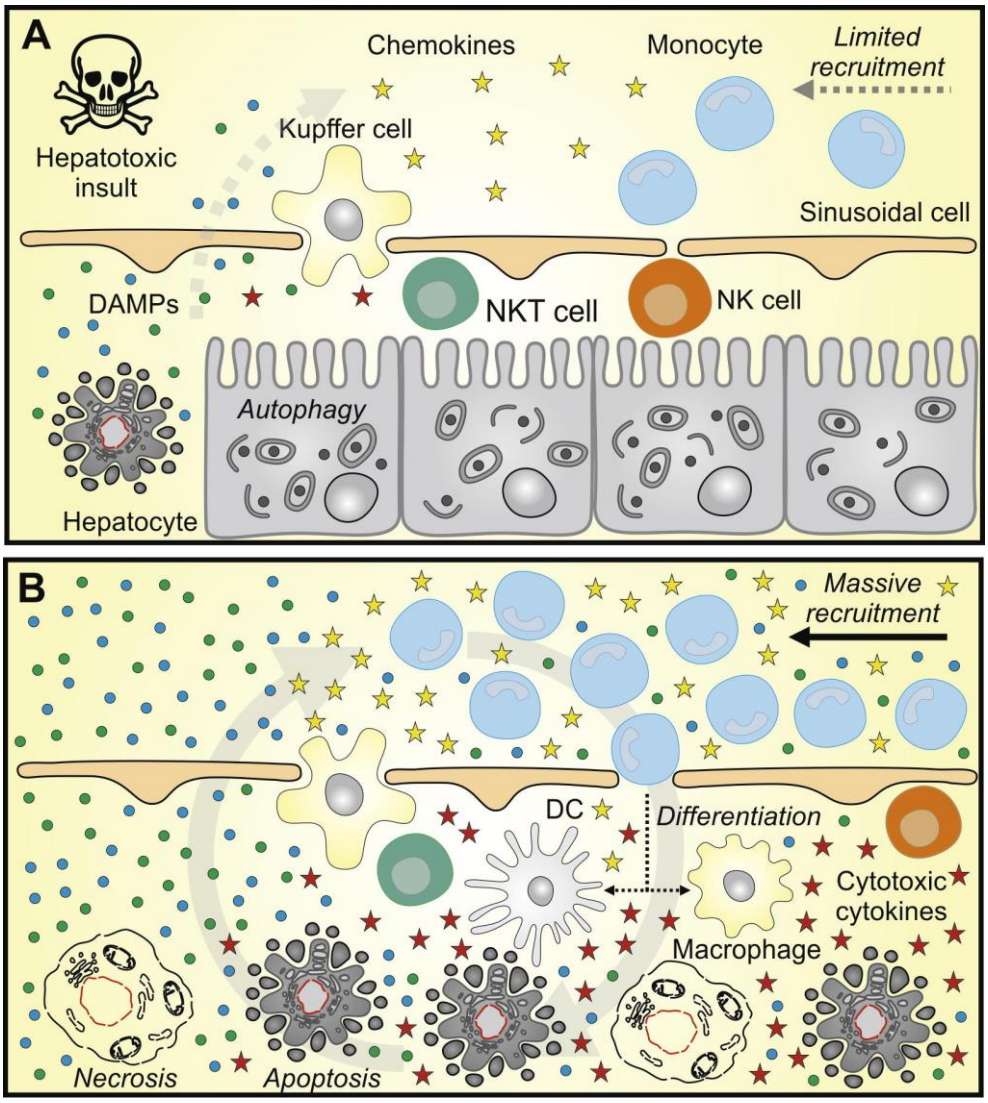


**Figure 5.** Mechanisms of hepatocyte cell death upon exposure to hepatotoxic conditions (A) and when the adaptive responses fail (B) (modified from Brenner *et al*, 2013).

Apoptosis, pyroptosis, autophagic cell death, necrosis and necroptosis are forms of hepatocyte cell death (Wree *et al*, 2014). Apoptosis is induced through the activation of death receptors (extrinsic pathway) or the mitochondria pathway (intrinsic pathway) (**Figure 5B**) (Ding and Yin, 2004). Both pathways lead to the activation of effector caspases 3 and 7, which produce the final apoptotic changes (Riedl and Shi, 2004). The extrinsic pathway is triggered by TNF-α, Fas ligand and TNF-related apoptosis-inducing ligand (TRAIL) (Eguchi *et al*, 2014). Hepatocytes are enriched in death receptors of the TNF protein superfamily such as TNF receptor 1 (TNFR1), CD95 (APO/FAS) and death receptors 3-6 (DR3-6). Upon binding to the receptors, death ligands activate caspase-8 and effector caspase-3 for cell death execution (Eguchi *et al*, 2014). The intrinsic pathway mediates apoptosis via members of the Bcl-2 family, which control the permeabilization of the mitochondrial outer membrane, cytochrome C release and subsequent caspase

activation (Martinou and Youle, 2011). Autophagy is the natural, programmed form to eliminate damaged organelles, but as explained in section 2.2.2, prolonged activation of autophagy can lead to irreversible cellular atrophy and collapse (**Figure 5A**) (Eguchi *et al*, 2014). Pyroptosis is mediated by the inflammasome and caspase-1 activation that produces the proteolytic maturation of proinflammatory cytokines IL-1β and IL-18, cellular leakage as well as the release of damage-associated molecular pattern molecules (DAMPs) (Cookson and Brennan, 2001, Eguchi *et al*, 2014). High mobility group box1 (HMGB1) is a DAMP secreted in response to inflammatory stimuli and/or from deceasing cells, including lipotoxic hepatocytes (Gan *et al*, 2014, Guzmán-Ruiz *et al*, 2014). TLR4 and the receptor for advanced glycation end products (RAGE) interact with extracellular HMGB1 to mediate the activation of JNK and caspase-1, which perpetuates liver inflammation and cell death (Gan *et al*, 2014). Necrosis is a passive cell death that does not require the activation of any particular signalling pathway and it is characterized by mitochondrial dysfunction, depletion of ATP and loss of the plasma membrane integrity followed by cytoplasmic leakage (**Figure 5B**) (Green and Llambi, 2015). Necroptosis is a type of regulated necrosis triggered by the same death receptor that activates the extrinsic pathway of apoptosis without the activation of caspase-8 (Holler *et al*, 2000, Degterev *et al*, 2005).

### 2.2.4. Mitochondrial dysfunction

Hepatocytes are rich in mitochondria, which not only are particularly prone to the effects of an altered substrate influx to the liver, but also to trigger pathways involved in cell survival (i.e., ATP production) and death (i.e., release of cytochrome C) (Grattagliano *et al*, 2019). In a short term, mitochondria protect hepatocytes from lipotoxicity by enhancing β-oxidation, TCA cycle induction and ATP synthesis through oxidative phosphorylation (OXPHOS) that are carried out by the electron transport chain (complexes I to IV) and ATP synthase (complex V) (Lemarie and Grimm, 2011, Simões *et al*, 2018). However, long-term metabolic adaptations of hepatic mitochondria are lost in NAFLD and NASH due to structural, molecular and functional alterations, including OXPHOS deficiency, resulting in electron leakage and ROS production (Begriche *et al*, 2006, Koliaki *et al*, 2015, Einer *et al*, 2018). Oxidative stress refers to an imbalance between the production of ROS and the antioxidant mechanisms such as, glutathione peroxidase, superoxide dismutase and catalase (Simões *et al*, 2018).

Mitochondrial DNA (mtDNA) is a circular double-stranded molecule located in the mitochondrial matrix. Each mitochondrion has several copies of the mtDNA molecule which encodes for only 37 genes: 13 are for proteins (polypeptides), 2 for the small and large subunits of ribosomal RNA (rRNA) and 22 for transfer RNA (tRNA), which are required for the synthesis of mtDNA-encoded polypeptides in the mitochondrial matrix (Begriche *et al*, 2006, Perks *et al*, 2017). These proteins are the core catalytic components of OXPHOS complexes I, III, IV and V. The mitochondrial genome is more prone to oxidative damage due to its proximity to the electron transport chain (the main cellular source of ROS), lack of protective histones or incomplete DNA repair mechanisms (Schon *et al*, 1997). NAFLD and NASH are associated with different types of mtDNA damage such as, DNA strand breaks, deletions, somatic mutations and increased levels of 8-hydroxydeoxyguanosine, a marker of oxidative stress-derived DNA damage (Koliaki *et al*, 2015). The accumulation of mtDNA mutations leads to a dysfunction of the OXPHOS complex, which in turn results in an increased ROS production and subsequent accumulation of more mtDNA mutations (Van Remmen *et al*, 2003). This triggers a vicious cycle of ROS production and oxidative damage promoting morphological changes, ultrastructural lesions, depletion of mtDNA and alterations in β-oxidation and OXPHOS activity (Simões *et al*, 2018). In addition, several lipid species involved in the development and progression of NAFLD are related to mitochondrial dysfunction (Peng *et al*, 2018). For instance, cardiolipin peroxidation alters the permeability and fluidity of the mitochondrial membrane, which is associated with the destabilization and loss of electron transport chain complex activity and the induction of mitochondrial permeability transition pore opening, leading to cytokine overproduction and apoptosis (Paradies *et al*, 2014, Peng *et al*, 2018).

### 2.2.5. Endoplasmic reticulum stress

The ER is a specialized organelle with important cellular functions including production, maturation and quality control of secretory and membrane proteins. NAFLD is associated with the accumulation of unfolded proteins, aggregation of misfolded proteins as well as altered redox status inducing ER stress, which triggers the unfolded protein response (UPR) in order to restore ER homeostasis (Malhotra and Kaufman, 2007, Puri *et al*, 2008). The UPR is mediated by three canonical branches: protein kinase R-like ER kinase (PERK), inositol-requiring enzyme-1 (IRE1$\alpha$) and activating transcription factor 6 (ATF6) (Malhi and Kaufman, 2011) (**Figure 6**).

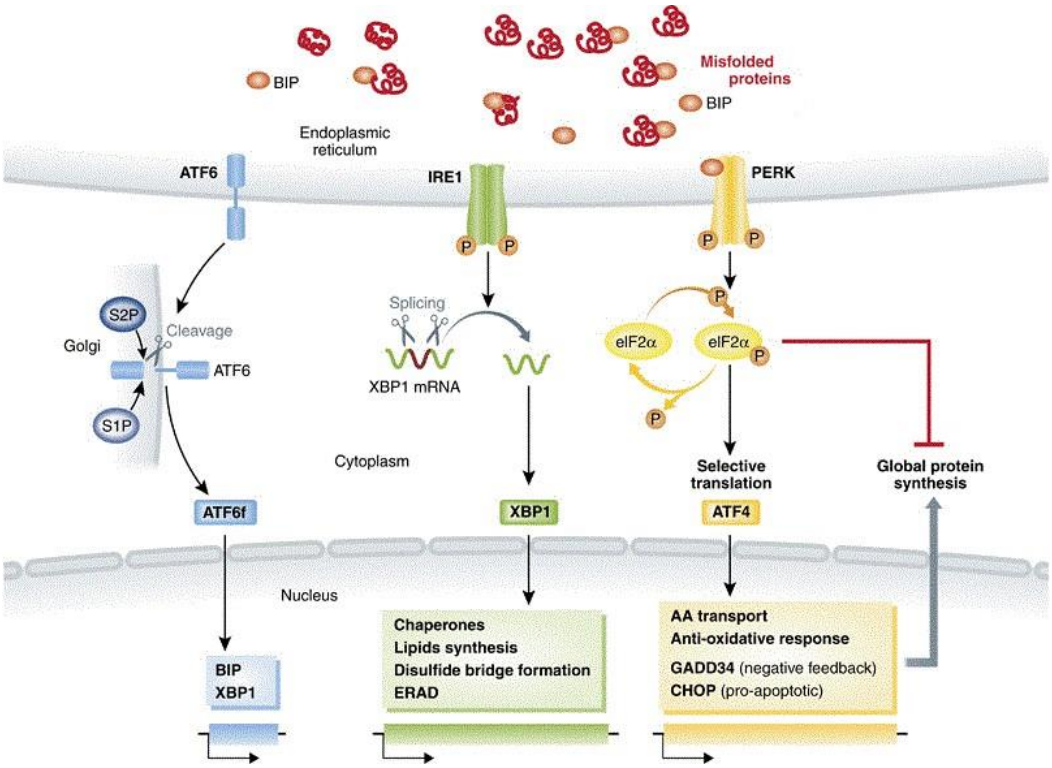


**Figure 6.** Scheme of the three canonical branches of the UPR (modified from Claudio *et al*, 2013).

Under normal conditions, PERK, IRE1α and ATF6 are inactivated and bound to 78 kDa glucose-regulated protein (GRP78). During ER stress, GRP78 is sequestered by misfolded proteins and UPR proteins are liberated and activated (Bertolotti *et al*, 2000). Activated PERK phosphorylates and activates the eukaryotic translation initiation factor 2 α (eIF2α) to inhibit protein synthesis, which leads to a decrease in protein translation. By contrast, eIF2α promotes the translation of ATF4 which enhances the expression of its downstream effectors C/EBP homologous protein (CHOP) and grown arrest and DNA damage inducible gene 34 (GADD34), which acts as a negative feedback loop that restores protein translation by dephosphorylation of eIF2α (Puri *et al*, 2008). The activation of IRE1α triggers the unconventional splicing of the mRNA encoding the transcription factor X-box binding protein 1 (XBP1), which upregulates the expression of ER-associated degradation (ERAD) machinery and chaperones to remove misfolded proteins as well as genes involved in fatty acid synthesis and ER biogenesis (Yoshida *et al*, 2001, Lee *et al*, 2008). Furthermore, the IRE-XBP1 pathway is involved in the activation of inflammatory signalling cascades, such as the JNK and NF-κB pathways (Sha *et al*, 2011). Finally, active ATF6 is translocated to the Golgi for its proteolytic activation. Mature proteins enter the nucleus and enhance the transcription of ER-related

genes (GRP78, CHOP and XBP1), which reflects the crosstalk among the three UPR pathways (Ye *et al*, 2000).

ER stress becomes chronic in the liver of animal models of obesity as well as in patients with NAFLD and NASH (Wang *et al*, 2006, Gregor *et al*, 2009). In addition to the accumulation of unfolded or misfolded proteins, the hepatic lipid overload is thought to be implicated in the initiation of chronic ER stress (Wei *et al*, 2006), which promote fat accumulation, mitochondrial dysfunction as well as impairments in VLDL secretion, protein stability and insulin signalling (Baiceanu *et al*, 2016). Failure of the UPR to resolve sustained ER stress results in the activation of oxidative and inflammatory pathways and, ultimately, in hepatocyte cell death (Puri *et al*, 2008).

### 2.2.6. Abnormal secretion of adipokines

Since the discovery of TNF-α (Hotamisligil *et al*, 1993) and leptin (Zhang *et al*, 1994) as adipocyte-secreted hormones, the adipose tissue has been identified as an extremely active endocrine organ. Currently, it is well known that the adipose tissue produces a huge variety of adipokines implicated in glucose and lipid metabolism, regulation of appetite, inflammation, cardiovascular homeostasis and reproduction, among other biological functions (Rodríguez *et al*, 2015) (**Figure 7**). Obesity, and especially visceral obesity, is associated with an abnormal secretion of adipokines that contributes to NAFLD (Rodríguez *et al*, 2007, Polyzos *et al*, 2009, Unamuno *et al*, 2018). During the pathological expansion of the adipose tissue, macrophages and other immune cells are recruited by the adipose tissue stimulating a chronic local inflammation (Ouchi *et al*, 2011). Adipose tissue-embedded immune cells secrete high amounts of pro-inflammatory cytokines that are directly transported across the portal vein to the liver (Weisberg *et al*, 2003, Frühbeck and Gómez-Ambrosi, 2013). In addition, a further relevant group of adipokines is altered in obesity and enhances hepatic inflammation and NAFLD progression: cytokines [IL-6, TNF-α, IL-10 and transforming growth factor β (TGF-β)], chemokines [macrophage inflammatory protein 2, monocyte chemoattractant protein 1 (MCP-1), CCL5 and IL-8/CXCL8], acute-phase reactants [C reactive protein (CRP), plasminogen activator inhibitor-1 and serum amyloid A], DAMPs (HMGB1, calprotectin and tenascin C), proinflammatory (leptin, osteopontin, resistin or chemerin) and anti-inflammatory (adiponectin, ghrelin, lipocalin-2 and omentin) factors (Rodríguez *et al*, 2015). Moreover, obesity is associated with a decreased expression of adiponectin,

an anti-inflammatory factor with a protective role against insulin resistance (Li *et al*, 2009).

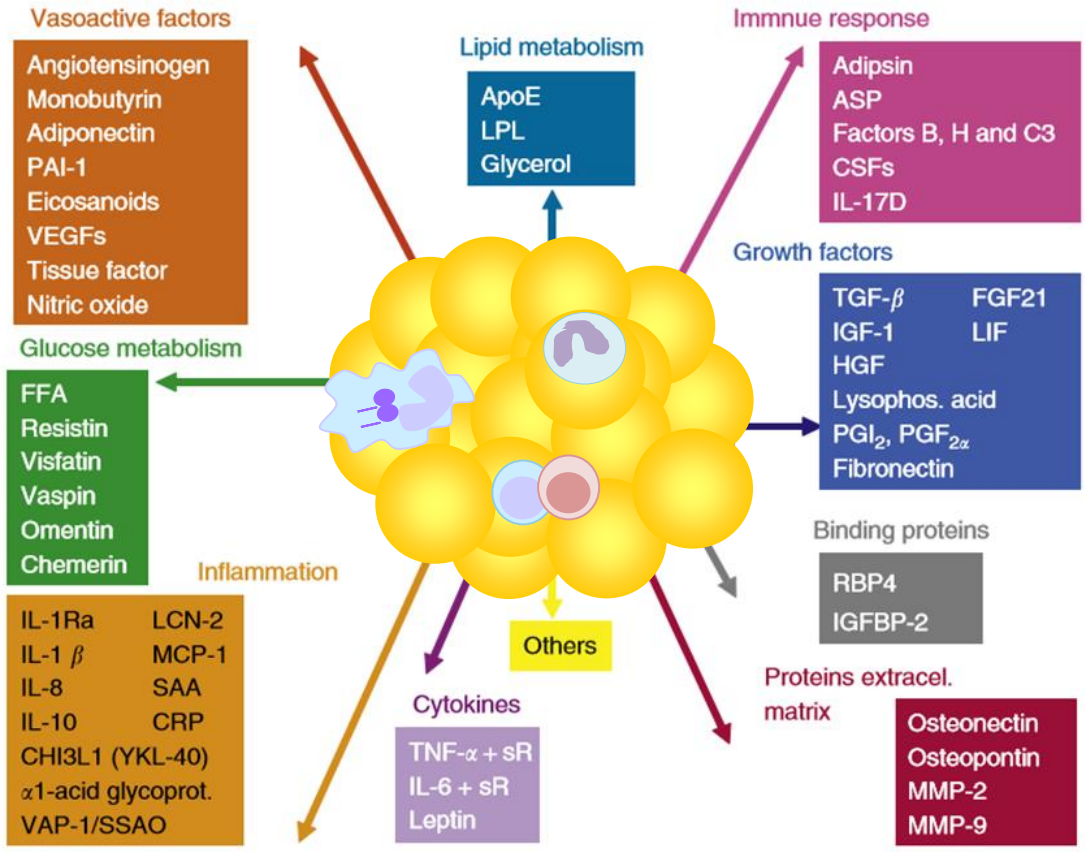


**Figure 7.** Factors secreted by white adipose tissue (modified from Frühbeck and Gómez-Ambrosi, 2013).

### 2.3. Impact of bariatric surgery in the resolution of NAFLD and NASH

Lifestyle interventions, including diet and exercise (150-min moderate weekly activity), have been used traditionally to manage overweight and obesity (Bray *et al*, 2016). However, lifestyle modifications alone do not produce sustained weight loss in most individuals, needing the implementation of effective pharmacological treatment (Anthes, 2014). Pharmacotherapy is indicated for individuals with a BMI≥30 kg/m$^2$ or a BMI ranging from 27.0 to 29.9 kg/m$^2$ with one major obesity-related comorbidity such as T2D, NAFLD and hypertension, among others (Toplak *et al*, 2015). In Europe, pharmacotherapy approved for obesity treatment includes orlistat, naltrexone/bupropion and liraglutide. Lorcaserin and phentermine/topiramate are also available in the USA (Bray *et al*, 2016). Lifestyle interventions and pharmacological options for weight loss present limited efficacy (Anthes, 2014, Toplak *et al*, 2015).

Bariatric surgery is the most effective medical approach for long-term weight loss in severely obese patients (Sjöström, 2013, Frühbeck, 2015). Standard indications for bariatric surgery require the presence of morbid obesity (BMI≥40 kg/m$^2$) or a BMI≥35 kg/m$^2$ with an important comorbidity associated, such as NAFLD, T2D or hypertension (Fried *et al*, 2014). These BMI thresholds should be reduced by 2.5 points for individuals of Asian genetic background (Fried *et al*, 2014). Moreover, the positive effects of bariatric surgery, especially with respect to improvements in insulin sensitivity have expanded the eligibility criteria for metabolic surgery to obese patients with T2D and a BMI of 30-35 kg/m$^2$ (Moncada *et al*, 2016a, Rubino *et al*, 2016). Most of the initial evidence is derived from the non-randomized, prospective, controlled Swedish Obese Subjects (SOS) study, which was the first long-term clinical trial to provide information on the beneficial effects of bariatric surgery on weight loss and maintenance as well as improvements in T2D, serum transaminase levels and NAFLD (Sjöström *et al*, 2004, Sjöström, 2008, Burza *et al*, 2013, Sjöström, 2013). The SOS study started in 1987 and included a surgery group [n=2,010; 19% gastric banding, 69% banded gastroplasty and 12% Roux-en-Y gastric bypass (RYGB)] and a control group of non-surgically treated obese subjects (n=2,037) that were followed up for over 30 years. In addition, several retrospective studies and one large prospective study with a 5-year follow-up period demonstrate that bariatric surgery can improve or even reverse NAFLD, NASH and NASH-fibrosis (Mathurin *et al*, 2009, Taitano *et al*, 2015). Weight loss reduces hepatic steatosis with the degree of liver improvement being directly proportional to weight loss (Wong *et al*, 2013).

### 2.3.1. Types of bariatric surgery procedures

Traditionally, surgical procedures are classified in three major categories: restrictive, malabsorptive and mixed techniques (**Figure 8**). Restrictive techniques, such as adjustable gastric banding, gastric plication, vertical banded gastroplasty or sleeve gastrectomy, reduce the capacity of the stomach limiting food intake. Malabsorptive procedures, including duodenal-jejunal bypass or jejuno-ileal bypass, remove parts of the small intestine, thereby decreasing the absorption of nutrients (Tack and Deloose, 2014). These techniques require the supplementation with minerals or vitamins in order to avoid deficiency diseases, including anemia or osteoporosis (Álvarez-Leite, 2004). Mixed interventions combine restrictive and malabsorptive procedures and include RYGB, biliopancreatic diversion and duodenal switch (DeMaria, 2007). Sleeve gastrectomy and RYGB are the most commonly used bariatric surgery procedures worldwide. The

selection of the bariatric surgery procedure depends on surgeon's experience to deal with the inevitable complications of each technique and to manage long-term follow-up care considerations (Neff *et al*, 2013).

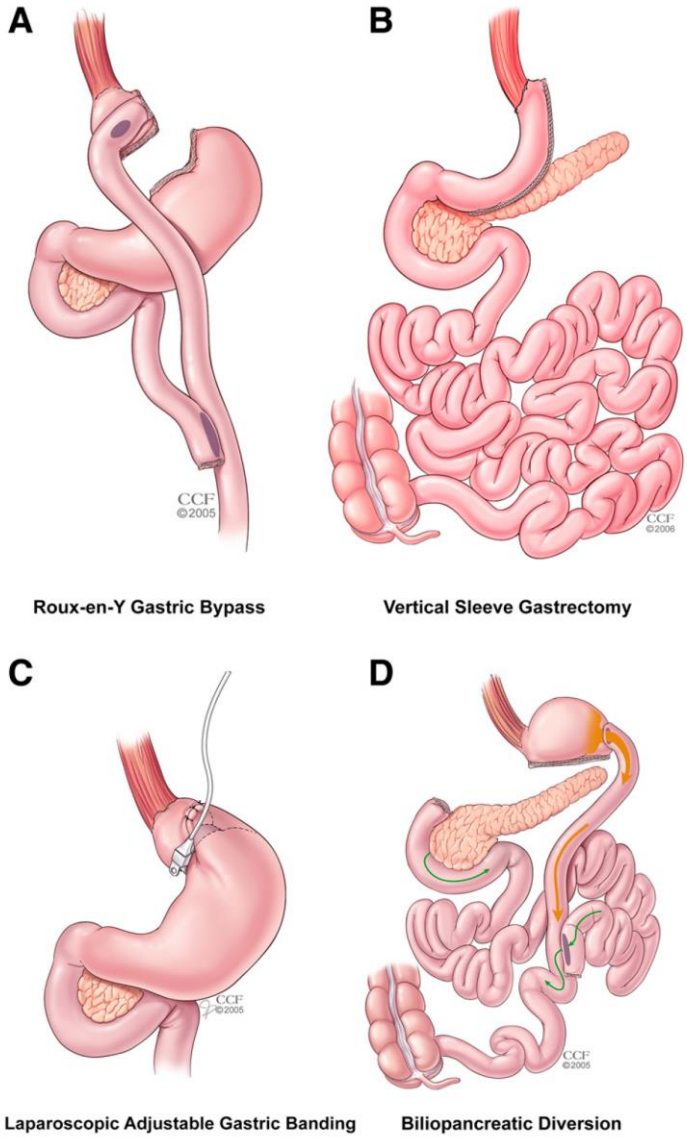


**Figure 8.** Several types of bariatric surgery (modified from Rubino *et al*, 2016).

*Sleeve gastrectomy*

Sleeve gastrectomy is a restrictive technique that involves the creation of a reduced stomach lumen by excising the gastric fundus and greater curvature of the stomach (Deitel *et al*, 2008, Katz *et al*, 2011). This technique is emerging as a popular procedure with effective results for the treatment of morbid obesity and its comorbidities in humans (Deitel *et al*, 2008) as well as in experimental models of genetic and diet-induced obesity (Valentí *et al*, 2011, Rodríguez *et al*, 2012b). Sleeve gastrectomy results in 75% and 47% improvement and resolution of T2D, respectively, and ameliorates

similarly to RYGB insulin sensitivity (Ribaric *et al*, 2014, Frühbeck, 2015). This procedure elicits an improvement in liver morphology and function in the different stages of NAFLD (Mattar *et al*, 2005, Mathurin *et al*, 2009, Taitano *et al*, 2015). In addition, hyperlipidaemia and risk of cardiovascular disease are also ameliorated after the surgery (Sjöström *et al*, 2004, Frühbeck, 2015). Experimental models of genetic and diet-induced obesity demonstrate that the beneficial effects in the resolution of comorbidities are independent of aging, surgical trauma and food intake reduction (Valentí *et al*, 2011, Rodríguez *et al*, 2012a, Rodríguez *et al*, 2012b, Moncada *et al*, 2016b). Sleeve gastrectomy has a favourable complication profile with leaks at the staple line, gastroesophageal reflux, dumping and vomiting syndrome being the main surgical complications (Deitel *et al*, 2008, Tack and Deloose, 2014). A key factor determining complications, mortality, readmissions and reoperations is the experience of operating surgeons (Birkmeyer *et al*, 2013); in experimented hands the mortality rate is 0.1-0.5%, similar to hysterectomy and cholecystectomy (Rubino *et al*, 2016).

*RYGB*

RYGB involves the resection of part of the stomach, creating a small gastric pouch, which is connected to the small intestine, bypassing the duodenum and the proximal part of the jejunum to promote malabsorption (DeMaria, 2007). This technique is one of the most used procedures and its popularity has increased due to significant and sustained weight loss in obese patients as well as improvements in obesity-associated comorbidities. In this regard, body weight is reduced approximately 25-30% at 12-18 months post-operatively and in most patients is maintained for almost 10 years (Sjöström *et al*, 2007). Body fat, especially visceral adipose tissue, is also decreased after RYGB as demonstrated by body composition studies (Gómez-Ambrosi *et al*, 2015). The improvement in glycaemia and T2D can be observed independently of any weight loss from the very beginning, with the remission of hyperglycemia and T2D resolution being 80-95% and 80%, respectively (Pories *et al*, 1995, Dirksen *et al*, 2012, Schauer *et al*, 2014). In addition, RYGB improves pancreatic β-cell function (Kashyap *et al*, 2013), hepatic steatosis, inflammation and fibrosis (Clark *et al*, 2005, Barker *et al*, 2006, Benjamin *et al*, 2018), hyperlipidaemia, hypertension and risk of cardiovascular disease (Sjöström *et al*, 2004, Frühbeck, 2015). The main complications of RYGB are anastomotic leakage of enteric contents, cholelithiasis, gastric fistulas, marginal ulceration, small bowel obstruction, internal hernia and nutritional complications (Higa

*et al*, 2000, Seeras and López, 2019), such as the chronic malabsorption of vitamin B12 and D, folate, iron, thiamine and calcium, ultimately leading to nutritional-related diseases including anemia and osteoporosis (DeMaria, 2007). In order to compensate the deficiency of micronutrients and vitamins, the intake of daily vitamin and mineral supplementations is required (Fried *et al*, 2013). Nowadays, the mortality rate of laparoscopic RYGB is 0.2% (Flum *et al*, 2009).

### 2.3.2. Mechanisms underlying post-surgical NAFLD and NASH improvement

The mechanisms underlying the beneficial effects of bariatric surgery on NAFLD are related to the improvement of metabolic dysfunction (Miras and le Roux, 2013). The precise mechanisms are not only the reduction of gastric size and malabsorption, but also changes in gastrointestinal hormones, bile flow alterations and modifications of gut microbiota, among others (Miras and le Roux, 2013, Frühbeck, 2015). These metabolic changes are weight loss-dependent or independent.

After bariatric surgery, the decrease in body fat can improve adipocyte function favouring an amelioration in insulin resistance, systemic inflammation and hepatic function (García-Marirrodriga *et al*, 2012, Illan-Gómez *et al*, 2012). The intestinal bypass produces alterations in gut hormones, such as ghrelin, gastric inhibitory peptide (GIP), glucagon-like peptide 1 (GLP-1) and polypeptide YY (PYY) (Preitner *et al*, 2004). The relationship between bariatric surgery and ghrelin levels remains controversial. Plasma ghrelin is markedly decreased after sleeve gastrectomy, which removes 70-80% of the stomach, and remains low after 1 year (Frühbeck *et al*, 2004a, Peterli *et al*, 2012). By contrast, patients undergoing RYGB exhibit reduced ghrelin levels, but not as pronounced as those observed with sleeve gastrectomy (Cummings *et al*, 2002, Frühbeck *et al*, 2004a), with ghrelin levels approaching preoperative values 12 months after surgery (Peterli *et al*, 2012, Malin *et al*, 2014). The decrease in ghrelin levels after sleeve gastrectomy and RYGB depends on the degree to which the surgical technique excludes the gastric fundus (Frühbeck *et al*, 2004a, Frühbeck *et al*, 2004b). The impact of ghrelin on hepatic function is extensively explained in section 3.3. GIP is mainly secreted from duodenal K-cells, whereas GLP-1 is primarily secreted by ileal L-cells, although both incretins are detected throughout the intestine (Mortensen *et al*, 2000). The increase in GIP and, especially GLP-1, due to proximal intestinal exclusion and accelerated nutrient delivery to the distal intestine can induce glucose-dependent insulin release (Salehi *et al*, 2011). In the liver, GLP-1 improves insulin resistance (Salehi *et al*, 2011), promotes lipid oxidation and

reduces the production of pro-inflammatory cytokines and ER stress (Ben-Shlomo *et al*, 2011). In addition, GLP-1 also has effects on central nervous system regulating central satiety, food intake, glucose homeostasis and activation of BAT thermogenesis and browning (Beiroa *et al*, 2014, Burcelin *et al*, 2014). On the other hand, $PYY_{3-36}$, the major circulating form of the 36-amino acid peptide PYY reduces food intake, enhances lipolysis, thermogenesis and post-prandial insulin and glucose responses (Sloth *et al*, 2007). Therefore, increased post-prandial levels of GLP-1 and $PYY_{3-36}$ are involved in the amelioration of glucose homeostasis after bariatric surgery (Strader *et al*, 2005).

The increase in bile acid secretion after RYGB produces an enhanced lipid absorption in the distal intestine (Steinert *et al*, 2013) as well as the binding to the intestinal nuclear farsenoid-X receptor (FXR) and the G-protein-coupled receptor (TGR5) to improve glucose tolerance by regulating insulin-independent glucose efflux (Ryan *et al*, 2014, Chávez-Talavera *et al*, 2017). Furthermore, bile acids induce the secretion of GLP-1 and PYY by the activation of TGR5, improving insulin sensitivity and glucose metabolism (Katsuma *et al*, 2005). Interestingly, bile acids are also involved in the changes of microbiota after bariatric surgery. The alterations in gut microbiota (Sweeney and Morton, 2013), including enhanced *Proteobacteria* and decreased *Firmicutes* species (Li *et al*, 2011), could be also due to changes in anatomical manipulations, dietary macronutrient composition and pH that induce a non-obesogenic state, improving energy profile and insulin sensitivity after bariatric surgery (Furet *et al*, 2010).

# 3. GHRELIN

## 3.1. Components of the ghrelin system

*Ghrelin forms*

Ghrelin is a 28-amino acid peptide, which was firstly identified in 1999 as the endogenous ligand of the growth hormone secretagogue receptor (GHS-R) (Kojima *et al*, 1999). Ghrelin is mainly produced in X/A cells of the oxyntic glands in the mucosa layer of the gastric fundus (Date *et al*, 2000, Dornonville de la Cour *et al*, 2001), but it can be also synthesized in other regions of the gastrointestinal tract, pancreas, brain, thyroid gland, pituitary, liver, placenta and testis, among others (Romero *et al*, 2010). The human *GHRL* gene is located on chromosome 3p26-p25 and encodes a polypeptide of 117 amino

acids, named preproghrelin that maintains its sequence highly conserved, among different mammals (Seim *et al*, 2009). After removing the 23-amino acid signal peptide by cleavage, the 94-amino acid segment, termed proghrelin, undergoes a proteolytic processing mainly by the prohormone convertase PC1/3 to generate the mature 28-amino acid long ghrelin, and also, a C-terminal peptide that after proteolytic process generates a peptide called obestatin (Zhu *et al*, 2006, Sato *et al*, 2012) (**Figure 9**). Ghrelin undergoes a post-translational modification consisting of the acylation of the Ser3 residue with an *n*-octanoyl group, which is necessary for ghrelin to bind to its receptor GHS-R1a (Gutiérrez *et al*, 2008). Therefore, there are two main isoforms of ghrelin: acylated ghrelin, representing ~ 10% of total ghrelin and desacyl ghrelin, without this post-translational modification and representing ~ 90% of total ghrelin (Hosoda *et al*, 2000). Several alternative ghrelin gene-derived peptides and mRNA splice variants have been also identified including des-Gln14-ghrelin (deletion of the amino acid Gln14), exon 3-deleted ghrelin and intron 1-retention ghrelin, which are overexpressed in certain types of cancer (Yeh *et al*, 2005, Seim *et al*, 2009). Certain genetic variants that cause changes in one amino acid of preproghrelin are associated with obesity, such as Arg51Gln, Leu72Met and Gln90Leu (Ukkola *et al*, 2001, Ukkola and Kesaniemi, 2003).

Circulating ghrelin levels are characterized by a preprandial increase and a postprandial decrease, supporting its role in meal initiation (Cummings *et al*, 2001). In this sense, ghrelin levels fluctuate in response to feeding and fasting, indicating that the ghrelin system is responding to energy status (Mao *et al*, 2019). In line with this observation, leptin upregulates ghrelin (Nogueiras *et al*, 2004, Gónzalez *et al*, 2008), whereas glucose and insulin decrease ghrelin levels (McCowen *et al*, 2002, Broglio *et al*, 2004). Another strong regulator of ghrelin action is liver-expressed antimicrobial peptide 2 (LEAP2), an intestinal hormone that acts as an endogenous antagonist of the ghrelin receptor as well as inhibits the production or secretion of ghrelin (Ge *et al*, 2018).

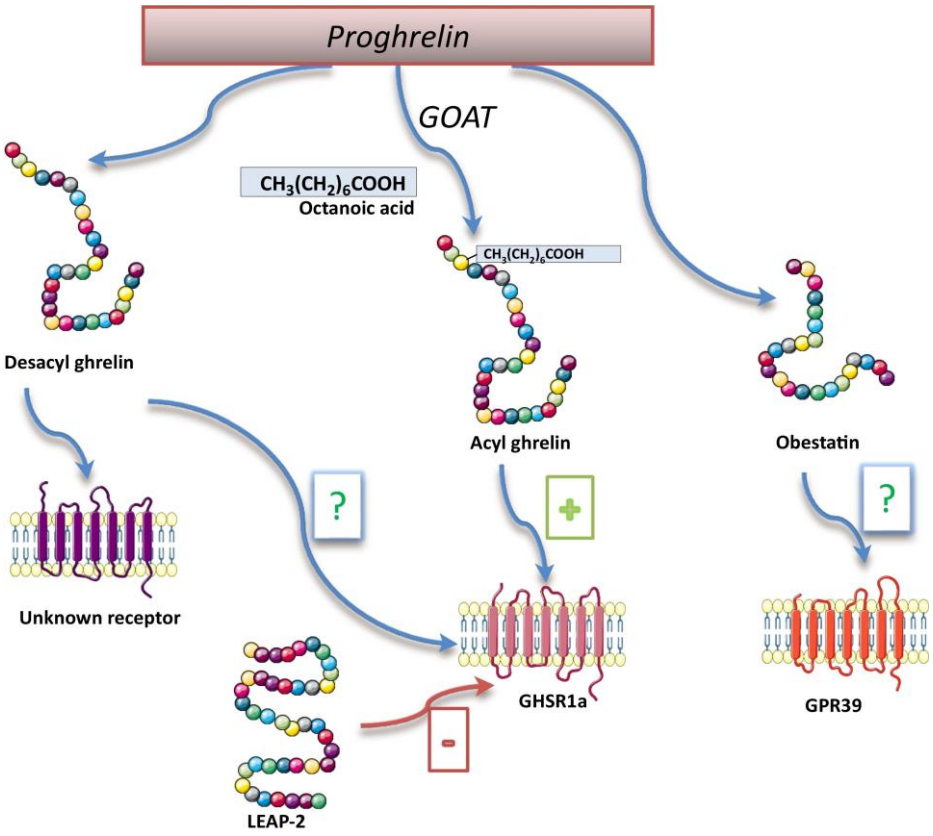


**Figure 9**. Main components of the ghrelin system (modified from Al Massadi *et al*, 2018).

*Ghrelin receptors*

In 1996, the GHS-R was isolated from the pituitary gland and hypothalamus and shown to be able to stimulate GH release (Howard *et al*, 1996). The gene encoding for human *GHSR* maps on chromosome 3q26.31 and produces two alternatively spliced proteins. GHS-R1a excises an intron, encodes a 366-amino acid protein with seven transmembrane domains that triggers $Ca^{2+}$signalling, and is considered the functional ghrelin receptor. GHS-R1a is primarily expressed in the brain and anterior pituitary gland, but also in several regions, including the pancreas, liver, ovaries and adrenal gland (Gnanapavan *et al*, 2002). GHS-R1b retains the intron, encodes a C-terminally truncated isoform of the ghrelin receptor, consisting of 289 amino acids and five transmembrane domains, and does not stimulate GH release (Gnanapavan *et al*, 2002). Usually, GHS-R1a forms a functional homodimer (Holst *et al*, 2005), whereas heterodimerization with GHS-R1b also occurs and reduces the signalling capacity (Leung *et al*, 2007). Furthermore, GHS-R1a can heterodimerize with other receptors, such as melanocortin 3 receptor, serotonin 2C receptor, dopamine receptors 1 and 2 and GPR83, among others, affecting ligand selectivity and downstream signalling (Müller *et al*, 2013, Schellekens *et al*, 2013). Notably, the action of desacyl ghrelin on GHS-R remains controversial and

several studies suggest the existence of an alternative, yet unknown, desacyl-ghrelin receptor (Callaghan and Furness, 2014, Heppner *et al*, 2014). Interestingly, other ghrelin receptors have been characterized in teleost fish such as GHS-R2b and GHS-R3b (Small *et al*, 2019).

*Ghrelin*-O-*acyltransferase*

The porcupine-like enzyme ghrelin *O*-acyltransferase (GOAT) is encoded by the human *MBOAT4* gene and is responsible for the acylation of ghrelin, which takes place in the ER (Gutiérrez *et al*, 2008, Yang *et al*, 2008). GOAT is expressed in the major ghrelin-secreting tissues, including stomach, gastrointestinal tract, pancreas and testes, among others (Lim *et al*, 2011a). Ingestion of medium-chain TG or medium-chain fatty acids can increase acylation of ghrelin (Nishi *et al*, 2005). The expression of GOAT is positively associated with fasting, GH releasing hormone (GHRH), insulin, leptin and acylated ghrelin, while being negatively regulated by refeeding and somatostatin (Gutiérrez *et al*, 2008, Yang *et al*, 2008, Gahete *et al*, 2010).

*Butyrylcholinesterase*

Butyrylcholinesterase (BChE) is well known for its role in metabolizing bioactive esters in medications and food as well as inactivating succinylcholine. However, De Vriese (De Vriese *et al*, 2004) reported that BChE is also responsible for the deacylation reaction of acylated ghrelin by cleaving the octanoyl group. Therefore, BChE has an important role in the regulation of circulating ghrelin and subsequently in many metabolic functions (Chen *et al*, 2017). BChE is synthesized by the liver and secreted into the circulation, being elevated in the bloodstream and also in the brain, muscles, stomach, kidney or heart (Chen *et al*, 2017).

### 3.2. Role of ghrelin in the regulation of body weight and adiposity

Ghrelin plays a major role in the short-term regulation of appetite and long-term regulation of adiposity (Chen *et al*, 2009, Rodríguez *et al*, 2009, Rodríguez, 2014). Ghrelin functions as a hunger signal necessary for meal initiation and anticipation, with its pulsatile secretion starting with a preprandial rise and postprandial fall 1 h after food intake (Cummings *et al*, 2001). The macronutrient composition of ingested food differentially affects postprandial ghrelin suppression, with total ghrelin levels being decreased more drastically after carbohydrate or protein ingestion than after lipids in the postabsortive state (Foster-Schubert *et al*, 2008). The central effect of ghrelin on adiposity

involves neural circuits that control food intake, energy expenditure, nutrient partitioning and reward neurons (Cowley *et al*, 2003, Al Massadi *et al*, 2017). Although the highest expression of GHS-R is detected in the pituitary and brain, lower levels of expression are detectable in some peripheral tissues, including white (WAT) and brown (BAT) adipose tissue (Rodríguez *et al*, 2009, Lin *et al*, 2011). In this sense, ghrelin stimulates lipid accumulation in WAT (Rodríguez *et al*, 2009, Miegueu *et al*, 2011), but suppresses norepinephrine release and thermogenesis in BAT (Mano-Otagiri *et al*, 2009, Mano-Otagiri *et al*, 2010). The other product of the *GHRL* gene, obestatin, is believed to have opposite effects to ghrelin on food intake and body weight through the GPR39 receptor (Zhang *et al*, 2005). Obestatin levels are increased in fasted rats and, after refeeding, plasma obestatin levels are significantly decreased but recovered quickly (Guo *et al*, 2008). However, there is some controversy regarding the role of obestatin in the regulation of adiposity, because other groups were not able to confirm these findings (Lauwers *et al*, 2006, Seoane *et al*, 2006, Nogueiras *et al*, 2007). Moreover, GPR39 was proposed as the putative receptor of obestatin, but other authors failed to reproduce GPR39-binding ability to obestatin *in vitro* (Lauwers *et al*, 2006).

### 3.2.1. Orexigenic effects through hypothalamic neurons

In 2000, Matthias Tschöp and colleagues discovered that ghrelin acts in the brain to regulate food intake, body weight and adiposity (Tschöp *et al*, 2000). Ghrelin reaches the hypothalamic neurons by crossing the blood-brain barrier, via the vagal afferent nerves and exerting paracrine actions in the hypothalamus, where it can be synthesized (Lim *et al*, 2011b). Central and peripheral ghrelin administration enhances the transcription of orexigenic peptides neuropeptide Y (NPY, agonist of Y receptors) and agouti-related protein (AgRP, antagonist of the melanocortin 4 receptor) as well as the inhibitory neurotransmitter GABA (Kamegai *et al*, 2000, Lawrence *et al*, 2002, Wang *et al*, 2002, Chen *et al*, 2004, López *et al*, 2008), which exerts inhibitory effects on anorexigenic proopiomelanocortin (POMC) neurons in the arcuate nucleus of the hypothalamus (Tong *et al*, 2008). The molecular mechanism whereby ghrelin exerts its orexigenic effects is mediated by the activation of the mTOR pathway (Martins *et al*, 2012) and sirtuin 1 (SIRT1), which deacetylates p53 and thereby activates AMPK (Velásquez *et al*, 2011). The activation of hypothalamic AMPK induced by ghrelin produces the inactivation of the *de novo* FFA synthetic pathway, resulting in a decrease in malonyl-CoA levels and activation of CPT1 (López *et al*, 2008). The pharmacological

inhibition of SIRT1 or the deletion of p53 blunt the orexigenic action of ghrelin (Porteiro *et al*, 2013). On the other hand, ghrelin induces a marked upregulation of hypothalamic mTOR, especially in the arcuate nucleus, producing the upregulation of several transcription factors, such as brain-specific homeobox domain, Forkhead box 1 (FoxO1) and phosphorylated cAMP response element-binding protein (pCREB), which ultimately increase the expression of NPY and AgRP (Diéguez *et al*, 2011, Martins *et al*, 2012). In addition, ghrelin also has the ability to increase food motivation acting on hypothalamic and extra-hypothalamic areas implicated in motivational and incentive behavior (ventral tegmental area [VTA] to the nucleus accumbens [NAc]) (Naleid *et al*, 2005, Skibicka *et al*, 2011, Al Massadi *et al*, 2019).

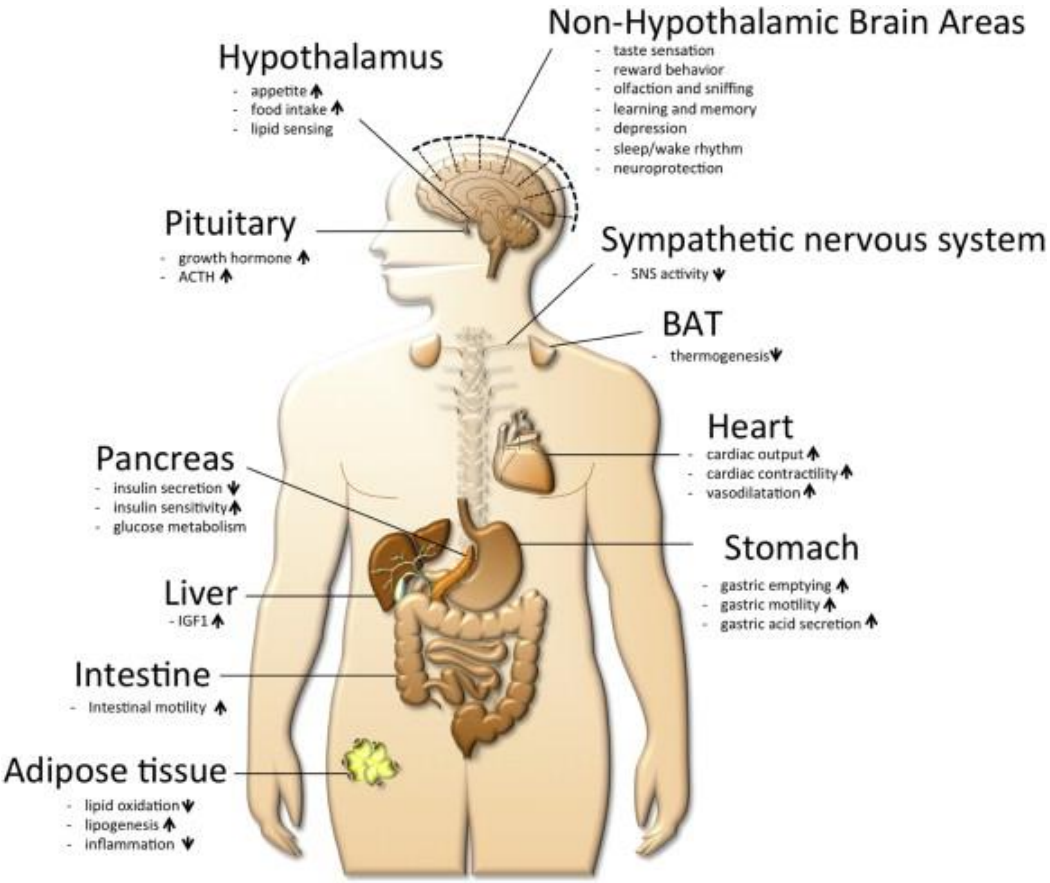


**Figure 10**. Physiological effects of ghrelin (modified from Müller *et al*, 2015).

Paradoxically, despite the orexigenic actions of ghrelin, obesity, insulin resistance, T2D and metabolic syndrome are associated with a decrease in circulating total ghrelin levels (Kojima *et al*, 1999, Tschöp *et al*, 2001, Pöykkö *et al*, 2005). In this regard, plasma desacyl ghrelin levels are dramatically decreased in these pathologies, while plasmatic concentrations of acylated ghrelin remain unchanged or enhanced (Rodríguez *et al*, 2009, Barazzoni *et al*, 2013).

### 3.2.2. Adipogenesis and lipogenesis in white adipose tissue

All the components of the ghrelin system are expressed in adipose tissue, suggesting an autocrine/paracrine effect on this tissue (Catalán *et al*, 2007, Rodríguez *et al*, 2009, Rodríguez *et al*, 2012c). During adipogenesis, the process whereby the preadipocytes are differentiated into mature adipocytes, ghrelin expression is increased and the *Ghrl* gene knockdown reduces insulin-mediated adipogenesis in 3T3-L1 adipocytes (Gurriarán-Rodríguez *et al*, 2011a). Both ghrelin isoforms induce human adipocyte differentiation *in vitro* with a concomitant enhancement in the mRNA expression of two key adipogenic transcription factors, PPARγ and SREBP (Kim *et al*, 2004, Rodríguez *et al*, 2009). In addition, acylated and desacyl ghrelin stimulate lipid accumulation by increasing the expression of several genes involved in lipogenesis, such as FAS, ACC, LPL and perilipin directly targeting visceral adipocytes (Rodríguez *et al*, 2009) or through central mechanisms (Theander-Carrillo *et al*, 2006). Moreover, acylated and desacyl ghrelin also exert anti-lipolytic effects, as demonstrated by the attenuation of isoproterenol-induced lipolysis through PI3K- and phosphodiesterase 3B-dependent mechanisms in 3T3-L1 cells and in rat visceral adipocytes (Baragli *et al*, 2011, Miegueu *et al*, 2011). In this regard, acylated and desacyl ghrelin reduce the expression of aquaporin 7 (AQP7) in human visceral adipocytes, supporting their role as anti-lipolytic and adipogenic hormones (Rodríguez *et al*, 2009). Obestatin also acts as a regulator of adipocyte metabolism by promoting adipogenesis and inhibiting lipolysis (Gurriarán-Rodríguez *et al*, 2011b, Wojciechowicz *et al*, 2015).

### 3.2.3. Thermoregulation in brown adipose tissue

Adaptive thermogenesis in BAT plays a key role in the regulation of energy homeostasis in both humans and rodents (Frühbeck *et al*, 2009). Under cold exposure or diet challenge, the sympathetic nervous system releases norepinephrine in order to activate β3-adrenergic receptors that initiate a signalling cascade activating protein kinase A, which phosphorylates hormone-sensitive lipase to produce the intracellular TG breakdown as well as the expression of mitochondrial uncoupling protein 1 (UCP1), a key protein involved in thermogenesis in brown adipocytes. Interestingly, central and peripheral ghrelin administration reduces energy expenditure due to the suppression of sympathetic activation of BAT as well as noradrenaline release and downregulation of UCP1 in brown adipocytes (Tsubone *et al*, 2005, Mano-Otagiri *et al*, 2009). In this regard, suppression of GHS-R in AgRP neurons mitigates diet-induced obesity by regulating

thermogenic activity in brown and beige adipocytes, suggesting the importance of centrally-mediated thermogenesis (Wu *et al*, 2017). Nonetheless, BAT expresses GHS-R and the ablation of *Ghsr* gene is associated with an activation of adaptive thermogenesis and energy expenditure in BAT (Mano-Otagiri *et al*, 2010), with aging *Ghsr*-null mice being lean, insulin-sensitive and with an increased thermogenic activation in brown adipocytes (Lin *et al*, 2014).

Human obesity is associated with a reduction in thermogenic capacity in BAT due to the downregulation of mitochondrial biogenesis and dynamics (Cypess *et al*, 2009, van Marken Lichtenbelt *et al*, 2009, Virtanen *et al*, 2009). Interestingly, cold-induced BAT activation is significantly associated with lower serum ghrelin concentrations, supporting the link between systemic ghrelin and BAT function (Chondronikola *et al*, 2017).

### 3.3. Potential impact of ghrelin in the pathogenesis of NAFLD

Experimental evidence supports the role of ghrelin in the development of NAFLD (Marchesini *et al*, 2003, Estep *et al*, 2011, Mykhalchyshyn *et al*, 2015). Moreover, the human liver synthesizes ghrelin, and a slight increase in ghrelin expression has been reported in patients with NASH (Uribe *et al*, 2008). The liver constitutes a target for the lipogenic actions of ghrelin, since both chronic central and peripheral administration of ghrelin stimulates hepatic TG content (Sangiao-Alvarellos *et al*, 2009, Porteiro *et al*, 2013). However, ghrelin also activates mechanisms to prevent lipotoxicity via autophagy induction or NF-κB inhibition in the liver (Mao *et al*, 2015b). Accordingly, acylated ghrelin treatment normalizes the proinflammatory markers NF-κB and TNF-α in the liver of obese rats (Barazzoni *et al*, 2014). Therefore, the metabolic and inflammatory pathways of ghrelin in the liver support its role in the development and progression of NAFLD (Zhang and Fan, 2015).

#### 3.3.1. Lipogenesis through central and peripheral mechanisms

It is well established that ghrelin induces lipogenesis in the liver through central and peripheral mechanisms (Zhang and Fan, 2015). Chronic central and systemic ghrelin infusion increases hepatic TG content and lipogenic factors, including PPARγ, SREBP, FAS, CCAAT/enhancer-binding protein α (CEBPα) or LPL (Davies *et al*, 2009, Sangiao-Alvarellos *et al*, 2009, Porteiro *et al*, 2013, Zhang and Fan, 2015). Ghrelin stimulates hepatic *de novo* lipogenesis by direct activation of its receptor in hepatocytes via a mechanism involving mTOR-PPARγ signalling (Li *et al*, 2014). In this sense, knockout

or inhibition of GHS-R1a produces a decrease in hepatic steatosis, without alteration in food intake in both diet-induced and genetically obese mice (Li *et al*, 2014). Moreover, the inhibition of mTOR signalling with rapamycin as well as the antagonism of PPARγ or PPARγ deficiency block the up-regulation of lipogenesis-related transcriptional factors and enzymes induced by ghrelin in hepatocytes (Li *et al*, 2014). Interestingly, the anabolic effects of ghrelin are at least partially independent of its appetite-stimulating effect and are also mediated by p53, which plays an essential role in the peripheral adipogenic and lipogenic gene expression (Porteiro *et al*, 2013).

### 3.3.2. Changes in insulin sensitivity

Insulin resistance is one of the hallmarks of NAFLD and one of the multiple hits involved in the progression of NAFLD to NASH (Zhang and Fan, 2015). Patients with NAFLD present a similar impairment in hepatic insulin sensitivity and glucose production as patients with overt T2D (Bugianesi *et al*, 2005). Ghrelin plays an important role in glucose homeostasis through the regulation of insulin secretion in β-cells as well as by the control of hepatic insulin signalling and glucose production. Nonetheless, acylated and desacyl ghrelin exert opposite effects on insulin sensitivity. Ghrelin is expressed in pancreatic islets (Date *et al*, 2002, Dezaki *et al*, 2004) and it is able to regulate insulin secretion as well as promote β-cell proliferation, survival and steatosis (Granata *et al*, 2007, Méndez-Giménez *et al*, 2017). Obestatin also ameliorates β-cell metabolism, survival and inflammation (Cowan *et al*, 2016, Khaleel and Abdel-Aleem, 2019). Broglio *et al*. firstly discovered that acylated ghrelin enhances blood glucose levels and decreases insulin secretion (Broglio *et al*, 2001). Diet-induced or genetically obese *ob/ob* mice lacking ghrelin or its receptor present an improvement in glucose tolerance and increase glucose-induced insulin secretion, thereby ameliorating insulin sensitivity in liver and other peripheral tissues (Sun *et al*, 2006). In addition, GOAT-specific inhibitor improves glucose tolerance providing evidence of the effect of acylated ghrelin on glucose homeostasis (Barnett *et al*, 2010). Interestingly, exogenous desacyl ghrelin treatment acts as a strong insulin secretagogue, while acylated ghrelin reduces glucose-induced insulin release and enhances glucose levels in both rodents and humans (Gauna *et al*, 2004, Gauna *et al*, 2005). In line with these observations, immunological, genetic and pharmacological blockade of ghrelin signalling increases glucose-stimulated insulin secretion and ameliorates peripheral insulin sensitivity (Alamri *et al*, 2016). The molecular mechanisms underlying acylated ghrelin effects seem to be mediated in

pancreatic β-cells by a non-canonical GHS-R1a signalling pathway, in which the receptor is heterodimerized with the somatostatin receptor subtype-5 (Park *et al*, 2012).

### 3.3.3. Anti-inflammatory and anti-fibrotic properties

Hepatic inflammation plays a pivotal role in the progression of NAFLD to NASH as well as in the initiation of fibrosis, in a process governed by the NF-κB signalling pathway (Elsharkawy and Mann, 2007). Following hepatocyte damage, Kuppfer and other inflammatory cells release proinflammatory cytokines, with TGF-β1 being the most critical one, that activates hepatic stellate cells (HSC) (Gressner *et al*, 2002). Activated HSC produce high quantities of collagen I and other proteins including, matrix metalloproteinases (MMPs), which produce extracellular matrix degradation, and tissue inhibitors of metalloproteinases (TIMPs), which are involved in extracellular matrix formation (De Minicis *et al*, 2007). Both MMP2 and TIMP1 regulate the process of liver fibrosis via TGF-β1 mediation (Senties-G´0mez *et al*, 2005). Administration of ghrelin has anti-inflammatory effects in multiple inflammatory diseases, such as intestinal ischemia and reperfusion injury, sepsis as well as cardiovascular, gastrointestinal and pancreatic disease (Kasimay *et al*, 2006, Chorny *et al*, 2008, Zhang and Fan, 2015). In this sense, administration of ghrelin in the gastrointestinal tract produces cell proliferation, improves the release of proinflammatory cytokines and decreases LPS- or TNF-α–induced apoptosis (Waseem *et al*, 2008). In addition, ghrelin exerts anti-inflammatory and anti-fibrotic properties in order to protect the liver against NALFD progression. Ghrelin-deficient mice develop exacerbated hepatic fibrosis and liver damage after chronic injury (Moreno *et al*, 2010, Mao *et al*, 2015b). Acylated ghrelin diminishes hepatic proinflammatory and oxidative changes in experimental models of oxidative damage, inflammation and fibrosis (Obay *et al*, 2008, Moreno *et al*, 2010). Ghrelin modulates hepatic inflammation via downregulation of the NF-κB signalling pathway, inhibiting the translocation of NF-κB into the nucleus (Mao *et al*, 2015b). Ghrelin attenuates liver fibrosis via the inhibition of the TGF-β1/Smad3 signalling pathway in models of liver injury (Moreno *et al*, 2010, Mao *et al*, 2015b). Interestingly, in patients with chronic liver diseases, serum ghrelin levels decrease in those with advanced fibrosis, and hepatic ghrelin gene expression correlates with expression of fibrogenic genes (Moreno *et al*, 2010, Mao *et al*, 2015b), supporting an important role of the hormone in liver fibrogenesis.

# Hypothesis and specific aims

## HYPOTHESIS

Bariatric surgery reduces the incidence of obesity-associated NAFLD and NASH, but the molecular mechanisms underlying these metabolic effects remain unclear. In this sense, ghrelin, a gut hormone with orexigenic, lipogenic and anti-inflammatory properties, plays a key role in the development of NAFLD and progression to NASH. The overall aim of the present thesis was to analyse the potential beneficial effects of ghrelin isoforms in the amelioration of hepatic steatosis and inflammation in diet-induced obese rats and in patients with severe obesity submitted to two different bariatric surgery techniques, namely sleeve gastrectomy and RYGB.

## SPECIFIC AIMS

Specifically, the aims of the present thesis were:

1. To study the potential role of ghrelin isoforms in the improvement of hepatic steatosis after sleeve gastrectomy and RYGB via the regulation of lipogenesis, β-oxidation and autophagy in an experimental model of diet-induced obesity that leads to NAFLD.

2. To explore the potential contribution of ghrelin isoforms in the amelioration of hepatic inflammation after RYGB through the inhibition of hepatocyte cell death (apoptosis, autophagic cell death and pyroptosis) in patients with severe obesity classified according to glucose tolerance status and hepatic function.

3. To evaluate the direct effects of acylated and desacyl ghrelin on markers of inflammation, mitochondrial dysfunction and ER stress under basal, lipotoxic and inflammatory conditions in primary rat hepatocytes.

# Articles

# STUDY I

## 1. Ghrelin and autophagy

### Article

**Ezquerro S**, Frühbeck G, Rodríguez A.
Ghrelin and autophagy.
*Curr Opin Clin Nutr Metab Care* 2017;20(5):402-408.

### Principal objective

The present review focuses on the role of ghrelin in the regulation of autophagy, an evolutionarily conserved pathway for bulk digestion of cytoplasmic organelles, maintenance of cellular homeostasis and survival, which is impaired in obesity, T2D, NAFLD, cardiovascular and neurodegenerative diseases.

### Specific objectives

- To describe the molecular mechanism involved in the process of autophagy.
- To review the impairment of the autophagy machinery in several disorders including, obesity, NAFLD, T2D, cardiovascular and neurodegenerative diseases.
- To outline the protective effect of ghrelin on intestinal mucosa, neurodegenerative, metabolic and cardiovascular diseases through autophagy activation.

Ezquerro S, Frühbeck G, Rodríguez A. Ghrelin and autophagy. Current Opinion in Clinical Nutrition & Metabolic Care, 2017, 20(5):402-408.

# STUDY II

## 2. Acylated and desacyl ghrelin are associated with hepatic lipogenesis, β-oxidation and autophagy: role in NAFLD amelioration after sleeve gastrectomy in obese rats

### Article

**Ezquerro S**, Méndez-Giménez L, Becerril S, Moncada R, Valentí V, Catalán V, Gómez-Ambrosi J, Frühbeck G, Rodríguez A.

Acylated and desacyl ghrelin are associated with hepatic lipogenesis, β-oxidation and autophagy: role in NAFLD amelioration after sleeve gastrectomy in obese rats.

*Sci Rep* 2016;6:39942.

### Hypothesis

Acylated and desacyl ghrelin are involved in the improvement of hepatic steatosis after sleeve gastrectomy, a restrictive bariatric surgery procedure, in diet-induced obese rats.

### Objectives

- To analyze *ex vivo* the effect of sleeve gastrectomy on hepatic steatosis through the regulation of hepatic lipogenesis, β-oxidation and autophagy.
- To study the potential differences in circulating acylated and desacyl ghrelin concentrations before and after sleeve gastrectomy as well as their association with hepatic lipogenesis, β-oxidation and autophagy.
- To evaluate *in vitro* the direct effects of both ghrelin isoforms on key regulatory molecules involved in these pathways in rat primary hepatocytes.

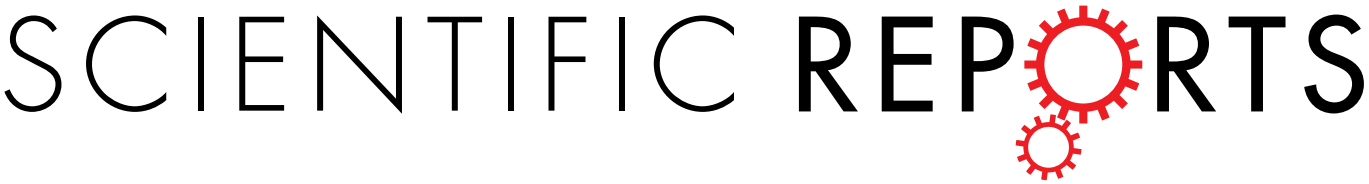

OPEN

# Acylated and desacyl ghrelin are associated with hepatic lipogenesis, β-oxidation and autophagy: role in NAFLD amelioration after sleeve gastrectomy in obese rats

Received: 29 September 2016
Accepted: 29 November 2016
Published: 23 December 2016

Silvia Ezquerro[1,2,3], Leire Méndez-Giménez[1,2,3], Sara Becerril[1,2,3], Rafael Moncada[2,3,4], Víctor Valentí[2,3,5], Victoria Catalán[1,2,3], Javier Gómez-Ambrosi[1,2,3], Gema Frühbeck[1,2,3,6] & Amaia Rodríguez[1,2,3]

**Bariatric surgery improves non-alcoholic fatty liver disease (NAFLD). Our aim was to investigate the potential role of ghrelin isoforms in the resolution of hepatic steatosis after sleeve gastrectomy, a restrictive bariatric surgery procedure, in diet-induced obese rats. Male Wistar rats (n = 161) were subjected to surgical (sham operation and sleeve gastrectomy) or dietary interventions [fed *ad libitum* a normal (ND) or a high-fat (HFD) diet or pair-fed]. Obese rats developed hepatosteatosis and showed decreased circulating desacyl ghrelin without changes in acylated ghrelin. Sleeve gastrectomy induced a dramatic decrease of desacyl ghrelin, but increased the acylated/desacyl ghrelin ratio. Moreover, sleeve gastrectomy reduced hepatic triglyceride content and lipogenic enzymes *Mogat2* and *Dgat1*, increased mitochondrial DNA amount and induced AMPK-activated mitochondrial FFA β-oxidation and autophagy to a higher extent than caloric restriction. In primary rat hepatocytes, the incubation with both acylated and desacyl ghrelin (10, 100 and 1,000 pmol/L) significantly increased TG content, triggered AMPK-activated mitochondrial FFA β-oxidation and autophagy. Our data suggest that the decrease in the most abundant isoform, desacyl ghrelin, after sleeve gastrectomy contributes to the reduction of lipogenesis, whereas the increased relative acylated ghrelin levels activate factors involved in mitochondrial FFA β-oxidation and autophagy in obese rats, thereby ameliorating NAFLD.**

Non-alcoholic fatty liver disease (NAFLD) is a pathology characterized by intrahepatic triacylglycerol (TG) over-accumulation[1,2], which is commonly associated with obesity, dyslipidemia, insulin resistance and type 2 diabetes[3]. NAFLD comprises a spectrum of liver disorders ranging from steatosis to non-alcoholic steatohepatitis (NASH) with risk of progression to liver cirrhosis and hepatocellular carcinoma[4]. The prevalence of NAFLD and NASH increases from around 20% and 3%, respectively, in the general population to 75% and 25–70%, respectively, in morbid obesity[5,6]. The excessive TG deposition in hepatocytes derives from an increased delivery of free fatty acids (FFA) into the liver from several different sources: excess dietary fat, higher FFA release from adipocytes via lipolysis, as well as increased *de novo* hepatic lipogenesis, ultimately leading to the development of obesity-associated NAFLD[7]. In addition, growing evidence indicates that hepatic mitochondrial dysfunction as well as alterations in autophagy are also involved in the development of this disease[8]. Bariatric surgery constitutes an effective treatment for morbid obesity achieving a more sustainable weight loss than that observed with lifestyle changes or pharmacological therapy[9]. Moreover, this procedure significantly improves, or even

[1]Metabolic Research Laboratory, Clínica Universidad de Navarra, Pamplona, Spain. [2]CIBER Fisiopatología de la Obesidad y Nutrición (CIBEROBN), Instituto de Salud Carlos III, Madrid, Spain. [3]Obesity & Adipobiology Group, Instituto de Investigación Sanitaria de Navarra (IdiSNA), Pamplona, Spain. [4]Department of Anesthesia, Clínica Universidad de Navarra, Pamplona, Spain. [5]Department of Surgery, Clínica Universidad de Navarra, Pamplona, Spain. [6]Department of Endocrinology & Nutrition, Clínica Universidad de Navarra, Pamplona, Spain. Correspondence and requests for materials should be addressed to A.R. (email: arodmur@unav.es)

| Determination | ND (n = 22) | HFD (n = 21) | *P* |
|---|---|---|---|
| Body weight (g) | 481 ± 15 | 606 ± 17 | **<0.001** |
| Whole-body white adiposity (g) | 33 ± 3 | 77 ± 6 | **<0.001** |
| Glucose (mg/dL) | 80 ± 2 | 90 ± 2 | **<0.01** |
| Insulin (ng/mL) | 2.1 ± 0.4 | 3.7 ± 0.6 | **<0.05** |
| HOMA | 0.52 ± 0.11 | 0.96 ± 0.17 | **<0.05** |
| Liver (g) | 12.3 ± 0.5 | 14.5 ± 0.5 | **<0.05** |
| Intrahepatic TG (mg/g) | 23.9 ± 1.6 | 34.7 ± 2.3 | **<0.001** |
| AST (IU/L) | 36 ± 3 | 41 ± 3 | >0.05 |
| ALT (IU/L) | 10 ± 1 | 11 ± 1 | >0.05 |

**Table 1. Body weight, insulin sensitivity and markers of hepatic function of lean and diet-induced obese rats.** ND, normal diet; HFD, high-fat diet; TG, triacylglycerols. Data are the mean ± S.E.M. Statistical differences were analyzed by Student's *t* test.

| Determination | Sham ND (n = 17) | Sleeve ND (n = 15) | Pair-fed ND (n = 17) | Sham HFD (n = 24) | Sleeve HFD (n = 22) | Pair-fed HFD (n = 23) |
|---|---|---|---|---|---|---|
| Body weight (g) | 503 ± 10 | 478 ± 11[b] | 495 ± 10 | 549 ± 18[a] | 514 ± 13[a,b] | 554 ± 13[a] |
| Total weight loss (%) | 14 ± 1 | 18 ± 1[b] | 12 ± 1 | 3 ± 1[a] | 10 ± 2[a,b] | 0 ± 1[a] |
| Whole-body white adiposity (g) | 41 ± 3 | 37 ± 3[b] | 49 ± 3 | 58 ± 7[a] | 55 ± 1[a,b] | 64 ± 3[a] |
| Glucose (mg/dL) | 79 ± 2 | 78 ± 2[b] | 90 ± 3 | 101 ± 4[a] | 103 ± 3[a,b] | 111 ± 5[a] |
| Insulin (ng/mL) | 2.4 ± 0.4 | 1.6 ± 0.3[b] | 2.2 ± 0.3 | 2.2 ± 0.3 | 1.8 ± 0.2[b] | 3.1 ± 0.4 |
| HOMA | 0.52 ± 0.10 | 0.44 ± 0.07[b] | 0.56 ± 0.08 | 0.66 ± 0.01[a] | 0.55 ± 0.05[a,b] | 1.00 ± 0.16[a] |
| Liver (g) | 12.4 ± 0.5 | 11.0 ± 0.5[b] | 12.1 ± 0.4 | 13.4 ± 0.5[a] | 12.1 ± 0.4[a,b] | 12.4 ± 0.4[a] |
| Intrahepatic TG (mg/g) | 23.4 ± 1.3 | 21.9 ± 1.6[b] | 23.2 ± 1.6 | 35.0 ± 0.4[a] | 25.3 ± 1.7[a,b] | 31.3 ± 2.3[a] |
| AST (IU/L) | 41 ± 3 | 26 ± 2[b] | 37 ± 2 | 40 ± 3 | 32 ± 2[b] | 36 ± 3 |
| ALT (IU/L) | 12 ± 1 | 9 ± 1 | 11 ± 2 | 11 ± 1 | 10 ± 1 | 9 ± 2 |

**Table 2. Body weight, insulin sensitivity and markers of hepatic function four weeks after surgical and dietary interventions in diet-induced obese rats.** ND, normal diet; HFD, high-fat diet; TG, triacylglycerols. Data are the mean ± S.E.M. Statistical differences were analyzed by two-way ANOVA. [a]$P < 0.05$ effect of diet; [b]$P < 0.05$ effect of surgery.

reverses, NAFLD, NASH and fibrosis in obese patients[10–12]. However, the molecular mechanisms underlying surgically-induced improvement of hepatic function remain unclear.

The orexigenic hormone ghrelin has been linked with the development of hepatosteatosis and the progression to NASH[13]. Ghrelin is a 28 amino acid peptide mainly synthesized in X/A cells of the oxyntic glands in the mucosa layer of the gastric fundus and circulates in two main forms: acylated ghrelin, with an *n*-octanoyl group at the serine 3 residue, and desacyl ghrelin, without this post-translational modification[14–16]. Administration of exogenous ghrelin increases food intake by activating hypothalamic neuropeptide Y/agouti-related peptide-containing neurons, which also express GHS-R type 1a, via the modulation of fatty acid metabolism[17,18]. Ghrelin also stimulates adiposity peripherally, through a direct stimulation of adipogenesis and lipogenesis in murine and human adipocytes[19,20]. The liver also constitutes a target for the lipogenic actions of ghrelin, since both chronic central and peripheral administration of ghrelin stimulate hepatic lipid storage[21,22]. In addition, opposite effects of ghrelin isoforms on hepatic glucose metabolism have been reported with desacyl ghrelin suppressing glucose release by hepatocytes as well as antagonizing the acylated ghrelin-induced increase in hepatic glucose output *in vitro*[23]. NAFLD is associated with alterations in total ghrelin concentrations[24,25], but the specific role of acylated and desacyl in hepatic lipid metabolism has not been disentangled.

Circulating ghrelin concentrations decrease after sleeve gastrectomy due to the resection of the gastric fundus[15] with RYGB additionally suppressing post-prandial ghrelin levels[26]. The aim of the present study was to analyze in diet-induced obese rats the implication of ghrelin isoforms in the improvement of hepatosteatosis after sleeve gastrectomy, a restrictive bariatric surgery procedure. In this regard, the potential differences in circulating acylated and desacyl ghrelin concentrations in obesity and after sleeve gastrectomy as well as their association with hepatic lipogenesis, lipophagy and mitochondrial FFA β-oxidation were evaluated. Moreover, the direct effects of the major isoforms of ghrelin on key regulatory molecules involved in these pathways were also studied in primary rat hepatocytes.

## Results

**Sleeve gastrectomy reduced serum desacyl ghrelin, but not the acylated form.** Sleeve gastrectomy improved body weight, adiposity and insulin sensitivity of experimental animals (Tables 1 and 2). As expected, serum desacyl ghrelin was decreased in obese rats ($P < 0.05$) (Fig. 1A), but no significant changes in circulating acylated ghrelin and the acylated/desacyl ghrelin ratio were found between lean and obese rats (Fig. 1C and E).

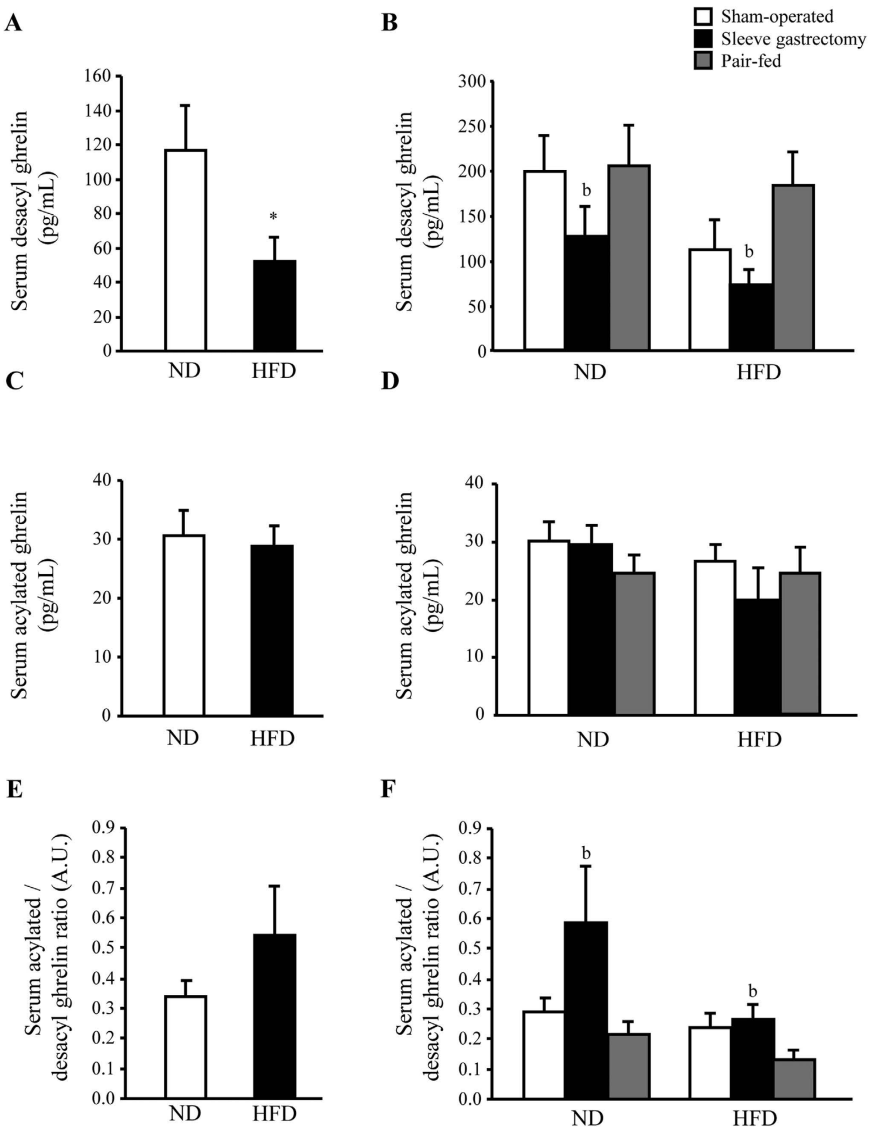


**Figure 1. Effect of sleeve gastrectomy on circulating ghrelin isoforms.** Bar graphs illustrate the impact of obesity and sleeve gastrectomy-induced weight loss on serum desacyl (**A**,**B**) and acylated (**C**,**D**) ghrelin levels as well as the acylated/desacyl ghrelin ratio (**E**,**F**). Differences were analyzed by Student's *t* test or two-way ANOVA, where appropriate. $^{*}P < 0.05$ *vs* lean control ND; $^{b}P < 0.05$ effect of surgery.

Rats undergoing bariatric surgery exhibited decreased ($P < 0.05$) desacyl ghrelin levels, without changes in acylated ghrelin concentrations ($P = 0.820$) (Fig. 1B and D). An increase in the acylated/desacyl ghrelin ratio ($P < 0.05$) was found after surgery (Fig. 1F).

**Sleeve gastrectomy improved hepatic function and steatosis through the regulation of lipogenic factors.** Obesity was associated with higher liver weight ($P < 0.05$), intrahepatic TG ($P < 0.001$) and serum AST and ALT levels, although the differences in transaminases did not read statistical significance (Table 1). Moreover, obese animals showed higher ($P < 0.05$) transcript levels of the lipogenic genes *Pparg*, *Srebf1*, *Mogat2* and *Dgat1* as well as a moderate-to-severe hepatic steatosis evidenced by the staining of the lipid droplet-coating protein adipophilin in liver sections (Fig. 2A–B and Supplemental Fig. 1). Liver weight ($P < 0.01$), intrahepatic TG ($P < 0.05$) and AST levels ($P < 0.001$) were decreased in rats subjected to bariatric surgery (Table 2). Accordingly, sleeve-gastrectomized rats exhibited a tendency towards a downregulation in hepatic *Pparg* ($P = 0.084$) and *Srebf1* ($P = 0.153$) transcription factors as well as lower ($P < 0.05$) mRNA levels of *Mogat2* and *Dgat1* and mild steatosis evidenced by adipophilin staining (Fig. 2B–C and Supplemental Fig. 1).

**Acylated and desacyl ghrelin stimulate lipogenesis in primary rat hepatocytes.** We next examined whether acylated and desacyl ghrelin levels are associated with the improvement in hepatic steatosis after sleeve gastrectomy. A positive correlation between desacyl ghrelin and ALT ($r = 0.23$, $P < 0.05$) was found, whereas acylated ghrelin was negatively correlated with intrahepatic TG ($r = -0.36$, $P < 0.001$). The direct effect of both ghrelin isoforms on lipogenesis was also evaluated in primary rat hepatocytes. Both acylated and desacyl

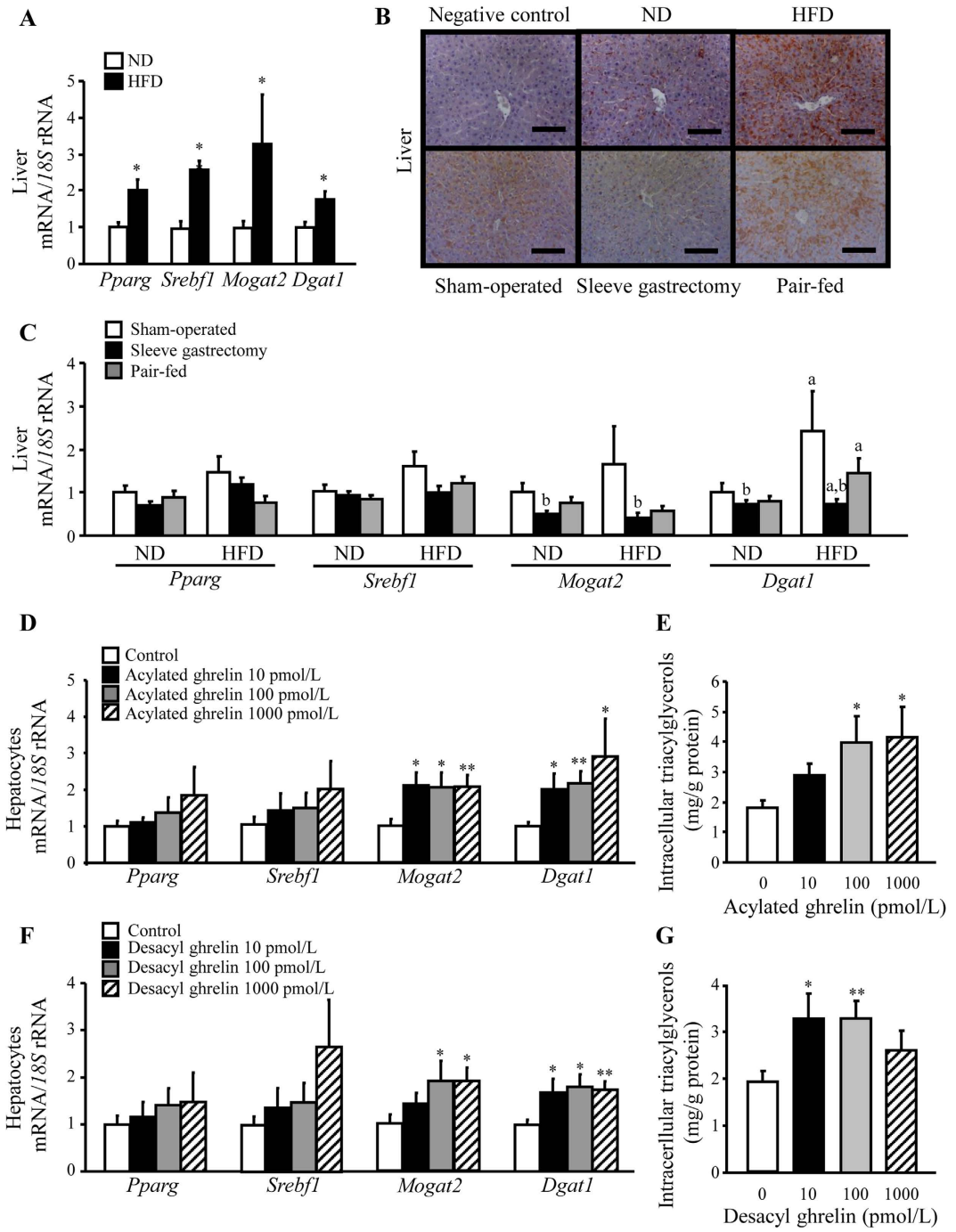


**Figure 2. Effect of acylated and desacyl ghrelin on the improvement of hepatic steatosis after sleeve gastrectomy.** Impact of obesity (**A**) and sleeve gastrectomy (**C**) on the mRNA expression levels of *Pparg, Srebf1, Mogat2* and *Dgat1* in liver samples of experimental animals. (**B**) Immunohistochemical detection of adipophilin in histological sections of rat liver (magnification 200x, *scale bar* = 100 μm). Effect of acylated (**D**,**E**) and desacyl (**F**,**G**) ghrelin on key lipogenic factors and intracellular triglycerides in rat hepatocyte cultures. The gene expression in lean rats, in the sham-operated groups fed a ND and in unstimulated hepatocytes was assumed to be 1. $^{*}P < 0.05$; $^{**}P < 0.01$ *vs* lean control ND or unstimulated hepatocytes; $^{a}P < 0.05$ effect of diet; $^{b}P < 0.05$ effect of surgery.

ghrelin increased ($P < 0.05$) the mRNA expression of *Mogat2* and *Dgat1* and intracellular TG content in rat hepatocytes (Fig. 2D–F), although no significant changes were observed in *Pparg* and *Srebf1* transcript levels.

**Acylated and desacyl ghrelin induced changes in factors related to AMPK-induced hepatic mitochondrial β-oxidation.** Since NAFLD is highly correlated with reduced mitochondrial lipid oxidation[27], the effect of sleeve gastrectomy on the regulation of mitochondrial FFA β-oxidation pathway was evaluated.

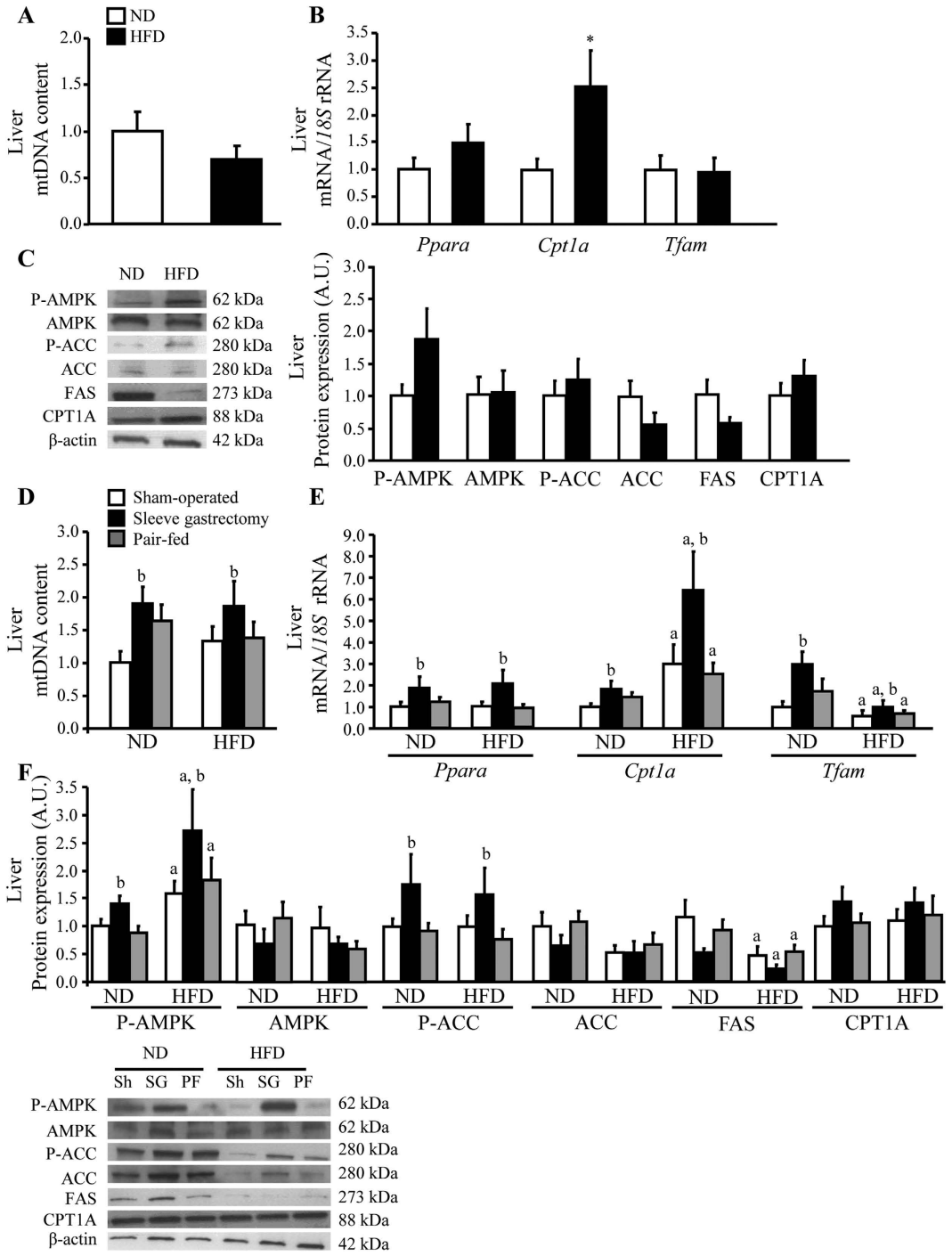


**Figure 3. Impact of sleeve gastrectomy on hepatic mitochondrial biogenesis and FFA β-oxidation.** Bar graphs show the effect of obesity (**A**,**B**) and sleeve gastrectomy (**D**,**E**) on the hepatic gene expression of molecules involved in mitochondrial biogenesis (mtDNA content and *Tfam*) and FFA β-oxidation (*Ppara* and *Cpt1a*). Representative cropped blots and Western-blot analysis show the impact of obesity (**C**) and sleeve gastrectomy (**F**) on the phosphorylation/activation of AMPK in Thr172 and the phosphorylation/inactivation of ACC in Ser79 as well as the basal expression of AMPK, ACC, FAS and CPT1A enzymes in liver samples of the experimental groups. The gene and protein expression in lean or in the sham group fed a ND was assumed to be 1. $^{*}P < 0.05$ *vs* lean control ND; $^{a}P < 0.05$ effect of diet; $^{b}P < 0.05$ effect of surgery.

Obesity did not change the hepatic mitochondrial number, as evidenced by a similar mtDNA copy number and transcript levels of *Tfam*, a factor involved in mitochondrial genome replication (Fig. 3A–B). Interestingly, a significant ($P < 0.05$) increase in both markers of mitochondrial biogenesis was observed following sleeve gastrectomy (Fig. 3D–E). It is well established that activated AMPK directly phosphorylates and inactivates ACC,

an enzyme that catalyzes the rate-limiting reaction for FFA synthesis[28]. The inhibition of ACC reduces the production of malonyl-CoA, an allosteric inhibitor of CPT1a, which is a key regulator of mitochondrial FFA uptake and its expression is positively regulated by PPARα[29]. Obese rats exhibited similar basal AMPK levels and AMPK phosphorylation/activation compared to lean rats (Fig. 3C). Accordingly, no differences ($P > 0.05$) in basal ACC levels, ACC phosphorylation/inactivation state as well as *Ppara,* CPT1A and FAS were observed in the obese group compared with lean rats (Fig. 3B–C). Interestingly, animals undergoing sleeve gastrectomy showed higher ($P < 0.05$) P-AMPK/AMPK and P-ACC/ACC ratios compared to the other interventional groups, as well as a marked upregulation ($P < 0.05$) of *Ppara* and *Cpt1a* expression, whereas CPT1A tended to increase (Fig. 3E–F).

The ability of acylated and desacyl ghrelin to modulate mitochondrial FFA β-oxidation was also tested in rat hepatocytes. Both isoforms enhanced ($P < 0.05$) AMPK and ACC phosphorylation rates (Fig. 4C and F), without changing FAS and *Tfam* expression (Fig. 4A–F). Furthermore, the physiological concentration of acylated ghrelin significantly increased ($P < 0.05$) *Ppara* and *Cpt1a* transcripts (Fig. 4A), whereas the protein expression of CPT1A showed a similar trend only after acylated ghrelin stimulation, but differences did not reach statistical significance (Fig. 4C).

**Acylated ghrelin, and to a lesser extent desacyl ghrelin, activated hepatic autophagy.** The role of autophagy, featured by an increased LC3B II/I ratio associated to a decreased p62/SQSTM1 protein content[30], on the improvement of NAFLD after sleeve gastrectomy was next analysed. Obese rats showed similar hepatic expression of the autophagy-related genes *Atg5* and *Atg7* as well as in the LC3B-II/I ratio and the p62 protein level than lean rats (Fig. 5A–C). By contrast, sleeve gastrectomy was associated with an increase in *Atg5* and *Atg7* mRNA (Fig. 5D) and LC3B-II/I ratio together with a down-regulation of p62 ($P < 0.05$) (Fig. 5E–F). Interestingly, the acylated/desacyl ghrelin ratio was positively correlated with hepatic transcript levels of *Atg5* ($r = 0.22$, $P < 0.05$). Thus, we next determined whether acylated and desacyl ghrelin directly affect autophagy in rat hepatocytes. The stimulation of hepatic cells with acylated ghrelin upregulated ($P < 0.05$) the expression of ATGs and LC3B-II/I ratio (Fig. 5G–H), while p62 levels were markedly diminished (Fig. 5I). However, desacyl ghrelin only modified the expression of p62 ($P < 0.01$) (Fig. 5L).

## Discussion

Obesity is associated with an increased risk of NAFLD[1,2] and surgically-induced weight loss improves serum transaminases and hepatic function[31–34]. In line with these observations, our data provide evidence that sleeve gastrectomy ameliorates hepatic function, as evidenced by an improved profile of AST and ALT, and hepatosteatosis, through the downregulation of lipogenic factors *Pparg, Srebf1, Mogat2* and *Dgat1*. However, the molecular mechanisms underlying this amelioration remain undefined. Ghrelin has been recently proposed as a potential link between obesity and NAFLD[35]. In spite of its orexigenic and adipogenic properties, circulating total ghrelin concentrations are paradoxically decreased in obesity[36]. Our findings show that obese rats exhibited lower serum desacyl ghrelin levels without changes in acylated ghrelin and acylated/desacyl ghrelin ratio, which is in agreement with previous reports[20,37–39]. Interestingly, obese individuals with low ghrelin levels are more prone to weight regain after following a hypocaloric diet intervention[40], suggesting an impaired central and/or peripheral ghrelin signalling that might explain the high-fat feeding in these subjects. One limitation of our study is that we only measured fasting ghrelin concentrations, and changes in post-feeding ghrelin levels are also important to understand their overall role in the regulation of appetite and metabolic flexibility. As expected, sleeve gastrectomy reduced desacyl ghrelin levels, due to the resection of the gastric fundus, the major production site of the hormone[15]. By contrast, plasma acylated ghrelin remained unchanged after bariatric surgery, which is in accordance with other authors[26,41], and the acylated/desacyl ghrelin ratio increased, suggesting an enhanced post-transcriptional modification in order to maintain the circulating levels of the acylated hormone. In a previous work of our group, we found that both acylated and desacyl ghrelin stimulated intracellular lipid accumulation in human differentiated omental adipocytes through the upregulation of PPARγ and SREBP-1c and other fat-storage related molecules[20]. Accordingly, we herein show that both ghrelin isoforms also increase intracellular TG content in rat hepatocytes by increasing the transcript levels of the lipogenic factors *Mogat2* and *Dgat1*. Since desacyl ghrelin represents ~90% of total ghrelin[20,42], the amelioration of the hepatic function after sleeve gastrectomy might be partially due to the decrease of the desacylated hormone after the removal of the gastric fundus.

Sleeve gastrectomy was associated with an improvement in insulin sensitivity, as evidenced by lower insulinemia and HOMA, as well as lower glycemia, which is in accordance with previous results[34]. Opposite effects of acylated and desacyl ghrelin on insulin sensitivity have been reported. Although this might seem paradoxical, tight homeostatic control in some physiological processes is achieved by fine-tuning hormonal actions with opposite effects of the diverse isoforms[43]. Thus, exogenous desacyl ghrelin administration acts as a potent insulin secretagogue, whereas acylated ghrelin decreases glucose-induced insulin release and increases glucose levels in both humans and rodents[44,45]. In line with these observations, genetic, immunological, and pharmacological blockade of ghrelin signalling enhances glucose-stimulated insulin secretion and improves peripheral insulin sensitivity[46]. Thus, it seems plausible that ghrelin changes after sleeve gastrectomy also contribute, at least in part, to the observed improvement in insulin sensitivity after sleeve gastrectomy.

Obesity is associated with an increased release of FFA from adipocytes due to increased lipolysis[7,47]. Circulating FFA are taken up by the liver and metabolized by two main pathways: i) the mitochondrial β-oxidation to generate ATP; and ii) esterification to produce TG, which can be either incorporated into very-low density lipoprotein (VLDL) particles or stored within the hepatocytes[48]. AMPK coordinates the changes in the activity of enzymes of hepatic lipid metabolism through the regulation of the partitioning of FFA both in oxidative and biosynthetic pathways with defects in this pathway leading to the development of NAFLD[49,50]. In the present study, lack of changes in the basal AMPK and ACC expression and activity as well as in the mitochondrial copy number in obese rats might reflect an impaired AMPK transduction signalling and dysfunction in

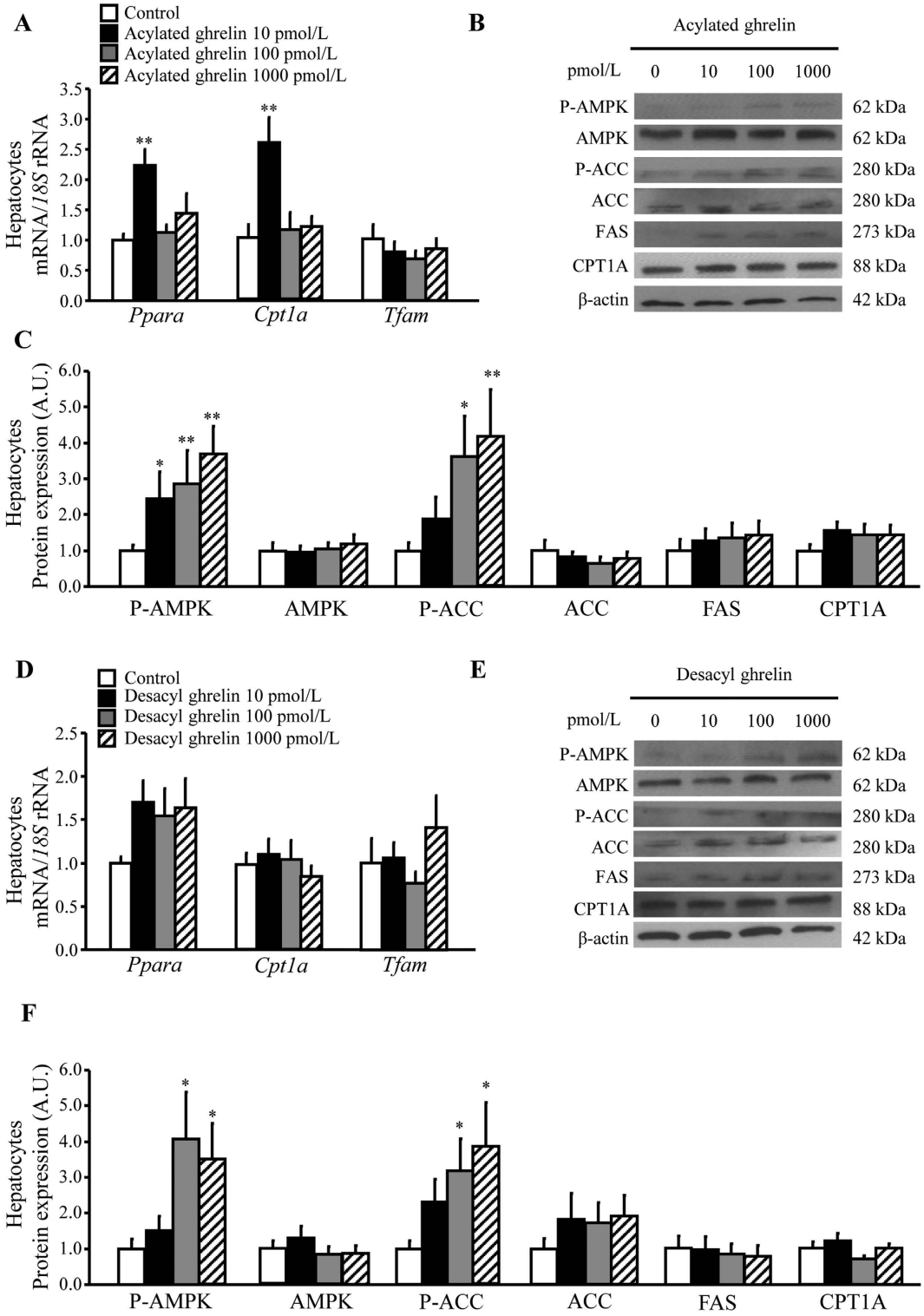


**Figure 4. Effect of acylated and desacyl ghrelin on mitochondrial biogenesis and FFA β-oxidation.** Bar graphs show the effect of acylated (**A**) and desacyl (**D**) ghrelin on the expression of molecules involved in mitochondrial biogenesis (*Tfam*) and FFA β-oxidation (*Ppara* and *Cpt1a*). Representative cropped blots and Western-blot analysis showing impact of acylated (**B**,**C**) and desacyl (**E**,**F**) ghrelin on P-AMPK/AMPK and P-ACC/ACC ratios as well as the basal expression of AMPK, ACC, FAS and CPT1A enzymes in primary cultures of rat hepatocytes. The gene and protein expression in unstimulated hepatocytes was assumed to be 1. $^{*}P < 0.05$; $^{**}P < 0.01$ *vs* unstimulated hepatocytes.

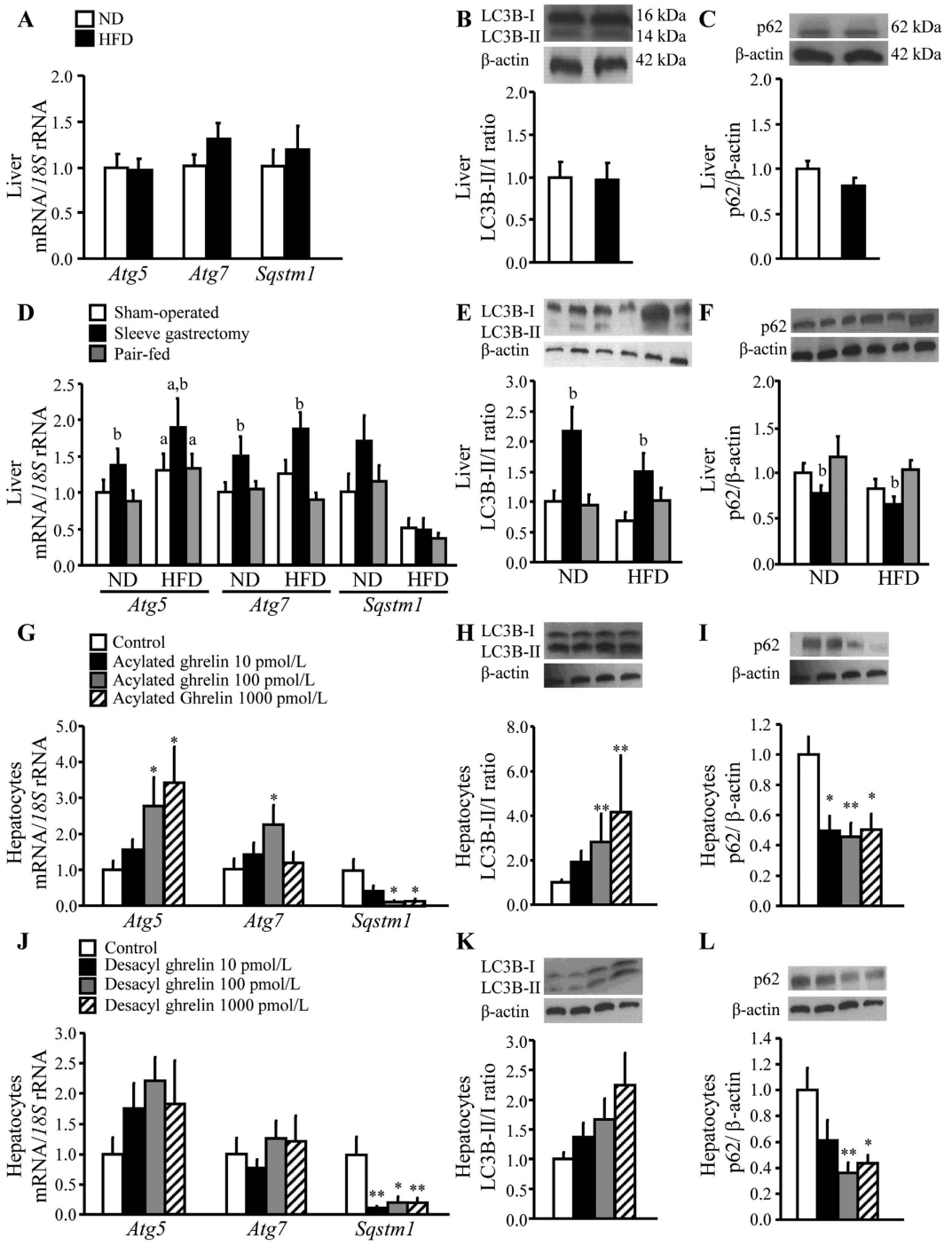


**Figure 5. Impact of acylated and desacyl ghrelin on the activation of autophagy after sleeve gastrectomy.** Effect of obesity and sleeve gastrectomy on the expression of *Atg5, Atg7* and *Sqstm1* genes (**A**,**D**), autophagosome formation as evidenced by the LC3B-II/I ratio (**B**,**E**) as well as autophagy inhibition determined by p62 accumulation (**C**,**F**) in liver samples of the experimental groups. Representative cropped blots are shown at the top of the figures. Effect of acylated (**G**,**H**,**I**) and desacyl (**J**,**K**,**L**) ghrelin on key autophagy factors in rat hepatocyte cultures. The gene expression in lean rats, in the sham-operated groups fed a normal diet and in unstimulated hepatocytes was assumed to be 1. $^{a}P < 0.05$ effect of diet; $^{b}P < 0.05$ effect of surgery. $^{*}P < 0.05$; $^{**}P < 0.01$ *vs* unstimulated hepatocytes.

mitochondrial biogenesis in the rat steatotic liver, which is in accordance with previous studies of our group[51] and others[52,53]. Interestingly, a notable increase in hepatic AMPK and ACC phosphorylation was found after sleeve gastrectomy, which is in agreement with other studies showing similar changes in AMPK and ACC activation

after bariatric surgery[54]. Accordingly, an upregulation of hepatic *Cpt1a* and its upstream molecule *Ppara* as well as an increase in mitochondrial content was observed after sleeve gastrectomy, suggesting an increased flux of FFA towards mitochondrial β-oxidation and higher mitochondrial copy number rather than inducing *de novo* TG synthesis. Interestingly, ghrelin triggers AMPK signalling in rat ventricular cardiomyocytes, myoblasts, hypothalamic neurons and hepatocytes[18,55–57]. Analogously, we found that acylated and desacyl ghrelin promoted AMPK and ACC activation in primary rat hepatocytes, suggesting that this hormone may be involved in the molecular mechanisms whereby sleeve gastrectomy improves hepatic mitochondrial function. In addition, acylated ghrelin also upregulates *Ppara* and *Cpt1a* expression, while the mitochondrial content was not affected. This observation leads to the notion that acylated ghrelin should be considered an important effector improving mitochondrial β-oxidation efficiency, whereas the beneficial effects on mitochondrial biogenesis after the surgery are not mediated by this hormone.

Autophagy plays an important role in the regulation of hepatic lipid metabolism. *In vitro* and *in vivo* studies in murine hepatocytes and hepatic tissue have demonstrated that autophagy mediates the breakdown of lipid stores and that an inhibition of autophagy increases TG storage in lipid droplets leading to the development of a fatty liver[8,58]. The inhibition of autophagy sensitizes hepatocytes to palmitic acid-induced apoptosis, suggesting a pro-survival function of autophagy against lipotoxicity[59]. In this sense, decreased levels of autophagy have been found in the liver of severely obese leptin-deficient *ob/ob* mice as well as in obese, diabetic OLETF rats, which might promote lipid accumulation and impaired hepatic function in these animal models[8,60]. However, our results showed no changes in the hepatic gene expression of the autophagy-related factors *Atg5* and *Atg7,* in the formation of autophagosomes evidenced by the LC3B-II/I conversion or in the inhibition of autophagy, expressed as p62 accumulation in obese rats. In this regard, hepatic autophagy is influenced by the degree of hepatic steatosis that might change the autophagosome formation during the ongoing NAFLD in adult obese rats. We herein report, for the first time, that sleeve gastrectomy is associated with an upregulation of the autophagy-related genes *Atg5* and *Atg7* and the LC3B-II/I ratio as well as with a decrease in the autophagy inhibition marker p62, suggesting that the induction of autophagy after this surgical procedure improves hepatic lipid clearance via lipophagy. Ghrelin isoforms are involved in the regulation of autophagy in several tissues, including the adipose tissue, small intestine, skeletal muscle and the heart[38,61–63]. Mao and colleagues reported that ghrelin induces autophagy in the liver via the activation of the AMPK signalling pathway[56], but the specific role of each isoform of the hormone remains unclear. Interestingly, *Mboat4*-knockout mice lacking the gene encoding GOAT, which catalyzes the acylation of ghrelin, show a marked reduction of hepatic autophagy during fasting, suggesting an important role of acylated ghrelin in the regulation of autophagy in the liver during energy depletion[35]. In the present study, acylated ghrelin increased *Atg5, Atg7* and the LC3B-II/I ratio and reduced p62 accumulation, while desacyl ghrelin only decreased p62 expression in hepatocytes, suggesting that acylated ghrelin and, to a lesser extent, desacyl ghrelin stimulate hepatic autophagy. Taken together, our findings suggest that the increase in acylated ghrelin levels after sleeve gastrectomy is involved in the induction of liver autophagy.

In summary, we herein show that the beneficial effects of bariatric surgery on NAFLD are mediated via a decrease in lipogenesis as well as an increase in autophagy and mitochondrial β-oxidation. The decrease in desacyl ghrelin after sleeve gastrectomy contributes to the reduction of lipogenesis, whereas the increased acylated ghrelin levels activate AMPK-activated mitochondrial FFA β-oxidation and autophagy in obese rats. These results support the notion that both ghrelin isoforms constitute key elements involved in the improvement of NAFLD after bariatric surgery.

## Methods

**Experimental animals and study design.** Four-week-old male Wistar rats (n = 161) were fed *ad libitum* during 4 months with either a normal diet (ND) (n = 22) or a high-fat diet (HFD) (n = 139). Obese rats were randomized into weight-matched groups to be submitted either to the sleeve gastrectomy (n = 37) or a sham operation (n = 41). Anesthesia, sham surgery and sleeve gastrectomy were performed as earlier described[64]. Following the surgical interventions, a group of animals were fed *ad libitum* a HFD, while another group was switched to a ND. In order to discriminate the effects of a reduced food intake following the bariatric surgery, two groups of obese rats were pair-fed to the amount of food eaten by the animals undergoing the sleeve gastrectomy switched to either the ND (n = 17) or maintaining the HFD (n = 23). Four weeks after the surgical and dietary interventions, rats were killed by decapitation after an 8-h fast. The methods were carried out in accordance with the relevant guidelines and regulations. All experimental procedures were approved by the Ethical Committee for Animal Experimentation of the University of Navarra (049/10) and conformed to the European Guidelines for the Care and Use of Laboratory Animals (directive 2010/63/EU).

**Blood and tissue analysis.** Serum alanine aminotransferase (ALT), aspartate aminotransferase (AST), and intrahepatic TG were determined by enzymatic methods, as previously described[65]. Fasting acylated and desacyl ghrelin levels were also assessed using a rat/mouse EIA Kit (A05117 and A05118, Cayman Chemical, Ann Harbor, MI, USA).

**RNA isolation and real-time PCR.** RNA isolation and purification were performed as earlier described[66]. Transcript levels of *Atg5, Atg7, Cav1, Cd36, Cpt1a, Dgat1, Fasn*, *Ghrl, Mboat4, Mogat2, Ppara, Pparg, Sqstm1, Srebf1* and *Tfam* (Supplementary Table S1) were quantified by real-time PCR (7300 Real Time PCR System, Applied Biosystems, Foster City, CA, USA). All results were normalized for the expression of *18S* rRNA (Applied Biosystems), and relative quantification was calculated as fold expression over the calibrator sample[66].

**Western-blot studies.** Blots were incubated overnight at 4 °C with rabbit polyclonal anti-ACC, rabbit polyclonal anti-phospho-ACC (Ser79), rabbit polyclonal anti-AMPKα, rabbit monoclonal anti-phospho-AMPKα

(Thr172), rabbit monoclonal anti-CPT1A, rabbit polyclonal anti-FAS, rabbit polyclonal anti-LC3B (Cell Signaling Technology, Inc., Danvers, MA, USA), rabbit polyclonal anti-p62 (Sigma St. Louis, MO, USA) antibodies or murine monoclonal anti-β-actin (Sigma). The antigen-antibody complexes were visualized using horseradish peroxidase (HRP)-conjugated secondary antibodies and the ECL Plus detection system (Amersham Biosciences, Buckinghamshire, UK).

**Immunohistochemistry of adipophilin.** The immunodetection of the lipid droplet-marker adipophilin in liver sections was performed by the indirect immunoperoxidase method[65], using a mouse monoclonal anti-adipophilin (Acris, Hiddenhausen, Germany) antibody. A semi-quantitative evaluation of steatosis in adipophilin-stained liver histological sections was performed. Hepatic steatosis was scored according to the staining of adipophilin by three blinded expert observers as: (0) none; (1) mild; (2) moderate; or (3) severe steatosis.

**DNA extraction and analysis of mitochondrial DNA amount.** The amount of mitochondrial DNA (mtDNA), extracted and purified using DNeasy Blood and Tissue Kit (Qiagen, Barcelona, Spain), was determined by real-time PCR of the mitochondrial cytochrome B (*Cytb*) gene normalized to the nuclear β-actin (*Actb*) gene (Supplementary Table S1), as previously described[67]. The real-time PCR was performed with 25 ng of total DNA using the TaqMan® Universal PCR Master Mix (Applied Biosystems), according to the manufacturer's instructions.

**Cell cultures.** Primary rat hepatocytes were purchased from Tebu-Bio (Barcelona, Spain) and cultured in a collagen sandwich configuration[68]. Rat hepatocytes were seeded into 6-well plates ($3 \times 10^5$ cells/well) and grown in Complete Growth Medium [DMEM/F-12 medium (Invitrogen) supplemented with 10% fetal bovine serum (FBS), 5 μg/mL insulin, 5 μg/mL transferrin, 5 ng/mL selenium (Invitrogen, Paisley, UK), 40 ng/mL dexamethasone (Sigma), 20 ng/mL epidermal growth factor (Sigma) and antibiotic-antimycotic] for 24 h. Then, cells were serum-starved for 24 h and stimulated with increasing concentrations (10, 100, 1000 pmol/L) of acylated and desacyl ghrelin, (Tocris, Ellisville, MO, USA) for 24 h. These physiological and supraphysiological concentrations of ghrelin isoforms to carry out the experiments were chosen on the basis of previous studies performed in our laboratory[20,38].

**Statistical analysis.** Data are expressed as the mean ± SEM. Statistical differences between mean values were analyzed using Student's *t* test, two-way ANOVA (diet × surgery), one-way ANOVA followed by Tukey's or Dunnett's *post-hoc* tests or the non-parametric Kruskal-Wallis test followed by *U* Mann-Whitney's pairwise comparisons, where appropriate. Pearson's correlation coefficients (*r*) were used to analyze the association between variables.

For more detailed Methods see Supplementary information.

## References


1. Chalasani, N. *et al.* The diagnosis and management of non-alcoholic fatty liver disease: practice Guideline by the American Association for the Study of Liver Diseases, American College of Gastroenterology, and the American Gastroenterological Association. *Hepatology*. **55,** 2005–2023 (2012).
2. European Association for the Study of the Liver (EASL), European Association for the Study of Diabetes (EASD) & European Association for the Study of Obesity (EASO). EASL-EASD-EASO Clinical Practice Guidelines for the management of non-alcoholic fatty liver disease. *J Hepatol*. **64,** 1388–1402 (2016).
3. Utzschneider, K. M. & Kahn, S. E. Review: The role of insulin resistance in nonalcoholic fatty liver disease. *J Clin Endocrinol Metab*. **91,** 4753–4761 (2006).
4. Rinella, M. E. Nonalcoholic fatty liver disease: a systematic review. *Jama*. **313,** 2263–2273 (2015).
5. Boza, C. *et al.* Predictors of nonalcoholic steatohepatitis (NASH) in obese patients undergoing gastric bypass. *Obes Surg*. **15,** 1148–1153 (2005).
6. Machado, M., Marques-Vidal, P. & Cortez-Pinto, H. Hepatic histology in obese patients undergoing bariatric surgery. *J Hepatol*. **45,** 600–606 (2006).
7. Zhang, J. *et al.* Association between serum free fatty acid levels and nonalcoholic fatty liver disease: a cross-sectional study. *Sci Rep*. **4,** 5832 (2014).
8. Yang, L., Li, P., Fu, S., Calay, E. S. & Hotamisligil, G. S. Defective hepatic autophagy in obesity promotes ER stress and causes insulin resistance. *Cell Metab*. **11,** 467–478 (2010).
9. Frühbeck, G. Bariatric and metabolic surgery: a shift in eligibility and success criteria. *Nat Rev Endocrinol*. **11,** 465–477 (2015).
10. Lassailly, G., Caiazzo, R., Pattou, F. & Mathurin, P. Bariatric surgery for curing NASH in the morbidly obese? *J Hepatol*. **58,** 1249–1251 (2013).
11. Taitano, A. A. *et al.* Bariatric surgery improves histological features of nonalcoholic fatty liver disease and liver fibrosis. *J Gastrointest Surg*. **19,** 429–436, discussion 436–427 (2015).
12. Mathurin, P. *et al.* Prospective study of the long-term effects of bariatric surgery on liver injury in patients without advanced disease. *Gastroenterology*. **137,** 532–540 (2009).
13. Zhang, S. R. & Fan, X. M. Ghrelin-ghrelin *O*-acyltransferase system in the pathogenesis of nonalcoholic fatty liver disease. *World J Gastroenterol*. **21,** 3214–3222 (2015).
14. Hosoda, H., Kojima, M., Matsuo, H. & Kangawa, K. Ghrelin and des-acyl ghrelin: two major forms of rat ghrelin peptide in gastrointestinal tissue. *Biochem Biophys Res Commun*. **279,** 909–913 (2000).
15. Frühbeck, G., Díez Caballero, A. & Gil, M. J. Fundus functionality and ghrelin concentrations after bariatric surgery. *N Engl J Med*. **350,** 308–309 (2004).
16. Rodríguez, A. Novel molecular aspects of ghrelin and leptin in the control of adipobiology and the cardiovascular system. *Obes Facts*. **7,** 82–95 (2014).
17. Chen, H. Y. *et al.* Orexigenic action of peripheral ghrelin is mediated by neuropeptide Y and agouti-related protein. *Endocrinology*. **145,** 2607–2612 (2004).
18. López, M. *et al.* Hypothalamic fatty acid metabolism mediates the orexigenic action of ghrelin. *Cell Metab*. **7,** 389–399 (2008).
19. Gurriarán-Rodríguez, U. *et al.* Preproghrelin expression is a key target for insulin action on adipogenesis. *J Endocrinol*. **210,** R1–7 (2011).

20. Rodríguez, A. *et al.* Acylated and desacyl ghrelin stimulate lipid accumulation in human visceral adipocytes. *Int J Obes*. **33,** 541–552 (2009).
21. Sangiao-Alvarellos, S. *et al.* Central ghrelin regulates peripheral lipid metabolism in a growth hormone-independent fashion. *Endocrinology*. **150,** 4562–4574 (2009).
22. Porteiro, B. *et al.* Ghrelin requires p53 to stimulate lipid storage in fat and liver. *Endocrinology*. **154,** 3671–3679 (2013).
23. Gauna, C. *et al.* Ghrelin stimulates, whereas des-octanoyl ghrelin inhibits, glucose output by primary hepatocytes. *J Clin Endocrinol Metab*. **90,** 1055–1060 (2005).
24. Estep, M. *et al.* Association of obestatin, ghrelin, and inflammatory cytokines in obese patients with non-alcoholic fatty liver disease. *Obes Surg*. **21,** 1750–1757 (2011).
25. Mykhalchyshyn, G., Kobyliak, N. & Bodnar, P. Diagnostic accuracy of acyl-ghrelin and it association with non-alcoholic fatty liver disease in type 2 diabetic patients. *J Diabetes Metab Disord*. **14,** 44 (2015).
26. Malin, S. K. *et al.* Improved acylated ghrelin suppression at 2 years in obese patients with type 2 diabetes: effects of bariatric surgery vs standard medical therapy. *Int J Obes*. **38,** 364–370 (2014).
27. Postic, C. & Girard, J. Contribution of de novo fatty acid synthesis to hepatic steatosis and insulin resistance: lessons from genetically engineered mice. *J Clin Invest*. **118,** 829–838 (2008).
28. Long, Y. C. & Zierath, J. R. AMP-activated protein kinase signaling in metabolic regulation. *J Clin Invest*. **116,** 1776–1783 (2006).
29. Rakhshandehroo, M., Hooiveld, G., Muller, M. & Kersten, S. Comparative analysis of gene regulation by the transcription factor PPARalpha between mouse and human. *PLoS One*. **4,** e6796 (2009).
30. Jansen, H. J. *et al.* Autophagy activity is up-regulated in adipose tissue of obese individuals and modulates proinflammatory cytokine expression. *Endocrinology*. **153,** 5866–5874 (2012).
31. Wang, Y. & Liu, J. Sleeve gastrectomy relieves steatohepatitis in high-fat-diet-induced obese rats. *Obes Surg*. **19,** 921–925 (2009).
32. Johansson, H. E., Haenni, A. & Zethelius, B. Platelet counts and liver enzymes after bariatric surgery. *J Obes*. **2013,** 567984 (2013).
33. Myronovych, A. *et al.* Vertical sleeve gastrectomy reduces hepatic steatosis while increasing serum bile acids in a weight-loss-independent manner. *Obesity*. **22,** 390–400 (2014).
34. Méndez-Giménez, L. *et al.* Sleeve gastrectomy reduces hepatic steatosis by improving the coordinated regulation of aquaglyceroporins in adipose tissue and liver in obese rats. *Obes Surg*. **25,** 1723–1734 (2015).
35. Zhang, Y., Fang, F., Goldstein, J. L., Brown, M. S. & Zhao, T. J. Reduced autophagy in livers of fasted, fat-depleted, ghrelin-deficient mice: reversal by growth hormone. *Proc Natl Acad Sci USA* **112,** 1226–1231 (2015).
36. Tschöp, M. *et al.* Circulating ghrelin levels are decreased in human obesity. *Diabetes*. **50,** 707–709 (2001).
37. Rodríguez, A. *et al.* Association of plasma acylated ghrelin with blood pressure and left ventricular mass in patients with metabolic syndrome. *J Hypertens*. **28,** 560–567 (2010).
38. Rodríguez, A. *et al.* The ghrelin *O*-acyltransferase-ghrelin system reduces TNF-alpha-induced apoptosis and autophagy in human visceral adipocytes. *Diabetologia*. **55,** 3038–3050 (2012).
39. Barazzoni, R. *et al.* Gastric bypass does not normalize obesity-related changes in ghrelin profile and leads to higher acylated ghrelin fraction. *Obesity*. **21,** 718–722 (2013).
40. Crujeiras, A. B. *et al.* Weight regain after a diet-induced loss is predicted by higher baseline leptin and lower ghrelin plasma levels. *J Clin Endocrinol Metab*. **95,** 5037–5044 (2010).
41. Patrikakos, P. *et al.* Long-term plasma ghrelin and leptin modulation after sleeve gastrectomy in Wistar rats in comparison with gastric tissue ghrelin expression. *Obes Surg*. **21,** 1432–1437 (2011).
42. Pacifico, L. *et al.* Acylated and nonacylated ghrelin levels and their associations with insulin resistance in obese and normal weight children with metabolic syndrome. *Eur J Endocrinol*. **161,** 861–870 (2009).
43. Frühbeck, G. & Gómez-Ambrosi, J. Control of body weight: a physiologic and transgenic perspective. *Diabetologia*. **46,** 143–172 (2003).
44. Gauna, C. *et al.* Administration of acylated ghrelin reduces insulin sensitivity, whereas the combination of acylated plus unacylated ghrelin strongly improves insulin sensitivity. *J Clin Endocrinol Metab*. **89,** 5035–5042 (2004).
45. Gauna, C. *et al.* Unacylated ghrelin acts as a potent insulin secretagogue in glucose-stimulated conditions. *Am J Physiol Endocrinol Metab*. **293,** E697–E704 (2007).
46. Alamri, B. N., Shin, K., Chappe, V. & Anini, Y. The role of ghrelin in the regulation of glucose homeostasis. *Horm Mol Biol Clin Investig*. **26,** 3–11 (2016).
47. Frühbeck, G., Méndez-Giménez, L., Fernández-Formoso, J. A., Fernández, S. & Rodríguez, A. Regulation of adipocyte lipolysis. *Nutr Res Rev*. **27,** 63–93 (2014).
48. Browning, J. D. & Horton, J. D. Molecular mediators of hepatic steatosis and liver injury. *J Clin Invest*. **114,** 147–152 (2004).
49. Kahn, B. B., Alquier, T., Carling, D. & Hardie, D. G. AMP-activated protein kinase: ancient energy gauge provides clues to modern understanding of metabolism. *Cell Metab*. **1,** 15–25 (2005).
50. Yin, X., Li, Y., Xu, G., An, W. & Zhang, W. Ghrelin fluctuation, what determines its production? *Acta Biochim Biophys Sin (Shanghai)*. **41,** 188–197 (2009).
51. Rodríguez, A. *et al.* Impaired adiponectin-AMPK signalling in insulin-sensitive tissues of hypertensive rats. *Life Sci*. **83,** 540–549 (2008).
52. Rector, R. S. *et al.* Daily exercise increases hepatic fatty acid oxidation and prevents steatosis in Otsuka Long-Evans Tokushima Fatty rats. *Am J Physiol Gastrointest Liver Physiol*. **294,** G619–626 (2008).
53. Finocchietto, P. V. *et al.* Defective leptin-AMP-dependent kinase pathway induces nitric oxide release and contributes to mitochondrial dysfunction and obesity in ob/ob mice. *Antioxid Redox Signal*. **15,** 2395–2406 (2011).
54. Peng, Y. *et al.* Does LKB1 mediate activation of hepatic AMP-protein kinase (AMPK) and sirtuin1 (SIRT1) after Roux-en-Y gastric bypass in obese rats? *J Gastrointest Surg*. **14,** 221–228 (2010).
55. Han, L. *et al.* Effects of ghrelin on triglyceride accumulation and glucose uptake in primary cultured rat myoblasts under palmitic acid-induced high fat conditions. *Int J Endocrinol*. **2015,** 635863 (2015).
56. Mao, Y. *et al.* Ghrelin attenuated lipotoxicity via autophagy induction and nuclear factor-kB inhibition. *Cell Physiol Biochem*. **37,** 563–576 (2015).
57. Yuan, M. J. *et al.* Ghrelin protects infarcted myocardium by induction of autophagy and AMP-activated protein kinase pathway. *Biochem Biophys Res Commun*. (2016).
58. Singh, R. *et al.* Autophagy regulates lipid metabolism. *Nature*. **458,** 1131–1135 (2009).
59. Tan, S. H. *et al.* Induction of autophagy by palmitic acid via protein kinase C-mediated signaling pathway independent of mTOR (mammalian target of rapamycin). *J Biol Chem*. **287,** 14364–14376 (2012).
60. Chang, E. *et al.* Ezetimibe improves hepatic steatosis in relation to autophagy in obese and diabetic rats. *World J Gastroenterol*. **21,** 7754–7763 (2015).
61. Slupecka, M., Wolinski, J. & Pierzynowski, S. G. The effects of enteral ghrelin administration on the remodeling of the small intestinal mucosa in neonatal piglets. *Regul Pept*. **174,** 38–45 (2012).
62. Yu, A. P. *et al.* Acylated and unacylated ghrelin inhibit doxorubicin-induced apoptosis in skeletal muscle. *Acta Physiol*. **211,** 201–213 (2014).
63. Pei, X. M. *et al.* Protective effects of desacyl ghrelin on diabetic cardiomyopathy. *Acta Diabetol*. **52,** 293–306 (2015).

64. Valentí, V. *et al.* Sleeve gastrectomy induces weight loss in diet-induced obese rats even if high-fat feeding is continued. *Obes Surg.* **21,** 1438–1443 (2011).
65. Rodríguez, A. *et al.* Reduced hepatic aquaporin-9 and glycerol permeability are related to insulin resistance in non-alcoholic fatty liver disease. *Int J Obes.* **38,** 1213–1220 (2014).
66. Catalán, V. *et al.* Validation of endogenous control genes in human adipose tissue: relevance to obesity and obesity-associated type 2 diabetes mellitus. *Horm Metab Res.* **39,** 495–500 (2007).
67. Heinonen, S. *et al.* Impaired mitochondrial biogenesis in adipose tissue in acquired obesity. *Diabetes.* **64,** 3135–3145 (2015).
68. Shulman, M. & Nahmias, Y. Long-term culture and coculture of primary rat and human hepatocytes. *Methods Mol Biol.* **945,** 287–302 (2013).

## Acknowledgements

The authors gratefully acknowledge Beatriz Ramírez (Metabolic Research Laboratory, Clínica Universidad de Navarra) for her technical assistance. SE was recipient of a predoctoral grant from the Asociación de Amigos of the University of Navarra. This work was supported by Fondo de Investigación Sanitaria-FEDER (PI12/00515 to GF and PI13/01430 to AR) from the Spanish Instituto de Salud Carlos III, the Department of Health of the Gobierno de Navarra (61/2014) to AR as well as by the Plan de Investigación de la Universidad de Navarra (PIUNA 2011-14) to AR.

## Author Contributions

A.R. and G.F. designed the study. S.E., L.M.-G., S.B., R.M., V.V., V.C., J.G.-A., G.F. and A.R. researched the data. S.E., L.M.-G., S.B., V.C., J.G.-A., G.F. and A.R. contributed to the discussion. S.E., G.F. and A.R. wrote the manuscript. All authors reviewed/edited the manuscript and approved the final version. A.R. and G.F. are the guarantors of this work, had full access to all the data and take full responsibility for the integrity of data and the accuracy of data analysis.

## Additional Information

**Supplementary information** accompanies this paper at http://www.nature.com/srep

**Competing financial interests:** The authors declare no competing financial interests.

**How to cite this article**: Ezquerro, S. *et al.* Acylated and desacyl ghrelin are associated with hepatic lipogenesis, β-oxidation and autophagy: role in NAFLD amelioration after sleeve gastrectomy in obese rats. *Sci. Rep.* **6**, 39942; doi: 10.1038/srep39942 (2016).

**Publisher's note:** Springer Nature remains neutral with regard to jurisdictional claims in published maps and institutional affiliations.

# Acylated and desacyl ghrelin are associated with hepatic lipogenesis, β-oxidation and autophagy: role in NAFLD amelioration after sleeve gastrectomy in obese rats

Silvia Ezquerro[1,5,6], Leire Méndez-Giménez[1,5,6], Sara Becerril[1,5,6], Rafael Moncada[2,5,6], Víctor Valentí[3,5,6], Victoria Catalán[1,5,6], Javier Gómez-Ambrosi[1,5,6], Gema Frühbeck[1,4,5,6], Amaia Rodríguez[1,5,6,*]

[1]Metabolic Research Laboratory, [2]Department of Anesthesia, [3]Department of Surgery, and [4]Department of Endocrinology & Nutrition, Clínica Universidad de Navarra, Pamplona, Spain; [5]CIBER Fisiopatología de la Obesidad y Nutrición (CIBEROBN), Instituto de Salud Carlos III, Madrid, Spain; [6]Obesity & Adipobiology Group, Instituto de Investigación Sanitario de Navarra (IdiSNA), Pamplona, Spain.

**Word count:** Abstract (200); Main text (3,355); Table (2); Figures (5); Supplemental data (2); References (69).

***Corresponding author:**

Amaia Rodríguez, PhD
Metabolic Research Laboratory
Clínica Universidad de Navarra
Irunlarrea 1
31008 Pamplona (Spain)
Phone: +34 948 42 56 00 (ext. 3357)
e-mail: arodmur@unav.es

## Supplementary methods

**Experimental animals and study design.** Four-week-old male Wistar rats (n=161) (breeding house of the University of Navarra) were housed in individual cages in a room with controlled temperature (22±2 ºC), ventilation (at least 15 complete air changes/h), 12:12-h light-dark cycle (lights on at 8:00 am) and relative humidity (50± 10%) under pathogen-free conditions. Animals were fed *ad libitum* during 4 months with either a normal diet (ND) (n=22) (12.1 kJ: 4% fat, 82% carbohydrate and 14% protein, diet 2014S, Harlan, Teklad Global Diets, Harlan Laboratories Inc., Barcelona, Spain) or a high-fat diet (HFD) (n=139) (23.0 kJ/g: 59% fat, 27% carbohydrate and 14% protein, diet F3282; Bio-Serv, Frenchtown, NJ, USA). Body weight and food intake were registered weekly to monitor the progression of DIO rats that reached a mean body weight of 630±15 g after 4 months on the HFD.

Obese rats were randomized into weight-matched groups to be submitted either to the sleeve gastrectomy (n=37) or a sham operation (n=41). Anesthesia and sleeve gastrectomy were performed according to previously described methodology[1-3]. Briefly, for the sleeve gastrectomy a laparotomy incision was made in the abdominal wall and the stomach was isolated outside the abdominal cavity. Loose gastric connections to the spleen and liver were released along the greater curvature and the great omentum was ligated and divided down to the level of the pylorus. About 60-70% of the forestomach and glandular stomach was excised out using an automatic stapler (AutoSuture TA DST Series, Tyco Healthcare group LP, Norwalk, CT, USA) with a TA30V3L load, leaving a tubular gastric remnant in continuity with the esophagus upwards and the pylorus and duodenum downwards. The sham surgery comprised the same laparotomic incision as well as handling of the stomach except for the gastrectomy. Following the surgical interventions [sham operation (n=24) or sleeve gastrectomy (n=22)], a group of obese animals continued to be fed *ad libitum* a HFD, while another group of obese rats was switched to a ND *ad libitum* [sham operation (n=17) or sleeve gastrectomy (n=15)]. In order to discriminate the effects of a reduced food intake following the bariatric surgery, two groups of obese rats were pair-fed to the amount of food eaten by the animals undergoing the sleeve gastrectomy switched to either the ND or the HFD [pair-fed ND (n=17) or pair-fed HFD (n=23)]. Four weeks after the surgical and dietary interventions, rats were killed by decapitation after an 8-h fasting period. The liver, epididymal

(EWAT), perirenal (PRWAT) and subcutaneous (SCWAT) white adipose tissues were carefully dissected out, weighed, frozen in liquid nitrogen and stored at -80 ºC until processed for the study. A small portion of the tissue was fixed in 4% paraformaldehyde for histological analyses. Blood samples were immediately collected and sera were obtained by cold centrifugation (4 ºC) at 700 *g* for 15 min. The percentage of total weight loss (%TWL) was calculated from the equation %TWL= (pre-interventional body weight- post-interventional body weight)/pre-interventional body weight x 100. All experimental procedures conformed to the European Guidelines for the care and use of Laboratory Animals (directive 2010/63/EU) and were approved by the Ethical Committee for Animal Experimentation of the University of Navarra (049/10).

**Blood and tissue analysis.** Serum glucose was determined by an automatic glucose sensor (Ascencia Elite, Bayer, Barcelona, Spain). Insulin was determined by ELISA (Crystal Chem, Inc., Chicago, IL, USA). Intra- and inter-assay coefficients of variation for measurements of insulin were 3.5%, for the former, and 5.4%, for the latter. Insulin resistance was calculated using the homeostasis model assessment (HOMA), calculated with the formula: fasting insulin (μU/mL) × fasting glucose (mmol/L)/22.5). Serum alanine aminotransferase (ALT), aspartate aminotransferase (AST), FFA and TG were measured by enzymatic methods using commercially available kits (Infinity$^{TM}$, Thermo Electron Corporation, Melbourne, Australia). Intrahepatic TG was determined by enzymatic methods, as previously described[4]. Fasting acylated and desacyl ghrelin levels were also assessed using a rat/mouse EIA Kit (A05117 and A05118**,** Cayman Chemical, Ann Harbor, MI, USA). Intra- and inter-assay coefficients of variation for measurements were 5.7% and 6.1%, respectively, for the former and 5.2% and 5.5 %, for the latter.

**RNA isolation and real-time PCR.** RNA isolation and purification were performed as earlier described[5]. Transcript levels of *Atg5, Atg7, Cav1, Cd36, Cpt1a, Dgat1, Fasn, Ghrl, Mboat4, Mogat2, Ppara, Pparg, Sqstm1, Srebf1* and *Tfam* were quantified by real-time PCR (7300 Real Time PCR System, Applied Biosystems, Foster City, CA, USA). Primers and probes (**Supplementary Table 1**) were designed using the software Primer Express 2.0 (Applied Biosystems) and acquired from Genosys (Sigma. St. Louis, MO, USA). Primers or TaqMan® probes encompassing fragments of the areas from the extremes of two exons were designed to ensure the detection of the corresponding

transcript avoiding genomic DNA amplification. The cDNA was amplified at the following conditions: 95 ºC for 10 min, followed by 45 cycles of 15 s at 95 ºC and 1 min at 59 ºC, using the TaqMan® Universal PCR Master Mix (Applied Biosystems). The primer and probe concentrations were 300 and 200 nmol/L, respectively. All results were normalized for the expression of *18S* rRNA (Applied Biosystems), and relative quantification was calculated as fold expression over the calibrator sample[5]. All samples were run in triplicate and the average values were calculated.

**Western-blot studies.** Tissues were harvested and homogenized in ice-cold lysis buffer (0.1% SDS, 1% Triton X-100, 5 mmol/L EDTA·$2H_2O$, 1 mol/L Tris-HCL, 150 mmol/L NaCl, 1% sodium deoxycholate, pH 7.40) complemented with a protease inhibitor cocktail (Complete™ Mini-EDTA free, Roche, Mannheim, Germany). Lysates were centrifuged at 12,000 *g* at 4 ºC for 15 min to remove nuclei and unruptured cells. Total protein concentrations were determined by the Bradford assay[6], using bovine serum albumin (BSA) (Sigma) as standard. Thirty micrograms of total protein of liver homogenates were diluted in loading buffer 4X (20% β-mercaptoethanol, 40 mmol/L dithiothreitol, 8% SDS, 40% glycerol, 0.016% bromophenol blue, 200 mmol/L Tris-HCl, pH 6.80) and heated for 10 min at 100 ºC. Samples were run out in Mini-PROTEAN® TGX™ precast gels (Bio-Rad Laboratories, Inc., Hercules, CA, USA), subsequently transferred to nitrocellulose membranes (Bio-Rad) and blocked in Tris-buffered saline (10 mmol/L Tris-HCl, 150 mmol/L NaCl, pH 8.00) with 0.05% Tween 20 (TBS-T) containing 5% non-fat dry milk for 1 h at room temperature (RT). Membranes were then incubated overnight at 4 ºC with rabbit polyclonal anti-ACC, rabbit polyclonal anti-phospho-ACC (Ser79), rabbit polyclonal anti-AMPKα, rabbit monoclonal anti-phospho-AMPKα (Thr172), rabbit monoclonal anti-CPT1A, rabbit polyclonal anti-FAS, rabbit polyclonal anti-LC3B (Cell Signaling Technology, Inc., Danvers, MA, USA), rabbit polyclonal anti-p62 (Sigma) antibodies (diluted 1:5,000 for ACC, phospho-ACC, FAS, LC3B and p62 and 1:2,000 for AMPK, phospho-AMPK and CPT1A in blocking solution) or murine monoclonal anti-β-actin (Sigma) (diluted 1:5,000 in blocking solution). The antigen-antibody complexes were visualized using horseradish peroxidase (HRP)-conjugated anti-rabbit or anti-mouse IgG antibodies (diluted 1:5,000 for ACC, phospho-ACC, FAS, LC3B, p62 and β-actin and 1:2,000 for AMPK, phospho-AMPK and CPT1A in blocking solution) and the enhanced

chemiluminescence ECL Plus detection system (Amersham Biosciences, Buckinghamshire, UK). The intensity of the bands was determined by densitometric analysis with the Gel Doc™ gel documentation system and the Quantity One 4.5.0 software (Bio-Rad) and normalized with β-actin density values.

**Immunohistochemistry of adipophilin.** The immunodetection of the specific marker of lipid accumulation adipophilin in histological sections of liver was performed by the indirect immunoperoxidase method, as previously described[4,7]. Sections of formalin-fixed paraffin-embedded liver (4 μm) were dewaxed in xylene, rehydrated in decreasing concentrations of ethanol and treated with 3% $H_2O_2$ (Sigma) in absolute methanol for 10 min at RT to quench endogenous peroxidase activity. Slides were blocked during 60 min with 1% goat serum (Sigma) diluted in Tris-buffer saline (TBS) (50 mmol/L Tris, 0.5 mol/L NaCl, pH 7.36) to prevent non-specific absorption. Sections were incubated overnight at 4 ºC with mouse monoclonal anti-adipophilin (Acris, Hiddenhausen, Germany) antibody diluted 1:200 in TBS. After washing three times with TBS (5 min each), slides were incubated with DAKO Real™ EnVision™ anti-rabbit/mouse (K5007; Dako, Golstrup, Denmark) for 1 h at RT. The peroxidase reaction was visualized using a 0.5 mg/mL diaminobenzidine (DAB)/0.03% $H_2O_2$ solution diluted in 50 mmol/L Tris-HCl, pH 7.36, and Harris hematoxylin solution (Sigma) as counterstaining. Negative control slides without primary antibody were included to assess non-specific staining. A semi-quantitative evaluation of steatosis in adipophilin-stained liver histological sections was performed. Hepatic steatosis was scored according to the staining of adipophilin by three blinded expert observers as: (0) none; (1) mild; (2) moderate; or (3) severe steatosis.

**DNA extraction and analysis of mtDNA amount**. The amount of mtDNA, extracted and purified using DNeasy Blood and Tissue Kit (Qiagen, Barcelona, Spain), was determined by real-time PCR of the mitochondrial cytochrome B (CYTB) gene normalized to the nuclear β-actin (ACTB) gene[8]. The RT-PCR was performed with 25 ng of total DNA using the TaqMan® Universal PCR Master Mix (Applied Biosystems), according to the manufacturer's instructions. The RT-PCR data were analyzed by the comparative "ΔΔCt method". The primer sequences are available in **Supplementary Table S1**.

**Cell cultures.** Non tumorigenic rat hepatocytes were purchased from Tebu-Bio (Barcelona, Spain). Cells were maintained in DMEMF-12 medium (Invitrogen, Paisley, UK) supplemented with 10% fetal bovine serum (FBS), 5 μg/mL insulin, 5 μg/mL transferrin, 5 ng/mL selenium (Invitrogen), 40 ng/mL dexamethasone (Sigma), 20 ng/mL epidermal growth factor (Sigma) and antibiotic-antimycotic (Complete Growth Medium). Rat hepatocytes were cultured in a collagen sandwich configuration as described by Shulman *et al*[9], were seeded into 6-well plates at $3x10^5$ cells/well and grown in Complete Growth Medium for 24h. Cells were serum starved for 24 h and then treated for 24 h with increasing concentrations (10, 100, 1000 pmol/L) of acylated ghrelin or desacyl ghrelin (Tocris, Ellisville, MO, USA) for 24 h. These physiological and supraphysiological concentrations of ghrelin isoforms to carry out the experiments were chosen on the basis of previous studies performed in our laboratory[10,11].

**Statistical analysis.** Data are expressed as the mean ± SEM. Statistical differences between mean values were analyzed using Student's *t* test, two-way ANOVA (diet x surgery), one-way ANOVA followed by Tukey's or Dunnett's *post-hoc* tests or the non-parametric Kruskal-Wallis test followed by *U* Mann-Whitney´s pairwise comparisons, where appropriate. Pearson's correlation coefficients (*r*) were used to analyze the association between variables. The statistical analyses were performed using the SPSS/Windows version 15.0 software (SPSS Inc., Chicago, IL, USA).

## References


1. Valentí, V. *et al.* Sleeve gastrectomy induces weight loss in diet-induced obese rats even if high-fat feeding is continued. *Obes Surg*. **21**, 1438-1443 (2011).
2. Rodríguez, A. *et al.* Sleeve gastrectomy reduces blood pressure in obese (*fa/fa*) Zucker rats. *Obes Surg*. **22**, 309-315 (2012).
3. Rodríguez, A. *et al.* Short-term effects of sleeve gastrectomy and caloric restriction on blood pressure in diet-induced obese rats. *Obes Surg*. **22**, 1481-1490 (2012).
4. Rodríguez, A. *et al.* Reduced hepatic aquaporin-9 and glycerol permeability are related to insulin resistance in non-alcoholic fatty liver disease. *Int J Obes*. **38**, 1213-1220 (2014).
5. Catalán, V. *et al.* Validation of endogenous control genes in human adipose tissue: relevance to obesity and obesity-associated type 2 diabetes mellitus. *Horm Metab Res*. **39**, 495-500 (2007).
6. Bradford, M. M. A rapid and sensitive method for the quantitation of microgram quantities of protein utilizing the principle of protein-dye binding. *Anal Biochem*. **72**, 248-254 (1976).

7. Rodríguez, A. *et al.* Insulin- and leptin-mediated control of aquaglyceroporins in human adipocytes and hepatocytes is mediated via the PI3K/Akt/mTOR signaling cascade. *J Clin Endocrinol Metab*. **96**, E586-597 (2011).
8. Heinonen, S. *et al.* Impaired mitochondrial biogenesis in adipose tissue in acquired obesity. *Diabetes*. **64**, 3135-3145 (2015).
9. Shulman, M. & Nahmias, Y. Long-term culture and coculture of primary rat and human hepatocytes. *Methods Mol Biol*. **945**, 287-302 (2013).
10. Rodríguez, A. *et al.* Acylated and desacyl ghrelin stimulate lipid accumulation in human visceral adipocytes. *Int J Obes.* **33**, 541-552 (2009).
11. Rodríguez, A. *et al.* The ghrelin *O*-acyltransferase-ghrelin system reduces TNF-alpha-induced apoptosis and autophagy in human visceral adipocytes. *Diabetologia*. **55**, 3038-3050 (2012).

**Supplementary Table S1. Sequences of primers and TaqMan® probes.**

| Gene (GenBank accession no.) | Oligonucleotide sequence (5'-3') | Nucleotides |
|---|---|---|
| *Actb* (NM_005111) | | |
| Forward | GGGAAATCGTGCGTGACATT | 2188-2207 |
| Reverse | GCTATGAGCTGCCTGACGGT | 2287-2306 |
| Taqman® probe | FAM-TGCCCTAGACTTCGAGCAAGAGATGGC-TAMRA | 2228-2254 |
| *Atg5* (NM_001014250.1) | | |
| Forward | CACACCCCTGAAATGGCATTAT | 449-470 |
| Reverse | TTCCAGAAAAGGACCTTCTGCA | 547-568 |
| Taqman® probe | FAM- TGCATCAAGCTCAGCT-TAMRA | 497-512 |
| *Atg7* (NM_001012097.1) | | |
| Forward | GGTCCGAGGATGGTGAACCT | 940-959 |
| Reverse | CTGAATCTCAAGCTGATGTGCT | 1006-1027 |
| Taqman® probe | FAM-ATGGACCCCAAAAGGC-TAMRA | 970-985 |
| *Cav1* (NM_031556.3) | | |
| Forward | ACGACGACGTGGTCAAGATTG | 334-354 |
| Reverse | TTGGTTTTACCGCTTGCTGTCT | 446-467 |
| Taqman® probe | FAM-TGCGGAACCAGAAGGGACACACAGTTT-TAMRA | 371-397 |
| *Cd36* (NM_031561.2) | | |
| Forward | GACATTTGCAGGTCCATCTATGC | 1041-1064 |
| Reverse | CAGAACCCAGACAACCACTGTTT | 1146-1168 |
| Taqman® probe | FAM-TTCTTCCAGCCAACGCCTTTGCCT-TAMRA | 1111-1137 |
| *Cpt1a* (NM_031559) | | |
| Forward | AACTTTGTGCAGGCCATGATG | 1942-1961 |
| Reverse | AGCTTGTGAGAAGCACCAGCA | 2007-2026 |
| Taqman® probe | FAM-ACCCCAAGTCAACGGCAGAGCAGA-TAMRA | 1964-1977 |
| *Cytb* (NC_001665.2) | | |
| Forward | GCCTTCCTACCATTCCTGCATA | 904-925 |
| Reverse | TTAACATGAATCGGAGGCCAA | 1001-1023 |
| Taqman® probe | FAM-CAAAACAACGCAGCTTAACATTCCGCC-TAMRA | 929-955 |
| *Dgat1* (NM_053437.1) | | |
| Forward | CGGTCCCCAACCATCTGATAT | 1048-1068 |
| Reverse | TTTCCACTCATGTCTCAATGCTGTGGCA | 1132-1152 |
| Taqman® probe | FAM-TTCCACTCATGTCTCAATGCTGTGGCA-TAMRA | 1091-2018 |
| *Fasn* (NM_017332.1) | | |
| Forward | AGAGCATTCTGGCCACATCCT | 4349-4369 |
| Reverse | TGTCTCCGAAAAGAGCCGG | 4435-4453 |
| Taqman® probe | FAM-CCCAGCCTGTGTGGCTAACAGCCAT-TAMRA | 4373-4397 |
| *Ghrl* (NM_021669.2) | | |
| Forward | AAGCCCAGCAGAGAAAGGAATC | 130-151 |

| | | |
|---|---|---|
| Reverse | TCAATGCTCCCTTCGATGTTG | 256-276 |
| Taqman® probe | FAM-AACTGCAGCCACGAGCTCTGGAAGG-TAMRA | 169-193 |
| *Ghsr* (NM_032075.3) | | |
| Forward | CAGAACCACAAGCAGACAGTGAA | 760-782 |
| Reverse | AGATACCTCTTTTCCAAGTCCTTCG | 841-865 |
| Taqman® probe | FAM-ATGCTTGCTGTGGTGGTGTTT-TAMRA | 784-804 |
| *Mboat4* (NM_001107317.2) | | |
| Forward | CACCTGGGTCTTCACTACAAGGA | 292-314 |
| Reverse | ACATTTCTGAAGGGAAGGTGGAG | 407-429 |
| Taqman® probe | FAM-TCCCCCTGTGAGGTTCTACATCAC-TAMRA | 333-356 |
| *Mogat2* (NM_001109436.2) | | |
| Forward | TCCCTGTCTCTTTGGTCAAGACA | 289-311 |
| Reverse | TTCTTAACCTGTGCACTGAAAGCA | 382-405 |
| Taqman® probe | FAM-CGGAACTACATCGCAGGCTTTCACCC-TAMRA | 330-355 |
| *Ppara* (NM_013196.1) | | |
| Forward | AAGGCCTCAGGATACCACTATGG | 699-721 |
| Reverse | CAGCTTCGATCACACTTGTCGTA | 783-805 |
| Taqman® probe | FAM-CTGCAAGGGCTTCTTTCGGCGAAC-TAMRA | 740-763 |
| *Pparg* (NM_013124) | | |
| Forward | CTGACCCAATGGTTGCTGATTAC | 257-279 |
| Reverse | CCTGTTGTAGAGTTGGGTTTTTTCA | 351-375 |
| Taqman® probe | FAM-TGAAGCTCCAAGAATACCAAAGTGCG-TAMRA | 290-315 |
| *Sqstm1* (NM_175843) | | |
| Forward | GCTCTCTAGACCCCTCACAGGAA | 1125-1147 |
| Reverse | CAGATGCTGTCCATGGGTTTCT | 1229-1250 |
| Taqman® probe | FAM-ACAGGGCTGAAGGAAGCTGCCCTGT-TAMRA | 1154-1178 |
| *Srebf1* (NM_001276707.1) | | |
| Forward | ATGCGGCTGTCGTCTACCAT | 2050-2069 |
| Reverse | AGTGTGCAGGAGATGCTATATCCAT | 2158-2182 |
| Taqman® probe | FAM-CATGCCATGGGCAAGTACACAGGAGG-TAMRA | 2085-2110 |
| *Tfam* (NM_031326.1) | | |
| Forward | ACACCCAGATGCAAAAGTTTCAG | 315-337 |
| Reverse | AAGCTGAGTGGAAGGTGTACAAAGA | 413-437 |
| Taqman® probe | FAM-AAAAATTGCAGCCATGTGGAGGGAGC-TAMRA | 348-373 |

*Actb*, β-actin; *Atg*, autophagy related; *Cav1*, caveolin 1; *Cd36*, CD36 molecule (thrombospondin receptor); *Cpt1a*, carnitine palmitoyl transferase 1a (liver); *Cytb*, cytochrome b; *Dgat1*, diacylglycerol *O*-acyltransferase 1; *Fasn*, fatty acid synthase; *Ghrl*, ghrelin; *Ghsr*, growth hormone secretagogue receptor; *Mboat4*, membrane bound *O*-acyltransferase domain containing 4; *Mogat2*, monoacylglycerol *O*-acyltransferase 2; *Ppara*, peroxisome proliferator-activator receptor α; *Pparg*, peroxisome proliferator-activator receptor γ; *Sqstm1*, sequestosome 1; *Srebf1*, sterol regulatory element binding factor 1c; *Tfam*, transcription factor A mitochondrial.

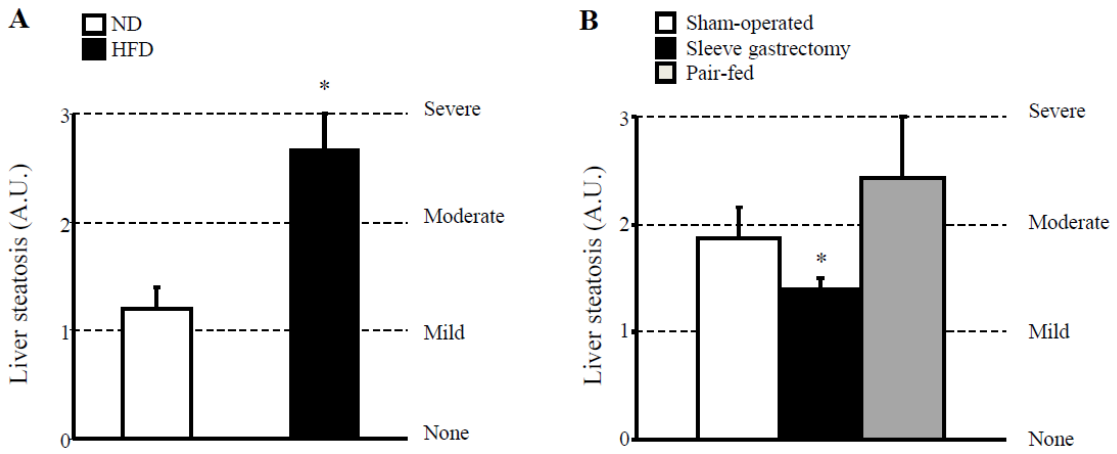


**Supplemental Fig. 1. Semi-quantitative evaluation of hepatic steatosis according to adipophilin staining.** Impact of obesity (A) and sleeve gastrectomy (B) on liver steatosis assessed by the staining of adipophilin in liver histological sections in a blind study. Differences were analyzed by $\chi^2$ test. *$P$<0.05 *vs* lean control ND or sham-operated ND.

# STUDY III

## 3. Ghrelin reduces TNF-α-induced human hepatocyte apoptosis, autophagy, and pyroptosis: role in obesity-associated NAFLD.

### Article

**Ezquerro S**, Mocha F, Frühbeck G, Guzmán-Ruiz R, Valentí V, Mugueta C, Becerril S, Catalán V, Gómez-Ambrosi J, Silva C, Salvador J, Colina I, Malagón MM, Rodríguez A.

Ghrelin reduces TNF-α-induced human hepatocyte apoptosis, autophagy, and pyroptosis: role in obesity-associated NAFLD.

*J Clin Endocrinol Metab* 2019;104(1):21-37.

### Hypothesis

Acylated and desacyl ghrelin protect against the pathogenic role of TNF-α in the development of NASH by inhibiting hepatocyte cell death in a series of patients with severe obesity classified according to their insulin resistance undergoing RYGB.

### Objectives

- To explore the potential differences in circulating acylated and desacyl ghrelin as well as TNF-α concentrations in obesity-associated insulin resistance and NAFLD before and after weight loss induced by bariatric surgery.
- To analyze *ex vivo* the hepatic expression of the components of the ghrelin system, TNF-α superfamily members, as well as key regulatory molecules of hepatocyte cell death.
- To determine the direct effects of acylated and desacyl ghrelin on basal and TNF-α induced apoptosis, autophagy and HMGB1-mediated pyroptosis in human HepG2 hepatocytes.

Ezquerro S, Mocha F, Frühbeck G, Guzmán-Ruiz R, Valentí V, Mugueta C, Becerril S, Catalán V, Gómez-Ambrosi J, Silva C, Salvador J, Colina I, Malagón MM, Rodríguez Ghrelin reduces TNF-α-induced human hepatocyte apoptosis, autophagy, and pyroptosis: role in obesity-associated NAFLD. J Clin Endocrinol Metab 2019;104(1):21-37.

# STUDY IV

## 4. Role of ghrelin isoforms in the mitigation of hepatic inflammation, mitochondrial dysfunction and endoplasmic reticulum stress after bariatric surgery in rats

### Article

**Ezquerro S**, Becerril S, Tuero C, Méndez-Giménez L, Mocha F, Moncada R, Valentí V, Cienfuegos JA, Catalán V, Gómez-Ambrosi J, Piper Hanley K, Frühbeck G, Rodríguez A.

Role of ghrelin isoforms in the mitigation of hepatic inflammation, mitochondrial dysfunction and endoplasmic reticulum stress after bariatric surgery in rats.

*Int J Obes* 2019; doi: 10.1038/s41366-019-0420-2.

### Hypothesis

Acylated and desacyl ghrelin improve the hepatic early inflammation, ER stress and mitochondrial dysfunction involved in the progression from NAFLD to NASH after sleeve gastrectomy or RYGB in diet-induced obese rats.

### Objectives

- To study the effect of sleeve gastrectomy and RYGB on several factors implicated in inflammation, ER stress and mitochondrial dysfunction.
- To analyze the circulating concentration of acylated and desacyl ghrelin before and after sleeve gastrectomy or RYGB and determine their association with inflammation.
- To evaluate the direct effects of both ghrelin isoforms on key regulatory molecules involved in inflammation, ER stress and mitochondrial dysfunction in primary rat hepatocytes under palmitic acid-induced lipotoxic conditions.

Ezquerro S, Becerril S, Tuero C, Méndez-Giménez L, Mocha F, Moncada R, Valentí V, Cienfuegos JA, Catalán V, Gómez-Ambrosi J, Piper Hanley K, Frühbeck G, Rodríguez A. Role of ghrelin isoforms in the mitigation of hepatic inflammation, mitochondrial dysfunction and endoplasmic reticulum stress after bariatric surgery in rats. International Journal of Obesity 2019; http://doi.org/10.1038/s41366-019-0420-2

## SUPPLEMENTARY METHODS

### Experimental animals and study design

Four-week-old male Wistar rats (n=129) (breeding house of the University of Navarra) were housed in individual cages in a room with controlled temperature (22±2 ºC), ventilation (at least 15 complete air changes/h), 12:12-h light-dark cycle (lights on at 8:00 am) and relative humidity (50± 10%) under pathogen-free conditions. Animals were fed *ad libitum* during 4 months with either a normal diet (ND) (n=28) (12.1 kJ: 4% fat, 82% carbohydrate and 14% protein, diet 2014S, Harlan, Teklad Global Diets, Harlan Laboratories Inc., Barcelona, Spain) or a high-fat diet (HFD) (n=101) (23.0 kJ/g: 59% fat, 27% carbohydrate and 14% protein, diet F3282; Bio-Serv, Frenchtown, NJ, USA) [1.1] Body weight and food intake were registered weekly to monitor the progression of diet-induced obesity with animals reaching a mean body weight of 630 ± 15 g after 4 months on the HFD.

Obese rats were randomly assigned to 6 different groups: i) sleeve gastrectomy (n=15); ii) sham surgery without gastric resection (n=11); iii) pair-fed to the same amount of food eaten by the sleeve gastrectomy group (n=17); iv) Roux-en-Y gastric bypass (RYGB) (n=6); v) sham surgery without gastric resection and intestinal bypass (n=11); vi) pair-fed to the same amount of food eaten by the RYGB group (n=8). Anaesthesia, sleeve gastrectomy and RYGB were performed according to previously described methodology.[2-5] Briefly, for the sleeve gastrectomy, a laparotomy incision was made in the abdominal wall and the stomach was isolated outside the abdominal cavity. Loose gastric connections to the spleen and liver were released along the greater curvature and the great omentum was ligated and divided down to the level of the pylorus. About 60-80% of the forestomach and glandular stomach was excised out using an automatic stapler (AutoSuture TA DST Series, Tyco Healthcare group LP, Norwalk, CT, USA) with a TA30V3L load, leaving a tubular gastric remnant in continuity with the esophagus upwards and the pylorus and duodenum downwards. The sham surgery for sleeve gastrectomy comprised the same laparotomic incision as well as handling of the stomach except for the gastrectomy. For the RYGB, a laparotomic incision was also made in the abdominal wall and the gut was isolated outside the abdominal capacity. Here too, about 60-80% of the forestomach and glandular stomach was excised out using an automatic stapler (AutoSuture TA DST Series) with a

TA30V3L load, to create a small gastric pouch. The remnant stomach was closed with 6-0 sutures. The jejunum was opened at 15 cm distal from the ligament of Treitz; subsequently, the distal jejunum was connected to the small gastric pouch with 6-0 sutures. A new anastomosis was made with 6-0 sutures between the biliopancreatic limb and the alimentary limb 10 cm distal from the gastrojejunal anastomosis to create the common channel. The sham surgery for RYGB comprised the same surgical procedure as well as handling of the stomach and gut except for the gastrectomy and the gastrointestinal bypass. Following the surgical interventions, the animals were fed a ND. Four weeks after the surgical and dietary interventions, rats were killed by decapitation after an 8-h fasting period. The liver, epididymal (EWAT), perirenal (PRWAT) and subcutaneous (SCWAT) white adipose tissues were carefully dissected out, weighed, frozen in liquid nitrogen and stored at -80 ºC until processed for the study. A small portion of the tissue was fixed in 4% paraformaldehyde for histological analyses. Blood samples were immediately collected and sera were obtained by cold centrifugation (4 ºC) at 700 *g* for 15 min. All experimental procedures conformed to the European Guidelines for the care and use of Laboratory Animals (directive 2010/63/EU) and were approved by the Ethical Committee for Animal Experimentation of the University of Navarra (049/10).

**Blood and tissue analysis**

Serum glucose was determined by an automatic glucose sensor (Ascencia Elite, Bayer, Barcelona, Spain). Insulin was determined by ELISA (Crystal Chem, Inc., Chicago, IL, USA). Intra- and inter-assay coefficients of variation for measurements of insulin were 3.5%, for the former, and 5.4%, for the latter. Insulin resistance was calculated using the homeostasis model assessment (HOMA), calculated with the formula: fasting insulin (μU/mL) × fasting glucose (mmol/L)/22.5). Serum alanine aminotransferase (ALT), aspartate aminotransferase (AST), free fatty acids (FFA) and triacylglycerols (TG) were measured by enzymatic methods using commercially available kits (Infinity$^{TM}$, Thermo Electron Corporation, Melbourne, Australia). Intrahepatic TG was determined by enzymatic methods, as previously described [6]. Fasting acylated and desacyl ghrelin levels were also assessed using a rat/mouse EIA Kit (A05117 and A05118**,** Cayman Chemical, Ann Harbor, MI, USA). Intra- and inter-assay coefficients of variation for measurements were 5.7% and 6.1%, respectively, for the former and 5.2% and 5.5 %, for the latter.

**RNA isolation and real-time PCR**

RNA isolation and purification were performed as earlier described.[7] Transcript levels of *Atf4*, *Atf6*, *Chop*, *Crp*, *Gadd34*, *Il6*, and *Tnf* were quantified by real-time PCR (7300 Real Time PCR System, Applied Biosystems, Foster City, CA, USA). Primers and probes (**Supplementary Table 1**) were designed using the software Primer Express 2.0 (Applied Biosystems) and acquired from Genosys (Sigma. St. Louis, MO, USA). Primers or TaqMan® probes encompassing fragments of the areas from the extremes of two exons were designed to ensure the detection of the corresponding transcript avoiding genomic DNA amplification. The cDNA was amplified at the following conditions: 95 ºC for 10 min, followed by 45 cycles of 15 s at 95 ºC and 1 min at 59 ºC, using the TaqMan® Universal PCR Master Mix (Applied Biosystems). The primer and probe concentrations were 300 and 200 nmol/L, respectively. All results were normalized for the expression of *18S* rRNA (Applied Biosystems), and relative quantification was calculated as fold expression over the calibrator sample.[7] All samples were run in triplicate and the average values were calculated.

**Western-blot**

Tissues were harvested and homogenized in ice-cold lysis buffer (0.1% SDS, 1% Triton X-100, 5 mmol/L EDTA·$2H_2O$, 1 mol/L Tris-HCL, 150 mmol/L NaCl, 1% sodium deoxycholate, pH 7.40) complemented with a protease inhibitor cocktail (Complete™ Mini-EDTA free, Roche, Mannheim, Germany). Lysates were centrifuged at 12,000 *g* at 4 ºC for 15 min to remove nuclei and unruptured cells. Total protein concentrations were determined by the Bradford assay,[8] using bovine serum albumin (BSA) (Sigma) as standard. Thirty or twenty micrograms of total protein of liver homogenates were diluted in loading buffer 4X (20% β-mercaptoethanol, 40 mmol/L dithiothreitol, 8% SDS, 40% glycerol, 0.016% bromophenol blue, 200 mmol/L Tris-HCl, pH 6.80) and heated for 10 min at 100 ºC. Samples were run out in Mini-PROTEAN® TGX™ precast gels (Bio-Rad Laboratories, Inc., Hercules, CA, USA), subsequently transferred to nitrocellulose membranes (Bio-Rad) and blocked in Tris-buffered saline (10 mmol/L Tris-HCl, 150 mmol/L NaCl, pH 8.00) with 0.05% Tween 20 (TBS-T) containing 5% non-fat dry milk for 1 h at room temperature (RT). Membranes were then incubated overnight at 4 ºC with rabbit monoclonal anti-ATF4 (#11815, Cell Signaling Technology, Inc., Danvers, MA, USA), mouse monoclonal anti-CHOP (#2895, Cell Signaling), rabbit polyclonal anti-eIF2α (#9722, Cell Signaling), rabbit polyclonal anti-

phospho-eIF2α (Ser51) (#9721, Cell Signaling), rabbit polyclonal anti-JNK (#9252, Cell Signaling), rabbit monoclonal anti-phospho-JNK (Thr183/Tyr185) (#4671, Cell Signaling), mouse monoclonal anti-complex-I (NDUFA9), anti-complex-II (SDHA), anti-complex-III (UQCRC2), anti-complex IV (MTCO1), anti-complex-V (ATP5A) and anti-porin (ab14713, ab14725, ab14745, ab14705, ab14748 and ab14734, respectively, abcam, Cambridge, UK), rabbit polyclonal anti-GRP78 (ab2168, abcam), rabbit polyclonal anti-IRE1 (ab37073, abcam), rabbit polyclonal anti-phospho-IRE (Ser724) (ab48187, abcam), rabbit monoclonal anti-phospho-PERK (Thr980) (MA5-15033, Thermo Fisher Scientific, San Jose, CA, USA), rabbit polyclonal anti-PERK (P0074, Sigma), rabbit polyclonal anti-XBP1 (SAB2102720, Sigma) antibodies (diluted 1:1,000 in blocking solution) or murine monoclonal anti-β-actin (A5441, Sigma) (diluted 1:5,000 in blocking solution). The antigen-antibody complexes were visualized using horseradish peroxidase (HRP)-conjugated anti-rabbit or anti-mouse IgG antibodies (diluted 1:5,000 in blocking solution) and the enhanced chemiluminescence ECL Plus detection system (Amersham Biosciences, Buckinghamshire, UK). The intensity of the bands was determined by densitometric analysis with the Gel Doc™ gel documentation system and the Quantity One 4.5.0 software (Bio-Rad) and normalized with β-actin density values.

**Histological analyses**

The immunodetection of adipophilin and CD68 in histological sections of liver was performed by the indirect immunoperoxidase method, as previously described.[6,9] Sections of formalin-fixed paraffin-embedded liver (4 μm) were dewaxed in xylene, rehydrated in decreasing concentrations of ethanol and treated with 3% $H_2O_2$ (Sigma) in absolute methanol for 10 min at RT to quench endogenous peroxidase activity. Slides were blocked during 60 min with 1% goat serum (Sigma) diluted in Tris-buffer saline (TBS) (50 mmol/L Tris, 0.5 mol/L NaCl, pH 7.36) to prevent non-specific absorption. Sections were incubated overnight at 4 ºC with mouse monoclonal anti-adipophilin (BM5051, Acris Antibodies GmbH, Herford, Germany) or mouse monoclonal anti-CD68 (ab31360, abcam) antibody diluted 1:200 in TBS. After washing three times with TBS (5 min each), slides were incubated with DAKO Real™ EnVision™ anti-rabbit/mouse (K5007; Dako, Golstrup, Denmark) for 1 h at RT. The peroxidase reaction was visualized using a 0.5 mg/mL diaminobenzidine (DAB)/0.03% $H_2O_2$ solution diluted in 50 mmol/L Tris-HCl, pH 7.36, and Harris hematoxylin solution (Sigma) as

counterstaining. Negative control slides without primary antibody were included to assess non-specific staining.

The TUNEL assay was performed using an *in situ* cell death detection kit (POD; Roche, Basel, Switzerland). Histological sections of formalin-fixed paraffin-embedded liver (4 μm) were dewaxed in xylene, rehydrated in decreasing concentrations of ethanol and treated with 3% $H_2O_2$ (Sigma) in absolute methanol for 10 min at RT to quench endogenous peroxidase activity. Then, slides were placed in citrate buffer 0.01 mol/L (pH 6.00) and heated in a microwave oven for 15 min at maximum power (800 W) and 15 min at medium power (400 W) for antigen retrieval. After washing three times with PBS, slides were incubated with 50 μL in a reaction mixture containing fluorescein-labelled dNTPs and terminal deoxynucleotidyl transferase (TdT) for 30 min at 37 ºC in a humidified atmosphere in the dark. Negative controls were incubated in the absence of TdT, and positive controls were pretreated for 10 min at RT with 100 μL of 100 U/ml DNase I from bovine pancreas (Roche) in 50 mmol/l Tris-HCl (pH 7.36) and 1 mg/mL BSA to induce DNA breaks, prior to labelling procedures. Slides were rinsed three times with PBS and, then, incubated with 50 μL of anti-fluorescein antibody conjugated with horseradish peroxidase for 30 min at 37 ºC in a humidified atmosphere in the dark. After washing three times with PBS, the peroxidase reaction was visualized with 50 μL of 3,3'-DAB/$H_2O_2$ solution for 10 min at RT. Slides were rinsed three times with PBS and analyzed under the light microscope.

The adipocyte cell surface area (CSA) was measured as previously described.[10] Briefly, biopsies of EWAT were fixed in 4% formaldehyde, embedded in paraffin, cut into sections of 6 μm and stained with hematoxylin-eosin. Images of three fields per section from each animal were captured with the 20× objective, and the adipocyte CSA from, at least, 100 cells/section was measured using the software AxioVision Release 4.6.3 (Zeiss, Göttingen, Germany)

**DNA extraction and analysis of mtDNA amount**

The amount of mtDNA, extracted and purified using DNeasy Blood and Tissue Kit (Qiagen, Barcelona, Spain), was determined by real-time PCR of the mitochondrial cytochrome B (*Cytb*) gene normalized to the nuclear β-actin (*Actb*) gene.[11] The primer and probes sequences are available in **Supplementary Table S1**. The real-time PCR was performed with 25 ng of total DNA using the TaqMan® Universal PCR Master Mix

(Applied Biosystems) and the obtained data were analyzed by the comparative "ΔΔCt method".

**Cell cultures**

Non-tumorigenic primary rat hepatocytes were purchased from Tebu-Bio (Barcelona, Spain). Cells were maintained in DMEM/F-12 medium (Invitrogen, Paisley, UK) supplemented with 10% fetal bovine serum (FBS), 5 μg/mL insulin, 5 μg/mL transferrin, 5 ng/mL selenium (Invitrogen), 40 ng/mL dexamethasone (Sigma), 20 ng/mL epidermal growth factor (Sigma) and antibiotic-antimycotic (Complete Growth Medium). Rat hepatocytes were cultured in a collagen sandwich configuration, as described by Shulman *et al,*[12] seeded into 6-well plates at $3x10^5$ cells/well and grown in Complete Growth Medium for 24 h. Cells were serum-starved for 24 h and then treated for 24 h with increasing concentrations (10, 100, 1000 pmol/L) of acylated ghrelin or desacyl ghrelin (Tocris, Ellisville, MO, USA) for 24 h. These physiological and supraphysiological concentrations of ghrelin isoforms to carry out the experiments were chosen on the basis of previous studies performed in our laboratory.[13,14] In a second subset of experiments, primary rat hepatocytes were stimulated with palmitate (200 μmol/L) (P0500, Sigma) in the presence or absence of acylated or desacyl ghrelin (100 pmol/L) for 24 h. Palmitate was dissolved in DMEM (1X) medium supplemented with 5% BSA.

**Statistical analysis**

Data are expressed as the mean ± SEM. The PS Power and Sample Size Calculations software (edition 3.0.43) was used to determine the power of the study and sample size calculation. Statistical differences between mean values were analyzed using Student's *t* test, one-way ANOVA followed by Tukey's or Dunnett's *post-hoc* tests or the non-parametric Kruskal-Wallis test followed by *U* Mann-Whitney´s pairwise comparisons, where appropriate. Pearson's correlation coefficients (*r*) were used to analyze the association between variables. The statistical analyses were performed using the SPSS/Windows version 15.0 software (SPSS Inc., Chicago, IL, USA).

## REFERENCES


1. Frühbeck G, Alonso R, Marzo F, Santidrián S. A modified method for the indirect quantitative analysis of phytate in foodstuffs. *Anal Biochem* 1995; **225**: 206-212.
2. Valentí V, Martín M, Ramírez B, Gómez-Ambrosi J, Rodríguez A, Catalán V *et al.* Sleeve gastrectomy induces weight loss in diet-induced obese rats even if high-fat feeding is continued. *Obes Surg* 2011; **21**: 1438-1443.
3. Rodríguez A, Becerril S, Valentí V, Ramírez B, Martin M, Méndez-Giménez L *et al.* Sleeve gastrectomy reduces blood pressure in obese (*fa/fa*) Zucker rats. *Obes Surg* 2012; **22**: 309-315.
4. Rodríguez A, Becerril S, Valentí V, Moncada R, Méndez-Giménez L, Ramérez B *et al.* Short-term effects of sleeve gastrectomy and caloric restriction on blood pressure in diet-induced obese rats. *Obes Surg* 2012; **22**: 1481-1490.
5. Bruinsma BG, Uygun K, Yarmush ML, Saeidi N. Surgical models of Roux-en-Y gastric bypass surgery and sleeve gastrectomy in rats and mice. *Nat Protoc* 2015; **10**: 495-507.
6. Rodríguez A, Gena P, Méndez-Giménez L, Rosito A, Valentí V, Rotellar F *et al.* Reduced hepatic aquaporin-9 and glycerol permeability are related to insulin resistance in non-alcoholic fatty liver disease. *Int J Obes* 2014; **38**: 1213-1220.
7. Catalán V, Gómez-Ambrosi J, Rotellar F, Silva C, Rodríguez A, Salvador J *et al.* Validation of endogenous control genes in human adipose tissue: relevance to obesity and obesity-associated type 2 diabetes mellitus. *Horm Metab Res* 2007; **39**: 495-500.
8. Bradford MM. A rapid and sensitive method for the quantitation of microgram quantities of protein utilizing the principle of protein-dye binding. *Anal Biochem* 1976; **72**: 248-254.
9. Rodríguez A, Catalán V, Gómez-Ambrosi J, García-Navarro S, Rotellar F, Valentí V *et al.* Insulin- and leptin-mediated control of aquaglyceroporins in human adipocytes and hepatocytes is mediated via the PI3K/Akt/mTOR signaling cascade. *J Clin Endocrinol Metab* 2011; **96**: E586-597.
10. Méndez-Giménez L, Becerril S, Moncada R, Valentí V, Ramírez B, Lancha A *et al.* Sleeve gastrectomy reduces hepatic steatosis by improving the coordinated regulation of aquaglyceroporins in adipose tissue and liver in obese rats. *Obes Surg* 2015; **25**: 1723-1734.
11. Heinonen S, Buzkova J, Muniandy M, Kaksonen R, Ollikainen M, Ismail K *et al.* Impaired mitochondrial biogenesis in adipose tissue in acquired obesity. *Diabetes* 2015; **64**: 3135-3145.
12. Shulman M, Nahmias Y. Long-term culture and coculture of primary rat and human hepatocytes. *Methods Mol Biol* 2013; **945**: 287-302.
13. Rodríguez A, Gómez-Ambrosi J, Catalán V, Gil MJ, Becerril S, Sáinz N *et al.* Acylated and desacyl ghrelin stimulate lipid accumulation in human visceral adipocytes. *Int J Obes* 2009; **33**: 541-552.
14. Rodríguez A, Gómez-Ambrosi J, Catalán V, Rotellar F, ValentI V, Silva C *et al.* The ghrelin *O*-acyltransferase-ghrelin system reduces TNF-alpha-induced apoptosis and autophagy in human visceral adipocytes. *Diabetologia* 2012; **55**: 3038-3050.

# Discussion

## 1. Summary of the main findings

Bariatric surgery improves NAFLD and NASH, but the underlying mechanisms remain unknown. The present thesis shows the potential role of acylated and desacyl ghrelin in the progression of NAFLD to NASH through the amelioration of hepatic steatosis and inflammation after bariatric surgery in an experimental model of obesity as well as in patients with morbid obesity. Diet-induced obese rats developed hepatosteatosis and showed decreased circulating desacyl ghrelin without changes in acylated ghrelin concentrations. Sleeve gastrectomy and RYGB induced a dramatic reduction in desacyl ghrelin levels, whereas the acylated/desacyl ghrelin ratio was augmented in obese rats. In patients with morbid obesity and NAFLD, desacyl ghrelin levels were diminished, while circulating TNF-α and the acylated/desacyl ghrelin ratio were increased. Interestingly, six months after bariatric surgery, decreased acylated/desacyl ghrelin levels were found in morbidly obese patients (**Table 3**). We demonstrated that bariatric surgery improved hepatic steatosis by reducing hepatic TG content and the lipogenic enzymes *Mogat2* and *Dgat1*, and triggering AMPK-activated mitochondrial FFA β-oxidation and autophagy to a higher extent than caloric restriction in diet-induced obese rats. In addition, both sleeve gastrectomy and RYGB ameliorated hepatic inflammation, as evidenced by a decrease in portal and lobulillar $CD68^+$ and apoptotic cells, proinflammatory JNK activation and a downregulation in the expression of inflammation-related genes (*Crp*, *Tnf* and *Il6*). In parallel, mitochondrial dysfunction was significantly attenuated after sleeve gastrectomy and RYGB via an increase in mitochondrial DNA amount as well as OXPHOS complexes I and II together with an amelioration of ER stress. Specifically, GRP78, spliced XBP-1, ATF4 and CHOP levels were reduced, as was phosphorylated eIF2α, following both bariatric surgical procedures.

Our results show that the stimulation of primary rat hepatocytes with acylated and desacyl ghrelin significantly increased TG content, but also prompted AMPK-activated mitochondrial FFA β-oxidation and autophagy. Furthermore, acylated and desacyl ghrelin also inhibited palmitate-triggered inflammation and UPR induction through the downregulation of IRE1α, PERK and ATF6 expression as well as their downstream effectors, ATF4 and CHOP, and chaperone GRP78. In human HepG2 hepatocytes, acylated and desacyl ghrelin treatment reduced TNF-α-induced apoptosis, evidenced by lower caspase-8 and caspase-3 cleavage, as well as TUNEL-positive cells and pyroptosis,

revealed by decreased caspase-1 activation and lower HMGB1 expression. Moreover, acylated ghelin suppressed TNF-α-activated hepatocyte autophagy, supported by decreased LC3B-II/I ratio and increased p62 accumulation via AMPK/mTOR, with acylated ghrelin being a protective factor against hepatocyte cell death. Thus, the decrease in the most abundant isoform, desacyl ghrelin, after bariatric surgery contributes to the reduction of lipogenesis, whereas the increased relative acylated ghrelin levels activate factors involved in mitochondrial FFA β-oxidation and autophagy as well as contribute to mitigate obesity-associated hepatic inflammation, mitochondrial dysfunction, ER stress and cell death, thereby ameliorating NAFLD (**Table 3**).

**Table 3**. Summary of the functional changes after bariatric surgery associated with ghrelin isoforms in patients with morbid obesity and experimental models of diet-induced obesity.

| **Ghrelin isoforms** | **HUMANS** | | **RATS** | | | **Functional changes associated with ghrelin isoforms** |
|---|---|---|---|---|---|---|
| | Changes in obesity | Changes after surgery | Changes in obesity | Changes after surgery | | |
| | | | | **SG** | **RYGB** | |
| **Desacyl ghrelin** | ▼ | ▼ | ▼ | ▼ | ▼ | Decrease in lipogenesis |
| **Acylated Ghrelin (*)** | ▼ | ▼ | = | = | = | Improvement in hepatic steatosis and inflammation |
| **Acylated/ desacyl Ghrelin (*)** | =▲ | ▼ | =▲ | ▲ | ▲ | Reduction in hepatocyte cell death |

▲Increase; ▼ Decrease; *Species-specific differences in absolute and relative acylated ghrelin are explained in page 61.

## 2. High prevalence of NAFLD and NASH in obesity

The incidence of NAFLD is rising due to the global epidemics of obesity, T2D and metabolic syndrome (Younossi *et al*, 2016, Younossi *et al*, 2018). In the study III, we confirmed the high prevalence of biopsy-proven NAFLD and NASH found in morbid obesity (70% and 55%, respectively), compared to those observed in the general population (24% and 3-5%, respectively) (Younossi *et al*, 2016, Younossi *et al*, 2018). Moreover, we also detected a sexual dimorphism of NAFLD, being more prevalent in males than in females, which is in accordance with previous reports (Ballestri *et al*, 2017). In order to gain further insight into the mechanisms underlying obesity-associated NAFLD, we used an experimental model of diet-induced obesity. In the studies II and IV, HFD feeding induced an increase in body weight, whole-body white adiposity and insulin

resistance as evidenced by higher insulinemia and HOMA as well as higher glycaemia, which is in agreement with previous results (Méndez-Giménez *et al*, 2015).

### 2.1. Mechanisms underlying the onset of obesity-associated NAFLD

*Alteration in lipogenesis and mitochondrial β-oxidation*

Obesity is associated with an increased release of FFA from the adipose tissue due to enhanced adipocyte lipolysis (Frühbeck *et al*, 2014, Zhang *et al*, 2014). Circulating FFA are taken up by the liver and metabolized by two main pathways: i) FFA esterification to produce TG, which can be either incorporated into VLDL particles or stored within the hepatocytes; and ii) the mitochondrial FFA β-oxidation to generate ATP (Browning and Horton, 2004, Kawano and Cohen, 2013, Ipsen *et al*, 2018). As shown in the studies II and IV, diet-induced obese rats developed hepatosteatosis, as evidenced by higher liver weight, increased intrahepatic TG content and staining of the lipid droplet-coating protein adipophilin together with an elevation of serum AST levels. Accordingly, obese animals showed an upregulation of the lipogenic genes *Pparg, Srebf1*, *Mogat2* and *Dgat1* compared with their lean counterparts. Moreover, AMPK regulates the partitioning of FFA both in oxidative and biosynthetic pathways with defects in this pathway leading to the development of NAFLD (Kahn *et al*, 2005). In this regard, lack of changes in the basal AMPK and ACC expression and activity as well as in the mitochondrial copy number in obese rats might reflect an impaired AMPK transduction signalling and dysfunction in mitochondrial biogenesis in the rat steatotic liver, in line with previous studies of our group (Rodríguez *et al*, 2008) and others (Rector *et al*, 2008, Finocchietto *et al*, 2011).

*Defective autophagy*

Autophagy also plays an important role in the regulation of hepatic lipid metabolism. *In vitro* and *in vivo* studies have shown that autophagy mediates the breakdown of lipid stores, and that an inhibition of autophagy promotes TG storage in lipid droplets leading to the development of fatty liver (Singh *et al*, 2009, Yang *et al*, 2010). The inhibition of autophagy sensitizes hepatocytes to palmitic acid-induced apoptosis, suggesting a pro-survival function of autophagy against lipotoxicity (Tan *et al*, 2012). In this sense, reduced levels of autophagy have been found in the liver of severely obese leptin-deficient *ob/ob* mice as well as in obese, diabetic OLETF rats, which might promote lipid accumulation and impaired hepatic function in these animal models

(Machado *et al*, 2006, Chang *et al*, 2015). However, our results in the study II showed no changes in the hepatic gene expression of the autophagy-related factors *Atg5* and *Atg7*, in the formation of autophagosomes evidenced by the LC3B-II/I conversion or in the inhibition of autophagy, expressed as p62 accumulation in obese rats. In this regard, hepatic autophagy is influenced by the degree of hepatic steatosis that might change the autophagosome formation during the ongoing NAFLD in adult obese rats.

### 2.2. Mechanisms underlying NAFLD to NASH progression in obesity

*Mitochondrial dysfunction and ER stress*

Mitochondria are key cellular components driving the metabolic shift in hepatocytes in an attempt to overcome the FFA and TG burden (Simões *et al*, 2018). Short-term lipid overload in hepatocytes stimulates the mitochondrial activity in order to maintain the bioenergetic demands, and, hence, serves to protect against NAFLD progression (Koliaki *et al*, 2015). In the study IV, lack of changes in mitochondrial DNA content together with the reduction in OXPHOS subunits in obese rats suggests that, in the long-term, this adaptation fails and cannot prevent lipotoxicity. Similar results have been reported by our group in rat steatotic liver (Rodríguez *et al*, 2008) and others in the liver of obese mice fed a Western diet (Einer *et al*, 2018) or choline-deficient diet (Teodoro *et al*, 2008), genetically obese *ob/ob* mice (Perfield *et al*, 2013) or obese patients with NASH (Koliaki *et al*, 2015) (**Figure 11**).

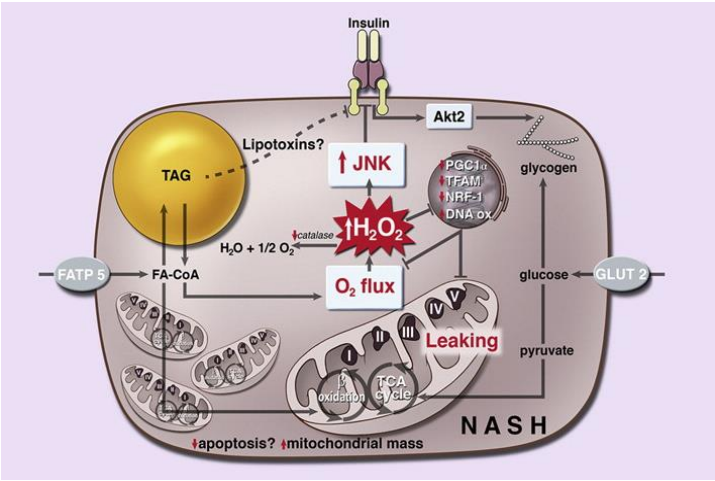


**Figure 11.** Mitochondrial metabolic adaptations are lost in NAFLD and NASH (modified from Koliaki *et al*, 2015).

Mitochondrial dysfunction can induce the accumulation of unfolded or misfolded proteins in the ER that is sensed by the chaperone GRP78 (Malhi and Kaufman, 2011). Under basal conditions, GPR78 is bound to the transmembrane proteins PERK, IRE1 and

ATF6 to block their activation (Kammoun *et al*, 2009). Upon ER stress, the accumulation of unfolded or misfolded proteins dissociates GPR78 and activates the UPR through the actions of the canonical sensors PERK, IRE1 and ATF6 in an attempt to restore ER homeostasis (Fu *et al*, 2012). The overexpression of the chaperone GPR78 inhibits the activation of the lipogenic transcription factor SREBP1c and decreases hepatic steatosis in the liver of genetically and diet-induced obese mice (Kammoun *et al*, 2009). Upon activation, XBP1 is translocated to the nucleus to upregulate the transcription of GRP78 during ER stress (Schroder and Kaufman, 2005). Furthermore, it has been proposed that the IRE1-XBP1 pathway is involved in the activation of inflammatory signalling cascades, such as the JNK and NF-κB pathways (Sha *et al*, 2011, Jiang *et al*, 2015). Accordingly, we demonstrated in the study IV that exposure to palmitic acid *in vitro* and HFD feeding *in vivo* induced steatosis, upregulation of the proinflammatory *Crp* and *Tnf* as well as chaperone GRP78 together with the activation of PERK, IRE1, ATF6 and their downstream effectors, eIF2α, ATF4, CHOP and XBP-1 in hepatocytes. To date, it is not clear whether changes in ER stress could precede or just occur after the development of hepatic steatosis (Dara *et al*, 2011). In our hands, it seems that lipid overload overwhelms the ER structure and chaperone activity, initiating a vicious circle of stress, mitochondrial dysfunction and worsening of ER stress, which is in agreement with previous reports (Fu *et al*, 2012, Jiang and Wan, 2018, Lee *et al*, 2018). Improving protein folding by chemical chaperones and/or genetic manipulation of UPR helps to normalize body weight, supporting the strong association between ER stress and obesity (Ozcan *et al*, 2006, Kammoun *et al*, 2009). Dysregulation of ER and mitochondrial functions contributes to the inflammatory signals and to the initiation and progression from NAFLD to NASH, since JNK activation accelerates lipid accumulation and causes hepatocyte inflammation and cell death (Yan *et al*, 2017).

*Increased hepatocyte cell death*

The members of the TNF protein superfamily are amongst the best-characterized inducers of hepatocyte cell death, a hallmark of liver damage (Ding and Yin, 2004, Eguchi *et al*, 2014). Several mechanisms have been proposed to cause hepatocyte demise, including apoptosis, defective autophagy, necrosis and/or pyroptosis (Ding and Yin, 2004, Eguchi *et al*, 2014). In the study III, we provided evidence for an overexpression of TNF-α and the death receptors TNF-R1 and DR3 as well as an activation of the apoptosis extrinsic pathway in the liver of morbidly obese patients with T2D, confirming

the role of insulin resistance as an independent risk factor for the onset of liver injury (Crespo *et al*, 2001). Furthermore, the patients with prediabetes of our cohort showed an upregulation of autophagy in spite of their hyperinsulinemia, evidenced by an increased LC3B II/I ratio, whereas no changes were observed in T2D patients. In line with this observation, impairment of liver autophagy in experimental models of NAFLD has been also related to changes in insulin signalling (Liu *et al*, 2009), a potent inhibitor of autophagy. These findings point to a compromised hepatic autophagy in patients with insulin resistance that may reflect the increased cell death of hepatocytes (Schneider and Cuervo, 2014). In this regard, a defective autophagy underlies several liver disorders, including NAFLD, and leaves hepatocytes vulnerable to stressors and unable to accommodate the extreme energetic demands, ultimately producing liver injury (Brenner *et al*, 2013, Eguchi *et al*, 2014, Schneider and Cuervo, 2014) (**Figure 12**).

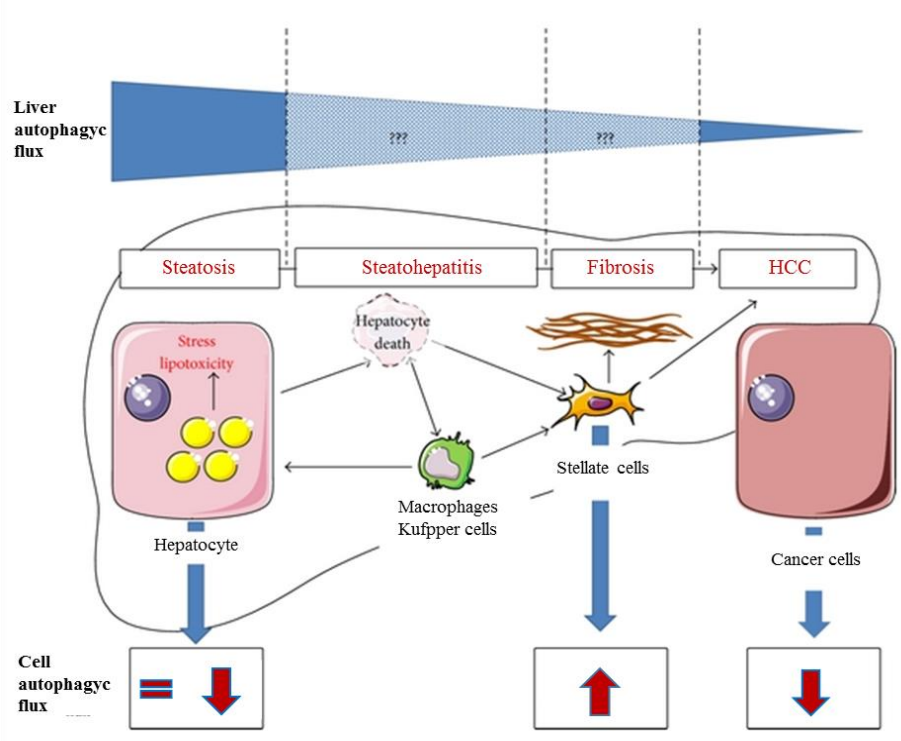


**Figure 12**. Autophagy and NAFLD. In the steatotic liver and hepatocytes, the autophagic flux is decreased or unchanged. In stellate cells, autophagy is activated and regulates HSC activation. In HCC, a reduction in autophagy in cancer cells facilitates tumor initiation (modified from Lavallard and Gual, 2014).

Another factor involved in hepatocyte cell death is the innate alarmin HMGB1, which plays a key role in the activation of pyroptosis following liver injury. Under physiological conditions, HMGB1 is a nuclear factor that maintains nuclear DNA structure and function (Guzmán-Ruiz *et al*, 2014). However, several liver injuries, such as heat shock (Geng *et al*, 2015), $CCl_4$ (Chen *et al*, 2014), acetaminophen (Yang *et al*,

2017) or infectious peritonitis (Yang *et al*, 2017), induce HMGB1 translocation from the nuclei to the cytoplasm for being secreted to the extracellular space. Extracellular HMGB1 binds its receptors TLR4 and RAGE, activating the NLRP3-inflammasome and caspase-1, ultimately leading to hepatocyte pyroptotic cell death (Geng *et al*, 2015). The anti-diabetic drug metformin directly binds HMGB1 and inhibits its inflammatory responses in a model of acetaminophen-induced acute liver injury (Horiuchi *et al*, 2017), suggesting that this process might be reversible. In the study III, we showed that insulin resistance strongly influenced hepatic expression of HMGB1, TLR4 and RAGE as well as caspase-1 cleavage in patients with morbid obesity. Our data revealed that insulin and MCM-LPS triggered HMGB1 translocation from the hepatocyte nucleus to cytosolic compartments resembling lysosomes, the organelles involved in HMGB1 secretion to the extracellular milieu (Gardella *et al*, 2002). Moreover, both insulin and TNF-α, one of the most abundant cytokines produced by LPS-activated macrophages, upregulated the expression of HMGB1 in HepG2 hepatocytes at the highest tested concentrations. Our findings demonstrate that hepatic HMGB1 expression and secretion is altered in insulin-resistant states contributing to the progression of NAFLD to NASH through the activation of pyroptosis.

In summary, during the development of obesity-associated NAFLD, several structural, molecular and functional alterations take place in different organelles of hepatocytes leading to the histological phenotypic alterations characteristic of NAFLD.

## 3. Changes in circulating ghrelin isoforms in obesity-associated NAFLD before and after bariatric surgery

Experimental and clinical evidence suggest a link between obesity-associated NAFLD and circulating ghrelin isoforms (Marchesini *et al*, 2003, Rodríguez *et al*, 2010, Estep *et al*, 2011, Mykhalchyshyn *et al*, 2015). In spite of its orexigenic and adipogenic properties, circulating total ghrelin concentrations are paradoxically decreased in obesity (Tschöp *et al*, 2001). In the studies II and IV, our findings showed that obese rats exhibited lower serum desacyl ghrelin levels without changes in acylated ghrelin concentrations, which is in agreement with previous reports (Rodríguez *et al*, 2009, Rodríguez *et al*, 2010, Rodríguez *et al*, 2012c, Barazzoni *et al*, 2013). Nonetheless, an increase in the acylated/desacyl ghrelin ratio was observed in obese animals compared with their lean counterparts. As expected, sleeve gastrectomy and RYGB dramatically

reduced plasma desacyl ghrelin levels, due to the surgical resection of the gastric fundus, the major production site of the hormone (Frühbeck *et al*, 2004b). By contrast, plasma acylated ghrelin remained unchanged after both bariatric surgeries, which is in accordance with other authors (Patrikakos *et al*, 2011, Malin *et al*, 2014), and the acylated/desacyl ghrelin ratio increased, suggesting an enhanced post-transcriptional modification in order to maintain the circulating levels of the acylated hormone. Interestingly, a positive correlation between post-surgical desacyl ghrelin and ALT was found, whereas acylated ghrelin levels were negatively correlated with intrahepatic TG and proinflammatory *Tnf* gene expression. In this sense, ghrelin acts as a survival factor for hepatocytes under lipotoxic and inflammatory conditions, as explained in the section 7 of the Discussion.

NAFLD is commonly associated with all the component features of the metabolic syndrome, which in turn, can increase the risk of development and progression of NAFLD. In humans, a progressive elevation in plasma acylated ghrelin and a reduction in plasma desacyl ghrelin is observed as the number of components of the metabolic syndrome increases in obese patients, indicating a potential role of both ghrelin isoforms in the pathogenesis and treatment of the metabolic syndrome (Rodríguez *et al*, 2010). Intriguingly, obese individuals with low ghrelin levels are more prone to weight regain after following a hypocaloric diet intervention (Crujeiras *et al*, 2010), denoting an impaired central and/or peripheral ghrelin signalling that might explain the high-fat feeding in these subjects. In the study III, we found that obese patients with NAFLD exhibited lower plasma desacyl ghrelin levels with an increase in the acylated/desacyl ghrelin ratio in parallel to the worsening of liver function, which is in agreement with previous reports (Rodríguez *et al*, 2009, Rodríguez *et al*, 2012c, Barazzoni *et al*, 2013). Accordingly, a reduction in circulating γ-GT was observed in morbidly obese patients after RYGB, with post-surgical desacyl and acylated ghrelin concentrations being negatively correlated with γ-GT levels. Moreover, the human liver synthesizes ghrelin, and a slight increase in ghrelin expression has been reported in patients with NASH (Uribe *et al*, 2008). We were not able to detect changes in the hepatic ghrelin, but a marked upregulation of the ghrelin-acylating enzyme GOAT was observed in the liver of obese patients with T2D. Interestingly, the proinflammatory TNF-α, also increased in the circulation and liver of obese patients with T2D, upregulated *MBOAT4* expression, suggesting that ghrelin acylation is activated during liver injury induced by TNF-α. Thus,

it seems plausible that the decrease in circulating acylated ghrelin after RYGB might reflect the improvement in insulin sensitivity and the mitigation of hepatic inflammation after bariatric surgery.

It is worth mentioning that the observed species-specific differences in absolute and relative acylated ghrelin levels after bariatric surgery (**Table 3**) might be related to the post-surgical period at which samples were collected (one month after surgical interventions in diet-induced obese rats, and six months after RYGB in patients with severe obesity). The temporal pattern of response elicited by bariatric surgery in ameliorating obesity and its comorbidities encompass weight loss-independent, weight-loss-dependent and adiposity-dependent effects (Frühbeck, 2015). It seems plausible that the inflammatory process accompanying the amelioration of NAFLD remains active one month after sleeve gastrectomy and RYGB, and requires increased relative acylated ghrelin levels to reduce hepatic inflammation. By contrast, the beneficial effects of bariatric surgery on hepatic function might have picked six months after bariatric surgery in patients with severe obesity, and the increased acylated/ghrelin ratio is no longer required. Further studies are necessary to analyze the impact of changes in the hepatic expression and activity of the ghrelin-acylating enzyme GOAT on the time-dependent amelioration of NAFLD.

## 4. Impact of sleeve gastrectomy and RYGB on hepatosteatosis in obesity

Bariatric surgery has emerged as the most effective treatment to induce sustainable weight loss and improve metabolic profile in obesity (Frühbeck, 2015). In this thesis, we have characterized the changes in body composition as well as the metabolic profile after two different bariatric surgical procedures, namely sleeve gastrectomy and RYGB. Both bariatric surgeries not only improve features of the metabolic syndrome, but also ameliorate NAFLD, NASH and NASH-fibrosis in diet-induced obese rats (Wang and Liu, 2009, Myronovych *et al*, 2014) and in morbidly obese patients (Mathurin *et al*, 2009, Lassailly *et al*, 2013, Frühbeck, 2015, Taitano *et al*, 2015, Bray *et al*, 2016).

In the studies II and IV, we provided evidence that four weeks after surgery, RYGB and, to a lesser extent, sleeve gastrectomy were associated with an improvement

in insulin sensitivity, supported by lower insulinemia, glycemia and HOMA index, which is in accordance with previous results of our group (Rodríguez *et al*, 2012a, Rodríguez *et al*, 2012b, Méndez-Giménez *et al*, 2015) and others (Ribaric *et al*, 2014, Schauer *et al*, 2014). Moreover, both techniques induced substantial loss of body weight and adiposity, improved metabolic profile and hepatosteatosis in diet-induced obese rats, according to other authors (Wang and Liu, 2009, Johansson *et al*, 2013, Myronovych *et al*, 2014). In line with these observations, our data confirmed that sleeve gastrectomy ameliorates hepatic function, as evidenced by an improved profile of AST and ALT, and hepatosteatosis, corroborated by the decrease in liver weight and intrahepatic TG as well as the downregulation of the lipogenic factors *Pparg*, *Srebf1*, *Mogat2* and *Dgat1*. Interestingly, hepatic AMPK and ACC phosphorylation was improved after sleeve gastrectomy, which is in agreement with other studies showing similar changes in AMPK and ACC activation after bariatric surgery (Peng *et al*, 2010). Accordingly, the upregulation of hepatic *Cpt1a* and its upstream molecule *Ppara* together with the enhance in mitochondrial DNA content after sleeve gastrectomy suggests an increased flux of FFA towards mitochondrial β-oxidation and higher mitochondrial copy number rather than inducing *de novo* TG synthesis. We demonstrated that sleeve gastrectomy is associated with an upregulation of the autophagy-related genes *Atg5* and *Atg7* and the LC3B-II/I ratio as well as with a reduction in the autophagy inhibition marker p62, suggesting that the induction of autophagy after this surgical procedure improves hepatic lipid clearance via lipophagy. In summary, we showed that the beneficial effects of bariatric surgery on NAFLD are mediated via a decrease in lipogenesis as well as an increase in autophagy and mitochondrial β-oxidation (**Figure 13**).

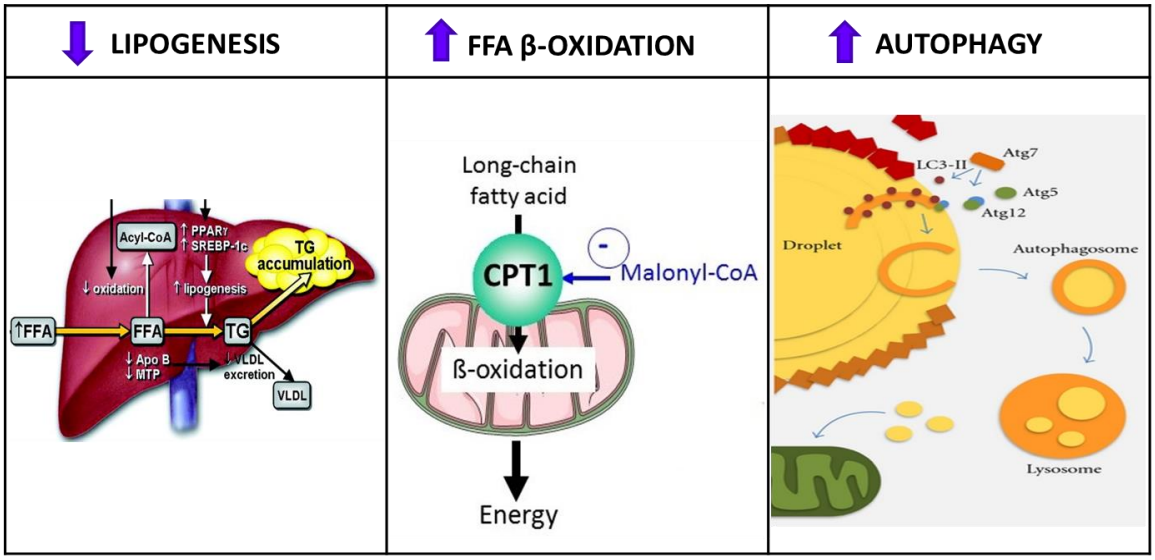

**Figure 13**. Mechanisms underlying the attenuation of NAFLD after sleeve gastrectomy (modified from Singh and Cuervo, 2012).

## 5. Role of ghrelin isoforms in the amelioration of obesity-associated NAFLD

The molecular mechanisms underlying surgically-induced amelioration of obesity-associated NAFLD remain unclear. The greater curvature of the stomach produces several factors, such as ghrelin, involved in the improvement of body weight and whole-body metabolism after bariatric surgery (Zhu *et al*, 2016). In this sense, it seems plausible that ghrelin changes after sleeve gastrectomy and RYGB contribute, at least in part, to the post-surgical improvements in hepatic function. Patients with obesity and NAFLD exhibit hypoghrelinemia, which is related to the degree of insulin resistance (Marchesini *et al*, 2003, Estep *et al*, 2011, Mykhalchyshyn *et al*, 2015). Interestingly, opposite effects of ghrelin isoforms on hepatic glucose metabolism have been reported (Gauna *et al*, 2005). Although this might seem paradoxical, tight homeostatic control in some physiological processes is achieved by fine-tuning hormonal actions with opposite effects of the diverse isoforms (Frühbeck and Gómez-Ambrosi, 2003). Thus, exogenous desacyl ghrelin administration acts as a potent insulin secretagogue, whereas acylated ghrelin decreases glucose-induced insulin release and increases glucose levels in both humans and rodents (Gauna *et al*, 2004, Gauna *et al*, 2007). Accordingly, blockade of ghrelin signalling stimulates glucose-stimulated insulin secretion and improves peripheral insulin sensitivity (Alamri *et al*, 2016). Thus, it seems plausible that ghrelin changes after sleeve gastrectomy also contribute, at least in part, to the observed improvement in insulin sensitivity after the surgical procedure.

Ghrelin isoforms also participate in the amelioration of NAFLD through a direct regulation of hepatic lipid metabolism. Previous work of our group, reported that both acylated and desacyl ghrelin stimulated intracellular lipid accumulation in human differentiated omental adipocytes through the upregulation of PPARγ and SREBP-1c and other fat-storage related molecules (Rodríguez *et al*, 2009). Accordingly, in the study II, we demonstrated that both ghrelin isoforms also increase intracellular TG content in rat hepatocytes through the upregulation of the lipogenic enzymes *Mogat2* and *Dgat1* (**Figure 14**). Since desacyl ghrelin represents ~90% of total ghrelin (Pacifico *et al*, 2009, Rodríguez *et al*, 2009), the amelioration of the hepatic function after sleeve gastrectomy might be partially due to the decrease of the desacylated hormone after the removal of the

gastric fundus. In addition, ghrelin triggers AMPK signalling in rat ventricular cardiomyocytes, myoblasts, hypothalamic neurons and hepatocytes (López *et al*, 2008, Han *et al*, 2015, Mao *et al*, 2015a, Yuan *et al*, 2016). Analogously, we found that acylated and desacyl ghrelin promoted AMPK and ACC activation in primary rat hepatocytes (**Figure 14**), suggesting that both isoforms of the hormone are involved in the molecular mechanisms whereby sleeve gastrectomy improves hepatic mitochondrial function. Furthermore, acylated ghrelin also upregulates *Ppara* and *Cpt1a* expression, while the mitochondrial DNA content was not affected. This observation leads to the notion that acylated ghrelin should be considered an important effector improving post-surgical mitochondrial β-oxidation efficiency, without changes in mitochondrial biogenesis.

Ghrelin isoforms are also involved in the regulation of autophagy in several tissues, including the adipose tissue, small intestine, skeletal muscle and the heart (Rodríguez *et al*, 2012c, Slupecka *et al*, 2012, Yu *et al*, 2014, Pei *et al*, 2015). Mao and colleagues reported that ghrelin induces autophagy in the liver via the activation of the AMPK signalling pathway (Mao *et al*, 2015a), but the specific role of each isoform of the hormone remains unclear. Interestingly, *Mboat4*-knockout, mice lacking the gene encoding GOAT, show a marked reduction of hepatic autophagy during fasting, suggesting an important role of acylated ghrelin in the regulation of autophagy in the liver during energy depletion (Zhang *et al*, 2015). In addition, ghrelin induces hepatic autophagy to prevent further cell injury in animal models of acute hepatitis and liver fibrosis (Mao *et al*, 2015a). In the study II, acylated ghrelin increased *Atg5, Atg7* and the LC3B-II/I ratio and reduced p62 accumulation, while desacyl ghrelin only decreased p62 expression in hepatocytes, indicating that acylated ghrelin and, to a lesser extent, desacyl ghrelin stimulate hepatic autophagy (**Figure 14**).

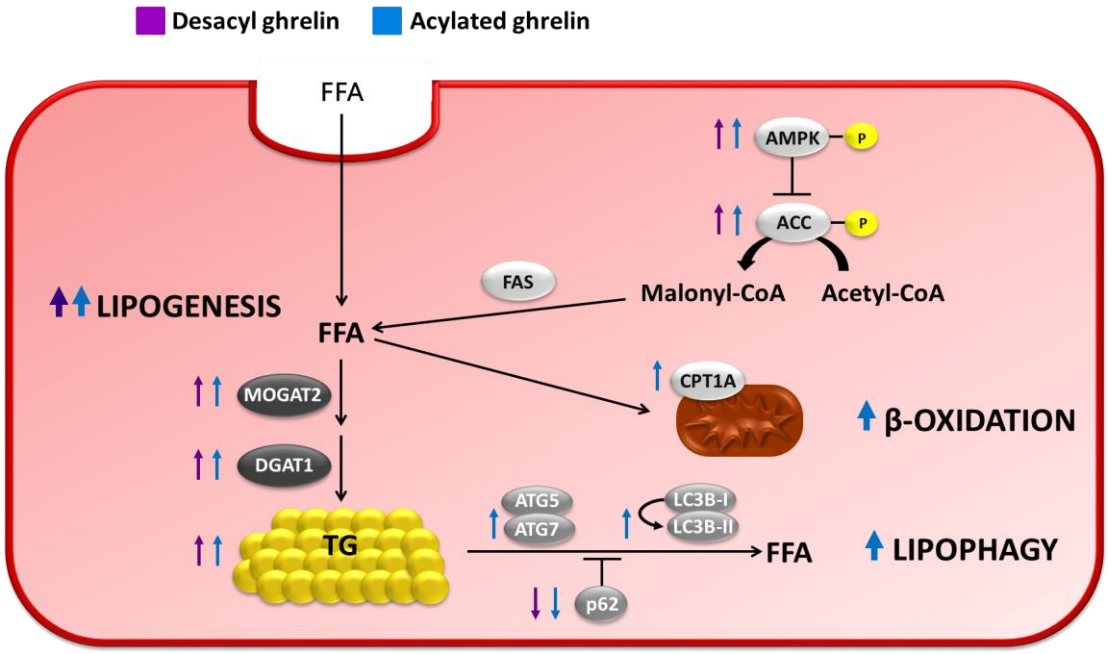


**Figure 14**. Effect of acylated and desacyl ghrelin on several factors involved in lipogenesis, β-oxidation and lipophagy.

Taken together, our findings suggest that the decrease in desacyl ghrelin after sleeve gastrectomy contributes to the reduction of lipogenesis, whereas the increased acylated ghrelin levels stimulate AMPK-activated mitochondrial FFA β-oxidation and autophagy in obese rats. These results support the notion that both ghrelin isoforms constitute key elements involved in the improvement of NAFLD after bariatric surgery.

## 6. Influence of sleeve gastrectomy and RYGB on hepatic inflammation in obesity

JNK signalling plays a crucial role in the initiation and progression of NAFLD, since JNK activation accelerates lipid accumulation and causes liver injury (Yan *et al*, 2017). Certain studies investigating the effect of bariatric surgery on obesity-associated hepatic inflammation have shown an improvement in mitochondrial dysfunction and ER stress as well as in the proinflammatory markers (Gregor *et al*, 2009, Mosinski *et al*, 2016, Sacks *et al*, 2018). In this regard, our study IV supports that both bariatric surgery procedures reduced proinflammatory JNK activation, the inflammation-related genes *Crp*, *Il6* and *Tnf* as well as inflammatory and apoptotic foci in the liver of obese rats. Sleeve gastrectomy reduced $CD68^{+}$ cells surrounding the portal vein, whereas RYGB decreased lobulillar macrophage infiltration compared to sham surgery. The caloric restriction induced by the reduction of the stomach size or intestine rerouting does not

sufficiently explain the post-surgical amelioration of hepatic inflammation. This observation is supported by the finding that pair-fed animals showed a mild reduction of hepatic inflammation compared with surgical groups. Thus, common endocrine changes resulting from the surgical procedures must be invoked (Koliaki *et al*, 2015).

Regarding the effect of bariatric surgery on mitochondrial dysfunction, it has been demonstrated that RYGB upregulates the hepatic expression of factors involved in mitochondrial biogenesis (PGC-1α, nuclear respiratory factors 1 and 2), fusion (mitofusin-1 and -2, and optic atrophy-1) and function (OXPHOS complexes I-V) in obese Sprague-Dawley rats (Peng and Murr, 2013, Sacks *et al*, 2018). Similarly, we observed an improvement of mitochondrial biogenesis and function in response to RYGB, evidenced by higher mtDNA and the OXPHOS complexes I and II in the liver of diet-induced obese rats. Moreover, sleeve gastrectomy effectively improved hepatic mitochondrial oxidative capacity, as shown by the upregulation of the OXPHOS complexes I-V. The lack of changes in the pair-fed groups also suggests that the upregulation of mitochondrial DNA and OXPHOS protein synthesis was caused independently of the surgically-induced caloric restriction.

Mitochondrial dysfunction can induce the accumulation of unfolded or misfolded proteins in the ER that is sensed by the chaperone GRP78 (Malhi and Kaufman, 2011). Interestingly, Gregor and colleagues reported that RYGB reduced the intense preoperative staining for GRP78 and phosphorylated eIF2α in liver sections of obese patients (Gregor *et al*, 2009). In line with this observation, we show that both bariatric surgical techniques, sleeve gastrectomy and RYGB, decreased the GRP78 protein at the same time as reducing the activation of the ER stress pathways PERK, IRE1 and ATF6, as well as in their downstream effectors. The absence of changes in the pair-fed groups indicated that the attenuation of ER stress after bariatric surgery was not related to food intake reduction. In summary, this study showed that the beneficial effect of bariatric surgery against the progression of NAFLD to NASH in the obese state was mediated through the mitigation of hepatic early inflammation, mitochondrial dysfunction and ER stress.

## 7. Role of ghrelin isoforms in the improvement of hepatic inflammation

Ghrelin acts as a survival factor for hepatocytes under lipotoxic and inflammatory conditions. In this sense, ghrelin treatment *in vitro* attenuates LPS-, palmitate- and TNF-α-induced hepatocyte apoptosis (Mao *et al*, 2016). In line with these observations, our study IV demonstrated that acylated ghrelin blunted palmitate-induced TG accumulation and inflammation in primary rat hepatocytes, as evidenced by the reduction in JNK activation as well as the decrease in the expression of proinflammatory markers, including *Crp*, *Il6* and *Tnf*.

We next investigated whether ghrelin improved mitochondrial OXPHOS respiration as a mechanism against the progression of NAFLD to NASH. In this regard, ghrelin promotes mitochondrial respiration and biogenesis in murine dopamine neurons in a UCP2-dependent manner (Andrews *et al*, 2009), murine C2C12 myocytes (Barazzoni *et al*, 2017) and rat kidney (Fujimura *et al*, 2014). Furthermore, a protective role of desacyl ghrelin against mitochondrial dysfunction has been also reported in a model of ischemia/reperfusion liver injury (Rossetti *et al*, 2017). However, Barazzoni and colleagues did not observe changes in hepatic mitochondrial oxidative enzyme activities after subcutaneous administration of ghrelin for 4 days in healthy rodents (Barazzoni *et al*, 2005). In the study IV, we found that palmitic acid treatment downregulated the mitochondrial OXPHOS protein subunits I-V in primary rat hepatocytes, which was reverted by the co-incubation with acylated ghrelin, and to a lesser extent, with desacyl ghrelin, supporting a defensive role of ghrelin isoforms against mitochondrial dysfunction induced by lipotoxicity. Furthermore, we observed that acylated and desacyl ghrelin diminished the protein expression of GRP78, suppressed phosphorylation of PERK, eIF2α and IRE1 as well as decreased *Atf4*, *Atf6* and *Chop* mRNA levels in palmitate-triggered UPR induction in hepatocytes. Given its demonstrated function inhibiting ER stress induced by tunicamycin or thapsigargin in primary rat cortical neurons (Chung *et al*, 2011), by ischemia/reperfusion injury in rat heart (Tian *et al*, 2018) and by sodium metabisulfite in the liver (Ercan *et al*, 2015), our data further confirm a protective role of ghrelin against lipid overload-induced ER stress by the suppression of UPR. Taken together, our findings suggest that the increased acylated ghrelin levels contributed, at least in part, to the reduction of JNK-induced inflammation and cell death, the improvement of mitochondrial oxidative capacity as well as the restoration of ER

homeostasis in steatotic hepatocytes after sleeve gastrectomy and RYGB. These results support the notion that ghrelin constitutes a key anti-inflammatory factor against NAFLD progression in obesity.

In the study III of the present thesis, we also studied the potential participation of ghrelin isoforms in TNF-α-induced cell death and we demonstrated, that acylated ghrelin and desacyl ghrelin inhibited the TNF-α-induced cleavage of caspase-8 and -3 and hepatocyte apoptosis in human HepG2 hepatocytes. This is consistent with our previous observation (Rodríguez *et al*, 2012c) that ghrelin isoforms reduced this proapoptotic signalling triggered by TNF-α in human visceral adipocytes. Analogously, Mao et al (Mao *et al*, 2016) recently revealed that ghrelin treatment attenuates the hepatocyte apoptosis induced by palmitic acid and LPS, two factors involved in liver injury associated with hyperlipidaemia and septic shock, respectively, through the inactivation of the proinflammatory JNK and P38 MAPK pathways and caspase 3. In line with this observation, both the administration of ghrelin to C57BL/6J mice fed a HFD (Mao *et al*, 2015a) and the administration of growth hormone-releasing peptide-2 (GHRP-2), a ghrelin receptor agonist, to LPS-treated rats (Granado *et al*, 2008) prevents the increase in transaminases and downregulates hepatic TNF-α expression, confirming the hepatic protective function of ghrelin in response to lipotoxicity and sepsis. In addition, we found that both ghrelin isoforms inhibited basal and TNF-α-induced HMGB1 expression and blocked caspase-1 autocatalytic activation induced by TNF-α, supporting their defensive role against pyroptosis also in hepatocytes. In this sense, ghrelin acts as an anti-inflammatory factor in experimental sepsis (Chorny *et al*, 2008) and myocardial ischemia/reperfusion injury (Sun *et al*, 2016) by inhibiting HMGB1. Acylated and desacyl ghrelin also blunted TNF-α-induced autophagy in human hepatocytes, acting as a protective agent against injury induced by TNF-α during an inflammatory state, which is also observed in human visceral adipocytes (Rodríguez *et al*, 2012c) (**Figure 15**). In conclusion, it seems plausible that the relative increase in acylated ghrelin levels contributes to the post-surgical amelioration of hepatic steatosis and inflammation. The increased acylated/desacyl ghrelin ratio in patients with obesity and NAFLD might constitute a compensatory mechanism to overcome TNF-α-induced hepatocyte apoptosis, autophagy and pyroptosis. The imbalance of ghrelin isoforms and TNF-α in the insulin-resistant state may contribute to the increased hepatocyte cell death found in T2D.

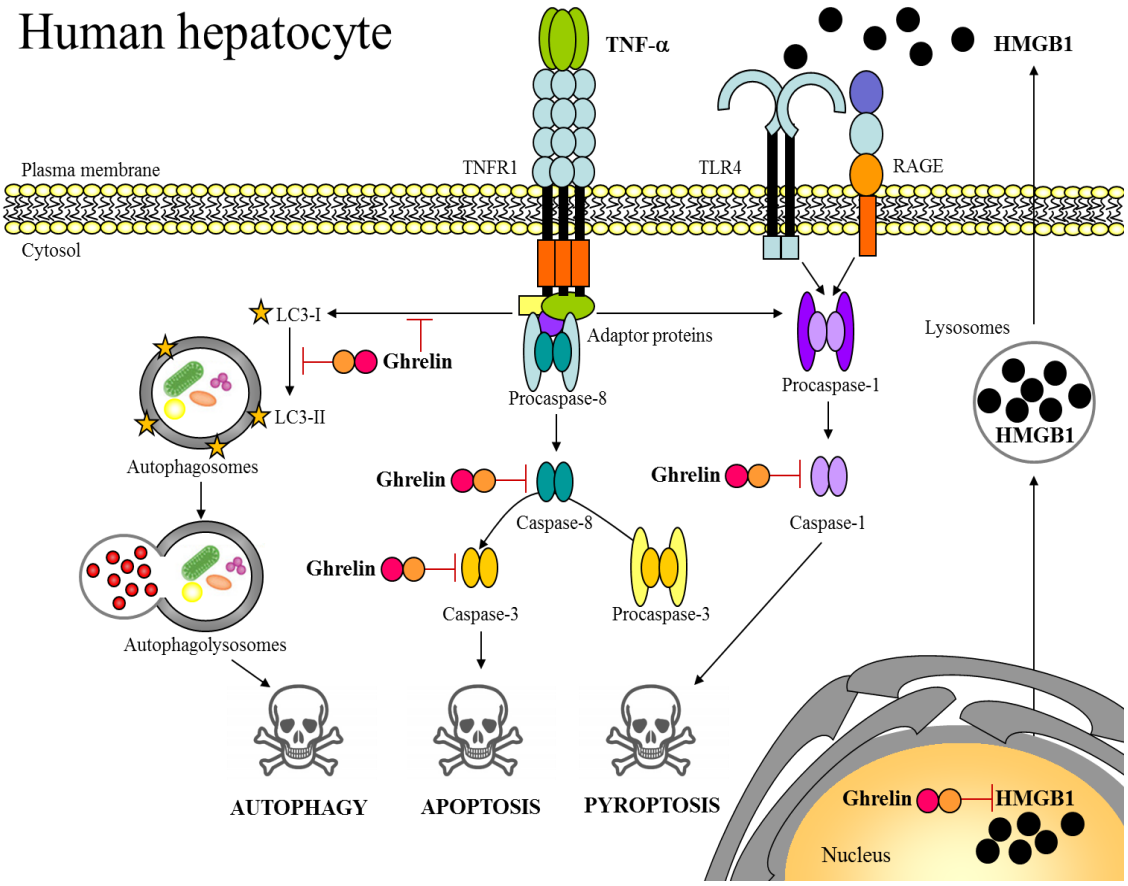


**Figure 15**. Effect of acylated and desacyl ghrelin on TNF-induced human hepatocyte cell death.

# Conclusions

1. Sleeve gastrectomy and RYGB protect against NAFLD progression through the reduction of hepatosteatosis, as well as the downregulation of factors involved in inflammation, mitochondrial dysfunction and ER stress.

2. Sleeve gastrectomy and RYGB dramatically reduce plasma desacyl ghrelin levels, without changes in acylated ghrelin concentrations in a model of diet-induced obesity. Nonetheless, both surgical procedures induce an increase in the acylated/desacyl ghrelin ratio in obese rats. By contrast, in patients with morbid obesity, desacyl and acylated ghrelin as well as the acylated/desacyl ghrelin ratio were decreased after bariatric surgery.

3. Both acylated and desacyl ghrelin promote lipogenesis in the liver, but acylated ghrelin also triggers mechanisms against lipotoxicity, such as the activation of mitochondrial FFA β-oxidation and autophagy. Therefore, the decrease in desacyl ghrelin participates in the reduction of hepatic lipogenesis after surgery, whereas the increased relative acylated ghrelin levels contribute to the post-surgical induction of AMPK-related mitochondrial FFA β-oxidation and autophagy in diet-induced obese rats.

4. Acylated ghrelin and desacyl ghrelin act as hepatoprotective factors by inhibiting the TNF-α-induced cleavage of caspase-8 and -3 and hepatocyte apoptosis. TNF-α also activates autophagy, probably due to the cellular collapse induced by liver injury, with acylated ghrelin reducing the autophagic flux induced by TNF-α. Finally, both ghrelin isoforms inhibit TNF-α-induced HMGB1 expression and blocked caspase-1 autocatalytic activation induced by TNF-α, supporting their protective role against pyroptosis in human hepatocytes.

5. Acylated and desacyl ghrelin alleviate palmitate-triggered inflammation, mitochondrial dysfunction as well as UPR induction. Thus, the relative increase in acylated ghrelin after sleeve gastrectomy and RYGB contributes to the reduction of JNK-induced inflammation and cell death, the improvement of mitochondrial oxidative capacity as well as the restoration of ER homeostasis in steatotic hepatocytes.

## Concluding remarks

Sleeve gastrectomy and RYGB constitute effective techniques to improve obesity-associated NAFLD. Our results identify ghrelin isoforms as key elements in mediating the beneficial effects of both bariatric surgeries via the regulation of hepatic TG accumulation and inflammation, hallmarks of NAFLD. Although acylated and desacyl ghrelin increase lipogenesis, both isoforms prevent lipotoxicity via the induction of β-oxidation and autophagy. In addition, they act as anti-inflammatory and survival factors under lipotoxic and inflammatory conditions. Therefore, the imbalance of ghrelin isoforms and TNF-α may contribute to the increased hepatocyte steatosis, inflammation and cell death found in the obese and insulin-resistant states. In this regard, the relative increase in acylated ghrelin after sleeve gastrectomy and RYGB might contribute, in part, to the amelioration of NAFLD and its progression to NASH in the obese state.

# Bibliography

Al Massadi O, López M, Tschöp M, Diéguez C, Nogueiras R. Current understanding of the hypothalamic ghrelin pathways inducing appetite and adiposity. *Trends Neurosci* 2017;40:167-80.

Al Massadi O, Müller T, Tschöp M, Diéguez C, Nogueiras R. Ghrelin and LEAP-2: Rivals in energy metabolism. *Trends Pharmacol Sci* 2018;39:685-94.

Al Massadi O, Nogueiras R, Diéguez C, Girault JA. Ghrelin and food reward. *Neuropharmacology* 2019;148:131-38.

Alamri BN, Shin K, Chappe V, Anini Y. The role of ghrelin in the regulation of glucose homeostasis. *Horm Mol Biol Clin Investig* 2016;26:3-11.

Álvarez-Leite JI. Nutrient deficiencies secondary to bariatric surgery. *Curr Opin Clin Nutr Metab Care* 2004;7:569-75.

Andrews ZB, Erion D, Beiler R, Liu ZW, Abizaid A, Zigman J, Elsworth JD, Savitt JM, DiMarchi R, Tschoep M, Roth RH, Gao XB, Horvath TL. Ghrelin promotes and protects nigrostriatal dopamine function via a UCP2-dependent mitochondrial mechanism. *J Neurosci* 2009;29:14057-65.

Anstee QM, Day CP. The genetics of NAFLD. *Nat Rev Gastroenterol Hepatol* 2013;10:645-55.

Anthes E. Treatment: Marginal gains. *Nature* 2014;508:S54-6.

Asrani SK. Incorporation of noninvasive measures of liver fibrosis into clinical practice: Diagnosis and prognosis. *Clin Gastroenterol Hepatol* 2015;13:2190-204.

Atkinson RL. Current status of the field of obesity. *Trends Endocrinol Metab* 2014;25:283-4.

Baiceanu A, Mesdom P, Lagouge M, Foufelle F. Endoplasmic reticulum proteostasis in hepatic steatosis. *Nat Rev Endocrinol* 2016;12:710-22.

Ballestri S, Nascimbeni F, Baldelli E, Marrazzo A, Romagnoli D, Lonardo A. NAFLD as a sexual dimorphic disease: Role of gender and reproductive status in the development and progression of nonalcoholic fatty liver disease and inherent cardiovascular risk. *Adv Ther* 2017;34:1291-326.

Baragli A, Ghe C, Arnoletti E, Granata R, Ghigo E, Muccioli G. Acylated and unacylated ghrelin attenuate isoproterenol-induced lipolysis in isolated rat visceral adipocytes through activation of phosphoinositide 3-kinase gamma and phosphodiesterase 3B. *Biochim Biophys Acta* 2011;1811:386-96.

Barazzoni R, Bosutti A, Stebel M, Cattin MR, Roder E, Visintin L, Cattin L, Biolo G, Zanetti M, Guarnieri G. Ghrelin regulates mitochondrial-lipid metabolism gene expression and tissue fat distribution in liver and skeletal muscle. *Am J Physiol Endocrinol Metab* 2005;288:E228-35.

Barazzoni R, Zanetti M, Nagliati C, Cattin MR, Ferreira C, Giuricin M, Palmisano S, Edalucci E, Dore F, Guarnieri G, de Manzini N. Gastric bypass does not normalize obesity-related changes in ghrelin profile and leads to higher acylated ghrelin fraction. *Obesity* 2013;21:718-22.

Barazzoni R, Semolic A, Cattin MR, Zanetti M, Guarnieri G. Acylated ghrelin limits fat accumulation and improves redox state and inflammation markers in the liver of high-fat-fed rats. *Obesity* 2014;22:170-7.

Barazzoni R, Gortan Cappellari G, Palus S, Vinci P, Ruozi G, Zanetti M, Semolic A, Ebner N, von Haehling S, Sinagra G, Giacca M, Springer J. Acylated ghrelin treatment normalizes skeletal muscle mitochondrial oxidative capacity and AKT phosphorylation in rat chronic heart failure. *J Cachexia Sarcopenia Muscle* 2017;8:991-98.

Barker KB, Palekar NA, Bowers SP, Goldberg JE, Pulcini JP, Harrison SA. Non-alcoholic steatohepatitis: effect of Roux-en-Y gastric bypass surgery. *Am J Gastroenterol* 2006;101:368-73.

Barnett BP, Hwang Y, Taylor MS, Kirchner H, Pfluger PT, Bernard V, Lin YY, Bowers EM, Mukherjee C, Song WJ, Longo PA, Leahy DJ, Hussain MA, Tschöp MH, Boeke JD, Cole PA. Glucose and weight control in mice with a designed ghrelin O-acyltransferase inhibitor. *Science* 2010;330:1689-92.

Begriche K, Igoudjil A, Pessayre D, Fromenty B. Mitochondrial dysfunction in NASH: causes, consequences and possible means to prevent it. *Mitochondrion* 2006;6:1-28.

Beiroa D, Imbernon M, Gallego R, Senra A, Herranz D, Villarroya F, Serrano M, Fernø J, Salvador J, Escalada J, Diéguez C, López M, Frühbeck G, Nogueiras R. GLP-1 agonism stimulates brown adipose tissue thermogenesis and browning through hypothalamic AMPK. *Diabetes* 2014;63:3346-58.

Ben-Shlomo S, Zvibel I, Shnell M, Shlomai A, Chepurko E, Halpern Z, Barzilai N, Oren R, Fishman S. Glucagon-like peptide-1 reduces hepatic lipogenesis via activation of AMP-activated protein kinase. *J Hepatol* 2011;54:1214-23.

Benjamin A, Zubajlo RE, Dhyani M, Samir AE, Thomenius KE, Grajo JR, Anthony BW. Surgery for obesity and related diseases: I. A novel approach to the quantification of the longitudinal speed of sound and its potential for tissue characterization. *Ultrasound Med Biol* 2018;44:2739-48.

Bertolotti A, Zhang Y, Hendershot LM, Harding HP, Ron D. Dynamic interaction of BiP and ER stress transducers in the unfolded-protein response. *Nat Cell Biol* 2000;2:326-32.

Birkmeyer JD, Finks JF, O'Reilly A, Oerline M, Carlin AM, Nunn AR, Dimick J, Banerjee M, Birkmeyer NJ. Surgical skill and complication rates after bariatric surgery. *N Engl J Med* 2013;369:1434-42.

Bjornsson OG, Sparks JD, Sparks CE, Gibbons GF. Regulation of VLDL secretion in primary culture of rat hepatocytes: involvement of cAMP and cAMP-dependent protein kinases. *Eur J Clin Invest* 1994;24:137-48.

Blundell JE, Dulloo AG, Salvador J, Frühbeck G. Beyond BMI--phenotyping the obesities. *Obes Facts* 2014;7:322-8.

Bray GA, Frühbeck G, Ryan DH, Wilding JP. Management of obesity. *Lancet* 2016;387:1947-56.

Brenner C, Galluzzi L, Kepp O, Kroemer G. Decoding cell death signals in liver inflammation. *J Hepatol* 2013;59:583-94.

Broglio F, Arvat E, Benso A, Gottero C, Muccioli G, Papotti M, van der Lely AJ, Deghenghi R, Ghigo E. Ghrelin, a natural GH secretagogue produced by the stomach, induces hyperglycemia and reduces insulin secretion in humans. *J Clin Endocrinol Metab* 2001;86:5083-6.

Broglio F, Gottero C, Prodam F, Destefanis S, Gauna C, Me E, Riganti F, Vivenza D, Rapa A, Martina V, Arvat E, Bona G, van der Lely AJ, Ghigo E. Ghrelin secretion is

inhibited by glucose load and insulin-induced hypoglycaemia but unaffected by glucagon and arginine in humans. *Clin Endocrinol* 2004;61:503-9.

Browning JD, Horton JD. Molecular mediators of hepatic steatosis and liver injury. *J Clin Invest* 2004;114:147-52.

Brunt EM, Kleiner DE, Wilson LA, Belt P, Neuschwander-Tetri BA. Nonalcoholic fatty liver disease (NAFLD) activity score and the histopathologic diagnosis in NAFLD: distinct clinicopathologic meanings. *Hepatology* 2011;53:810-20.

Bugianesi E, Gastaldelli A, Vanni E, Gambino R, Cassader M, Baldi S, Ponti V, Pagano G, Ferrannini E, Rizzetto M. Insulin resistance in non-diabetic patients with non-alcoholic fatty liver disease: sites and mechanisms. *Diabetologia* 2005;48:634-42.

Burcelin R, Gourdy P, Dalle S. GLP-1-based strategies: a physiological analysis of differential mode of action. *Physiology* 2014;29:108-21.

Burza MA, Romeo S, Kotronen A, Svensson PA, Sjöholm K, Torgerson JS, Lindroos AK, Sjöström L, Carlsson LM, Peltonen M. Long-term effect of bariatric surgery on liver enzymes in the Swedish Obese Subjects (SOS) study. *PLoS One* 2013;8:e60495.

Buzzetti E, Pinzani M, Tsochatzis EA. The multiple-hit pathogenesis of non-alcoholic fatty liver disease (NAFLD). *Metabolism* 2016;65:1038-48.

Caballería L, Pera G, Auladell MA, Toran P, Muñoz L, Miranda D, Alumà A, Casas JD, Sánchez C, Gil D, Aubà J, Tibau A, Canut S, Bernad J, Aizpurua MM. Prevalence and factors associated with the presence of nonalcoholic fatty liver disease in an adult population in Spain. *Eur J Gastroenterol Hepatol* 2010;22:24-32.

Caesar R, Tremaroli V, Kovatcheva-Datchary P, Cani PD, Backhed F. Crosstalk between gut microbiota and dietary lipids aggravates WAT inflammation through TLR signaling. *Cell Metab* 2015;22:658-68.

Callaghan B, Furness JB. Novel and conventional receptors for ghrelin, desacyl-ghrelin, and pharmacologically related compounds. *Pharmacol Rev* 2014;66:984-1001.

Camhi SM, Bray GA, Bouchard C, Greenway FL, Johnson WD, Newton RL, Ravussin E, Ryan DH, Smith SR, Katzmarzyk PT. The relationship of waist circumference and BMI to visceral, subcutaneous, and total body fat: sex and race differences. *Obesity* 2011;19:402-8.

Canbay A, Friedman S, Gores GJ. Apoptosis: the nexus of liver injury and fibrosis. *Hepatology* 2004;39:273-8.

Castera L, Friedrich-Rust M, Loomba R. Non-invasive assessment of liver disease in patients with NAFLD. *Gastroenterology* 2019;

Catalán V, Gómez-Ambrosi J, Rotellar F, Silva C, Gil MJ, Rodríguez A, Cienfuegos JA, Salvador J, Frühbeck G. The obestatin receptor (GPR39) is expressed in human adipose tissue and is down-regulated in obesity-associated type 2 diabetes mellitus. *Clin Endocrinol* 2007;66:598-601.

Clark JM, Alkhuraishi AR, Solga SF, Alli P, Diehl AM, Magnuson TH. Roux-en-Y gastric bypass improves liver histology in patients with non-alcoholic fatty liver disease. *Obes Res* 2005;13:1180-6.

Claudio N, Dalet A, Gatti E, Pierre P. Mapping the crossroads of immune activation and cellular stress response pathways. *EMBO J* 2013;32:1214-24.

Cookson BT, Brennan MA. Pro-inflammatory programmed cell death. *Trends Microbiol* 2001;9:113-4.

Cowan E, Kumar P, Burch KJ, Grieve DJ, Green BD, Graham SF. Treatment of lean and diet-induced obesity (DIO) mice with a novel stable obestatin analogue alters plasma metabolite levels as detected by untargeted LC-MS metabolomics. *Metabolomics* 2016;12:124.

Cowley MA, Smith RG, Diano S, Tschöp M, Pronchuk N, Grove KL, Strasburger CJ, Bidlingmaier M, Esterman M, Heiman ML, García-Segura LM, Nillni EA, Méndez P, Low MJ, Sotonyi P, Friedman JM, Liu H, Pinto S, Colmers WF, Cone RD, Horvath TL. The distribution and mechanism of action of ghrelin in the CNS demonstrates a novel hypothalamic circuit regulating energy homeostasis. *Neuron* 2003;37:649-61.

Crespo J, Cayon A, Fernández-Gil P, Hernández-Guerra M, Mayorga M, Domínguez-Díez A, Fernández-Escalante JC, Pons-Romero F. Gene expression of tumor necrosis factor alpha and TNF-receptors, p55 and p75, in nonalcoholic steatohepatitis patients. *Hepatology* 2001;34:1158-63.

Croci I, Byrne NM, Choquette S, Hills AP, Chachay VS, Clouston AD, O'Moore-Sullivan TM, Macdonald GA, Prins JB, Hickman IJ. Whole-body substrate metabolism is associated with disease severity in patients with non-alcoholic fatty liver disease. *Gut* 2013;62:1625-33.

Crujeiras AB, Goyenechea E, Abete I, Lage M, Carreira MC, Martínez JA, Casanueva FF. Weight regain after a diet-induced loss is predicted by higher baseline leptin and lower ghrelin plasma levels. *J Clin Endocrinol Metab* 2010;95:5037-44.

Cummings DE, Purnell JQ, Frayo RS, Schmidova K, Wisse BE, Weigle DS. A preprandial rise in plasma ghrelin levels suggests a role in meal initiation in humans. *Diabetes* 2001;50:1714-9.

Cummings DE, Weigle DS, Frayo RS, Breen PA, Ma MK, Dellinger EP, Purnell JQ. Plasma ghrelin levels after diet-induced weight loss or gastric bypass surgery. *N Engl J Med* 2002;346:1623-30.

Cypess AM, Lehman S, Williams G, Tal I, Rodman D, Goldfine AB, Kuo FC, Palmer EL, Tseng YH, Doria A, Kolodny GM, Kahn CR. Identification and importance of brown adipose tissue in adult humans. *N Engl J Med* 2009;360:1509-17.

Chalasani N, Younossi Z, Lavine JE, Diehl AM, Brunt EM, Cusi K, Charlton M, Sanyal AJ. The diagnosis and management of non-alcoholic fatty liver disease: practice Guideline by the American Association for the Study of Liver Diseases, American College of Gastroenterology, and the American Gastroenterological Association. *Hepatology* 2012;55:2005-23.

Chan YK, Estaki M, Gibson DL. Clinical consequences of diet-induced dysbiosis. *Ann Nutr Metab* 2013;63 Suppl 2:28-40.

Chang E, Kim L, Park SE, Rhee EJ, Lee WY, Oh KW, Park SW, Park CY. Ezetimibe improves hepatic steatosis in relation to autophagy in obese and diabetic rats. *World J Gastroenterol* 2015;21:7754-63.

Chávez-Talavera O, Tailleux A, Lefebvre P, Staels B. Bile acid control of metabolism and inflammation in obesity, type 2 diabetes, dyslipidemia, and nonalcoholic fatty liver disease. *Gastroenterology* 2017;152:1679-94 e3.

Chen CY, Asakawa A, Fujimiya M, Lee SD, Inui A. Ghrelin gene products and the regulation of food intake and gut motility. *Pharmacol Rev* 2009;61:430-81.

Chen HY, Trumbauer ME, Chen AS, Weingarth DT, Adams JR, Frazier EG, Shen Z, Marsh DJ, Feighner SD, Guan XM, Ye Z, Nargund RP, Smith RG, Van der Ploeg LH, Howard AD, MacNeil DJ, Qian S. Orexigenic action of peripheral ghrelin is mediated by neuropeptide Y and agouti-related protein. *Endocrinology* 2004;145:2607-12.

Chen M, Huang W, Wang C, Nie H, Li G, Sun T, Yang F, Zhang Y, Shu K, Gong Q. High-mobility group box 1 exacerbates CCl(4)-induced acute liver injury in mice. *Clin Immunol* 2014;153:56-63.

Chen VP, Gao Y, Geng L, Brimijoin S. Butyrylcholinesterase regulates central ghrelin signaling and has an impact on food intake and glucose homeostasis. *Int J Obes* 2017;41:1413-19.

Chirieac DV, Cianci J, Collins HL, Sparks JD, Sparks CE. Insulin suppression of VLDL apo B secretion is not mediated by the LDL receptor. *Biochem Biophys Res Commun* 2002;297:134-7.

Chondronikola M, Porter C, Malagaris I, Nella AA, Sidossis LS. Brown adipose tissue is associated with systemic concentrations of peptides secreted from the gastrointestinal system and involved in appetite regulation. *Eur J Endocrinol* 2017;177:33-40.

Chorny A, Anderson P, González-Rey E, Delgado M. Ghrelin protects against experimental sepsis by inhibiting high-mobility group box 1 release and by killing bacteria. *J Immunol* 2008;180:8369-77.

Chung H, Chung HY, Bae CW, Kim CJ, Park S. Ghrelin suppresses tunicamycin- or thapsigargin-triggered endoplasmic reticulum stress-mediated apoptosis in primary cultured rat cortical neuronal cells. *Endocr J* 2011;58:409-20.

Dara L, Ji C, Kaplowitz N. The contribution of endoplasmic reticulum stress to liver diseases. *Hepatology* 2011;53:1752-63.

Dasarathy S, Dasarathy J, Khiyami A, Joseph R, López R, McCullough AJ. Validity of real time ultrasound in the diagnosis of hepatic steatosis: a prospective study. *J Hepatol* 2009;51:1061-7.

Dasarathy S, Yang Y, McCullough AJ, Marczewski S, Bennett C, Kalhan SC. Elevated hepatic fatty acid oxidation, high plasma fibroblast growth factor 21, and fasting bile acids in nonalcoholic steatohepatitis. *Eur J Gastroenterol Hepatol* 2011;23:382-8.

Date Y, Kojima M, Hosoda H, Sawaguchi A, Mondal MS, Suganuma T, Matsukura S, Kangawa K, Nakazato M. Ghrelin, a novel growth hormone-releasing acylated peptide, is synthesized in a distinct endocrine cell type in the gastrointestinal tracts of rats and humans. *Endocrinology* 2000;141:4255-61.

Date Y, Nakazato M, Hashiguchi S, Dezaki K, Mondal MS, Hosoda H, Kojima M, Kangawa K, Arima T, Matsuo H, Yada T, Matsukura S. Ghrelin is present in pancreatic alpha-cells of humans and rats and stimulates insulin secretion. *Diabetes* 2002;51:124-9.

Davies JS, Kotokorpi P, Eccles SR, Barnes SK, Tokarczuk PF, Allen SK, Whitworth HS, Guschina IA, Evans BA, Mode A, Zigman JM, Wells T. Ghrelin induces abdominal obesity via GHS-R-dependent lipid retention. *Mol Endocrinol* 2009;23:914-24.

De Minicis S, Seki E, Uchinami H, Kluwe J, Zhang Y, Brenner DA, Schwabe RF. Gene expression profiles during hepatic stellate cell activation in culture and in vivo. *Gastroenterology* 2007;132:1937-46.

De Vriese C, Gregoire F, Lema-Kisoka R, Waelbroeck M, Robberecht P, Delporte C. Ghrelin degradation by serum and tissue homogenates: identification of the cleavage sites. *Endocrinology* 2004;145:4997-5005.

Degterev A, Huang Z, Boyce M, Li Y, Jagtap P, Mizushima N, Cuny GD, Mitchison TJ, Moskowitz MA, Yuan J. Chemical inhibitor of nonapoptotic cell death with therapeutic potential for ischemic brain injury. *Nat Chem Biol* 2005;1:112-9.

Deitel M, Crosby RD, Gagner M. The First International Consensus Summit for Sleeve Gastrectomy (SG), New York City, October 25-27, 2007. *Obes Surg* 2008;18:487-96.

DeMaria EJ. Bariatric surgery for morbid obesity. *N Engl J Med* 2007;356:2176-83.

Desvergne B, Wahli W. Peroxisome proliferator-activated receptors: nuclear control of metabolism. *Endocr Rev* 1999;20:649-88.

Dezaki K, Hosoda H, Kakei M, Hashiguchi S, Watanabe M, Kangawa K, Yada T. Endogenous ghrelin in pancreatic islets restricts insulin release by attenuating Ca2+ signaling in beta-cells: implication in the glycemic control in rodents. *Diabetes* 2004;53:3142-51.

Diéguez C, Vázquez MJ, Romero A, López M, Nogueiras R. Hypothalamic control of lipid metabolism: focus on leptin, ghrelin and melanocortins. *Neuroendocrinology* 2011;94:1-11.

Ding WX, Yin XM. Dissection of the multiple mechanisms of TNF-alpha-induced apoptosis in liver injury. *J Cell Mol Med* 2004;8:445-54.

Dirksen C, Jørgensen NB, Bojsen-Møller KN, Jacobsen SH, Hansen DL, Worm D, Holst JJ, Madsbad S. Mechanisms of improved glycaemic control after Roux-en-Y gastric bypass. *Diabetologia* 2012;55:1890-901.

Donnelly KL, Smith CI, Schwarzenberg SJ, Jessurun J, Boldt MD, Parks EJ. Sources of fatty acids stored in liver and secreted via lipoproteins in patients with nonalcoholic fatty liver disease. *J Clin Invest* 2005;115:1343-51.

Dornonville de la Cour C, Björkqvist M, Sandvik AK, Bakke I, Zhao CM, Chen D, Håkanson R. A-like cells in the rat stomach contain ghrelin and do not operate under gastrin control. *Regul Pept* 2001;99:141-50.

Ducheix S, Vegliante MC, Villani G, Napoli N, Sabba C, Moschetta A. Is hepatic lipogenesis fundamental for NAFLD/NASH? A focus on the nuclear receptor coactivator PGC-1beta. *Cell Mol Life Sci* 2016;73:3809-22.

Eaton S, Bartlett K, Pourfarzam M. Mammalian mitochondrial beta-oxidation. *Biochem J* 1996;320 345-57.

Eguchi A, Wree A, Feldstein AE. Biomarkers of liver cell death. *J Hepatol* 2014;60:1063-74.

Einer C, Hohenester S, Wimmer R, Wottke L, Artmann R, Schulz S, Gosmann C, Simmons A, Leitzinger C, Eberhagen C, Borchard S, Schmitt S, Hauck SM, von Toerne C, Jastroch M, Walheim E, Rust C, Gerbes AL, Popper B, Mayr D, Schnurr M, Vollmar AM, Denk G, Zischka H. Mitochondrial adaptation in steatotic mice. *Mitochondrion* 2018;40:1-12.

Elam MB, Wilcox HG, Solomon SS, Heimberg M. In vivo growth hormone treatment stimulates secretion of very low density lipoprotein by the isolated perfused rat liver. *Endocrinology* 1992;131:2717-22.

Elsharkawy AM, Mann DA. Nuclear factor-kappaB and the hepatic inflammation-fibrosis-cancer axis. *Hepatology* 2007;46:590-7.

Ercan S, Kencebay C, Basaranlar G, Derin N, Aslan M. Induction of xanthine oxidase activity, endoplasmic reticulum stress and caspase activation by sodium metabisulfite in rat liver and their attenuation by Ghrelin. *Food Chem Toxicol* 2015;76:27-32.

Ertunc ME, Hotamisligil GS. Lipid signaling and lipotoxicity in metaflammation: indications for metabolic disease pathogenesis and treatment. *J Lipid Res* 2016;57:2099-114.

Eslam M, Valenti L, Romeo S. Genetics and epigenetics of NAFLD and NASH: Clinical impact. *J Hepatol* 2018;68:268-79.

Estep M, Abawi M, Jarrar M, Wang L, Stepanova M, Elariny H, Moazez A, Goodman Z, Chandhoke V, Baranova A, Younossi ZM. Association of obestatin, ghrelin, and inflammatory cytokines in obese patients with non-alcoholic fatty liver disease. *Obes Surg* 2011;21:1750-7.

European Association for the Study of the Liver (EASL), European Association for the Study of Diabetes (EASD), European Association for the Study of Obesity (EASO). EASL-EASD-EASO Clinical Practice Guidelines for the management of non-alcoholic fatty liver disease. *J Hepatol* 2016;64:1388-402.

Fabbrini E, Sullivan S, Klein S. Obesity and nonalcoholic fatty liver disease: biochemical, metabolic, and clinical implications. *Hepatology* 2010;51:679-89.

Farah BL, Landau DJ, Sinha RA, Brooks ED, Wu Y, Fung SYS, Tanaka T, Hirayama M, Bay BH, Koeberl DD, Yen PM. Induction of autophagy improves hepatic lipid metabolism in glucose-6-phosphatase deficiency. *J Hepatol* 2016;64:370-79.

Fazel Y, Koenig AB, Sayiner M, Goodman ZD, Younossi ZM. Epidemiology and natural history of non-alcoholic fatty liver disease. *Metabolism* 2016;65:1017-25.

Federico A, Dallio M, Godos J, Loguercio C, Salomone F. Targeting gut-liver axis for the treatment of nonalcoholic steatohepatitis: translational and clinical evidence. *Transl Res* 2016;167:116-24.

Finocchietto PV, Holod S, Barreyro F, Peralta JG, Alippe Y, Giovambattista A, Carreras MC, Poderoso JJ. Defective leptin-AMP-dependent kinase pathway induces nitric oxide release and contributes to mitochondrial dysfunction and obesity in ob/ob mice. *Antioxid Redox Signal* 2011;15:2395-406.

Flum DR, Belle SH, King WC, Wahed AS, Berk P, Chapman W, Pories W, Courcoulas A, McCloskey C, Mitchell J, Patterson E, Pomp A, Staten MA, Yanovski SZ, Thirlby R, Wolfe B. Perioperative safety in the longitudinal assessment of bariatric surgery. *N Engl J Med* 2009;361:445-54.

Foster-Schubert KE, Overduin J, Prudom CE, Liu J, Callahan HS, Gaylinn BD, Thorner MO, Cummings DE. Acyl and total ghrelin are suppressed strongly by ingested proteins, weakly by lipids, and biphasically by carbohydrates. *J Clin Endocrinol Metab* 2008;93:1971-9.

Fried M, Yumuk V, Oppert JM, Scopinaro N, Torres AJ, Weiner R, Yashkov Y, Frühbeck G. Interdisciplinary European Guidelines on metabolic and bariatric surgery. *Obes Facts* 2013;6:449-68.

Fried M, Yumuk V, Oppert JM, Scopinaro N, Torres A, Weiner R, Yashkov Y, Frühbeck G. Interdisciplinary European guidelines on metabolic and bariatric surgery. *Obes Surg* 2014;24:42-55.

Frühbeck G, Gómez-Ambrosi J. Control of body weight: a physiologic and transgenic perspective. *Diabetologia* 2003;46:143-72.

Frühbeck G, Díez-Caballero A, Gil MJ, Montero I, Gómez-Ambrosi J, Salvador J, Cienfuegos JA. The decrease in plasma ghrelin concentrations following bariatric surgery depends on the functional integrity of the fundus. *Obes Surg* 2004a;14:606-12.

Frühbeck G, Díez Caballero A, Gil MJ. Fundus functionality and ghrelin concentrations after bariatric surgery. *N Engl J Med* 2004b;350:308-9.

Frühbeck G, Becerril S, Sáinz N, Garrastachu P, García-Velloso MJ. BAT: a new target for human obesity? *Trends Pharmacol Sci* 2009;30:387-96.

Frühbeck G, Gómez-Ambrosi J. Adipose tissue: structure, function and metabolism. In: Caballero B, editor. Encyclopedia of human nutrition. 3rd edition ed: Elsevier Ltd; 2013. p. 1-13.

Frühbeck G, Toplak H, Woodward E, Yumuk V, Maislos M, Oppert JM, Executive committee of the European Association for the Study of Obesity. Obesity: the gateway to ill health - an EASO position statement on a rising public health, clinical and scientific challenge in Europe. *Obes Facts* 2013;6:117-20.

Frühbeck G, Méndez-Giménez L, Fernández-Formoso JA, Fernández S, Rodríguez A. Regulation of adipocyte lipolysis. *Nutr Res Rev* 2014;27:63-93.

Frühbeck G. Bariatric and metabolic surgery: a shift in eligibility and success criteria. *Nat Rev Endocrinol* 2015;11:465-77.

Fu S, Watkins SM, Hotamisligil GS. The role of endoplasmic reticulum in hepatic lipid homeostasis and stress signaling. *Cell Metab* 2012;15:623-34.

Fujimura K, Wakino S, Minakuchi H, Hasegawa K, Hosoya K, Komatsu M, Kaneko Y, Shinozuka K, Washida N, Kanda T, Tokuyama H, Hayashi K, Itoh H. Ghrelin protects against renal damages induced by angiotensin-II via an antioxidative stress mechanism in mice. *PLoS One* 2014;9:e94373.

Fujita K, Nozaki Y, Wada K, Yoneda M, Fujimoto Y, Fujitake M, Endo H, Takahashi H, Inamori M, Kobayashi N, Kirikoshi H, Kubota K, Saito S, Nakajima A. Dysfunctional very-low-density lipoprotein synthesis and release is a key factor in nonalcoholic steatohepatitis pathogenesis. *Hepatology* 2009;50:772-80.

Furet JP, Kong LC, Tap J, Poitou C, Basdevant A, Bouillot JL, Mariat D, Corthier G, Dore J, Henegar C, Rizkalla S, Clement K. Differential adaptation of human gut microbiota to bariatric surgery-induced weight loss: links with metabolic and low-grade inflammation markers. *Diabetes* 2010;59:3049-57.

Gahete MD, Córdoba-Chacón J, Salvatori R, Castano JP, Kineman RD, Luque RM. Metabolic regulation of ghrelin *O*-acyl transferase (GOAT) expression in the mouse hypothalamus, pituitary, and stomach. *Mol Cell Endocrinol* 2010;317:154-60.

Gallagher D, Heymsfield SB, Heo M, Jebb SA, Murgatroyd PR, Sakamoto Y. Healthy percentage body fat ranges: an approach for developing guidelines based on body mass index. *Am J Clin Nutr* 2000;72:694-701.

Gan LT, Van Rooyen DM, Koina ME, McCuskey RS, Teoh NC, Farrell GC. Hepatocyte free cholesterol lipotoxicity results from JNK1-mediated mitochondrial injury and is HMGB1 and TLR4-dependent. *J Hepatol* 2014;61:1376-84.

García-Marirrodriga I, Amaya-Romero C, Ruiz-Díaz GP, Fernández S, Ballesta-López C, Pou JM, Romeo JH, Vilahur G, Vilhur G, Badimon L, Ybarra J. Evolution of lipid profiles after bariatric surgery. *Obes Surg* 2012;22:609-16.

Gardella S, Andrei C, Ferrera D, Lotti LV, Torrisi MR, Bianchi ME, Rubartelli A. The nuclear protein HMGB1 is secreted by monocytes via a non-classical, vesicle-mediated secretory pathway. *EMBO Rep* 2002;3:995-1001.

Gauna C, Meyler FM, Janssen JA, Delhanty PJ, Abribat T, van Koetsveld P, Hofland LJ, Broglio F, Ghigo E, van der Lely AJ. Administration of acylated ghrelin reduces insulin sensitivity, whereas the combination of acylated plus unacylated ghrelin strongly improves insulin sensitivity. *J Clin Endocrinol Metab* 2004;89:5035-42.

Gauna C, Delhanty PJ, Hofland LJ, Janssen JA, Broglio F, Ross RJ, Ghigo E, van der Lely AJ. Ghrelin stimulates, whereas des-octanoyl ghrelin inhibits, glucose output by primary hepatocytes. *J Clin Endocrinol Metab* 2005;90:1055-60.

Gauna C, Kiewiet RM, Janssen JA, van de Zande B, Delhanty PJ, Ghigo E, Hofland LJ, Themmen AP, van der Lely AJ. Unacylated ghrelin acts as a potent insulin secretagogue in glucose-stimulated conditions. *Am J Physiol Endocrinol Metab* 2007;293:E697-E704.

Ge X, Yang H, Bednarek MA, Galon-Tilleman H, Chen P, Chen M, Lichtman JS, Wang Y, Dalmas O, Yin Y, Tian H, Jermutus L, Grimsby J, Rondinone CM, Konkar A, Kaplan DD. LEAP2 is an endogenous antagonist of the ghrelin receptor. *Cell Metab* 2018;27:461-69 e6.

Geisler CE, Renquist BJ. Hepatic lipid accumulation: cause and consequence of dysregulated glucoregulatory hormones. *J Endocrinol* 2017;234:R1-R21.

Geng Y, Ma Q, Liu YN, Peng N, Yuan FF, Li XG, Li M, Wu YS, Li BL, Song WB, Zhu W, Xu WW, Fan J, Su L. Heatstroke induces liver injury via IL-1beta and HMGB1-induced pyroptosis. *J Hepatol* 2015;63:622-33.

Gnanapavan S, Kola B, Bustin SA, Morris DG, McGee P, Fairclough P, Bhattacharya S, Carpenter R, Grossman AB, Korbonits M. The tissue distribution of the mRNA of ghrelin and subtypes of its receptor, GHS-R, in humans. *J Clin Endocrinol Metab* 2002;87:2988.

Gómez-Ambrosi J, Silva C, Galofré JC, Escalada J, Santos S, Millán D, Vila N, Ibañez P, Gil MJ, Valentí V, Rotellar F, Ramírez B, Salvador J, Frühbeck G. Body mass index classification misses subjects with increased cardiometabolic risk factors related to elevated adiposity. *Int J Obes* 2012;36:286-94.

Gómez-Ambrosi J, Moncada R, Valentí V, Silva C, Ramírez B, Catalán V, Rodríguez A, Andrada P, Escalada J, Pastor C, Cienfuegos JA, Gil MJ, Salvador J, Frühbeck G. Cardiometabolic profile related to body adiposity identifies patients eligible for bariatric surgery more accurately than BMI. *Obes Surg* 2015;25:1594-603.

Gónzalez CR, Vázquez MJ, López M, Diéguez C. Influence of chronic undernutrition and leptin on GOAT mRNA levels in rat stomach mucosa. *J Mol Endocrinol* 2008;41:415-21.

Granado M, Martín AI, López-Menduiña M, López-Calderón A, Villanúa MA. GH-releasing peptide-2 administration prevents liver inflammatory response in endotoxemia. *Am J Physiol Endocrinol Metab* 2008;294:E131-41.

Granata R, Settanni F, Biancone L, Trovato L, Nano R, Bertuzzi F, Destefanis S, Annunziata M, Martinetti M, Catapano F, Ghe C, Isgaard J, Papotti M, Ghigo E, Muccioli G. Acylated and unacylated ghrelin promote proliferation and inhibit apoptosis of pancreatic beta-cells and human islets: involvement of 3',5'-cyclic adenosine monophosphate/protein kinase A, extracellular signal-regulated kinase 1/2, and phosphatidyl inositol 3-Kinase/Akt signaling. *Endocrinology* 2007;148:512-29.

Grattagliano I, Montezinho LP, Oliveira PJ, Frühbeck G, Gómez-Ambrosi J, Montecucco F, Carbone F, Wieckowski MR, Wang DQ, Portincasa P. Targeting mitochondria to oppose the progression of nonalcoholic fatty liver disease. *Biochem Pharmacol* 2019;160:34-45.

Green DR, Llambi F. Cell death signaling. *Cold Spring Harb Perspect Biol* 2015;7:

Gregor MF, Yang L, Fabbrini E, Mohammed BS, Eagon JC, Hotamisligil GS, Klein S. Endoplasmic reticulum stress is reduced in tissues of obese subjects after weight loss. *Diabetes* 2009;58:693-700.

Gressner AM, Weiskirchen R, Breitkopf K, Dooley S. Roles of TGF-beta in hepatic fibrosis. *Front Biosci* 2002;7:d793-807.

Guo ZF, Ren AJ, Zheng X, Qin YW, Cheng F, Zhang J, Wu H, Yuan WJ, Zou L. Different responses of circulating ghrelin, obestatin levels to fasting, re-feeding and different food compositions, and their local expressions in rats. *Peptides* 2008;29:1247-54.

Gurriarán-Rodríguez U, Al-Massadi O, Crujeiras AB, Mosteiro CS, Amil-Diz M, Beiroa D, Nogueiras R, Seoane LM, Gallego R, Pazos Y, Casanueva FF, Camiña JP. Preproghrelin expression is a key target for insulin action on adipogenesis. *J Endocrinol* 2011a;210:R1-7.

Gurriarán-Rodríguez U, Al-Massadi O, Roca-Rivada A, Crujeiras AB, Gallego R, Pardo M, Seoane LM, Pazos Y, Casanueva FF, Camiña JP. Obestatin as a regulator of adipocyte metabolism and adipogenesis. *J Cell Mol Med* 2011b;15:1927-40.

Gutiérrez-Fisac JL, Guallar-Castillón P, León-Muñoz LM, Graciani A, Banegas JR, Rodríguez-Artalejo F. Prevalence of general and abdominal obesity in the adult population of Spain, 2008-2010: the ENRICA study. *Obes Rev* 2012;13:388-92.

Gutiérrez JA, Solenberg PJ, Perkins DR, Willency JA, Knierman MD, Jin Z, Witcher DR, Luo S, Onyia JE, Hale JE. Ghrelin octanoylation mediated by an orphan lipid transferase. *Proc Natl Acad Sci USA* 2008;105:6320-5.

Guzmán-Ruiz R, Ortega F, Rodríguez A, Vázquez-Martínez R, Díaz-Ruiz A, García-Navarro S, Giralt M, García-Rios A, Cobo-Padilla D, Tinahones FJ, López-Miranda J, Villarroya F, Frühbeck G, Fernández-Real JM, Malagón MM. Alarmin high-mobility group B1 (HMGB1) is regulated in human adipocytes in insulin resistance and influences insulin secretion in beta-cells. *Int J Obes* 2014;38:1545-54.

Hall AM, Kou K, Chen Z, Pietka TA, Kumar M, Korenblat KM, Lee K, Ahn K, Fabbrini E, Klein S, Goodwin B, Finck BN. Evidence for regulated monoacylglycerol acyltransferase expression and activity in human liver. *J Lipid Res* 2012;53:990-9.

Han L, Li J, Chen Y, Wang W, Zhang D, Liu G. Effects of ghrelin on triglyceride accumulation and glucose uptake in primary cultured rat myoblasts under palmitic acid-induced high fat conditions. *Int J Endocrinol* 2015;2015:635863.

Hannah WN, Jr., Harrison SA. Noninvasive imaging methods to determine severity of nonalcoholic fatty liver disease and nonalcoholic steatohepatitis. *Hepatology* 2016;64:2234-43.

Heppner KM, Piechowski CL, Müller A, Ottaway N, Sisley S, Smiley DL, Habegger KM, Pfluger PT, Dimarchi R, Biebermann H, Tschöp MH, Sandoval DA, Pérez-Tilve D. Both acyl and des-acyl ghrelin regulate adiposity and glucose metabolism via central nervous system ghrelin receptors. *Diabetes* 2014;63:122-31.

Higa KD, Boone KB, Ho T. Complications of the laparoscopic Roux-en-Y gastric bypass: 1,040 patients--what have we learned? *Obes Surg* 2000;10:509-13.

Holst B, Brandt E, Bach A, Heding A, Schwartz TW. Nonpeptide and peptide growth hormone secretagogues act both as ghrelin receptor agonist and as positive or negative allosteric modulators of ghrelin signaling. *Mol Endocrinol* 2005;19:2400-11.

Holler N, Zaru R, Micheau O, Thome M, Attinger A, Valitutti S, Bodmer JL, Schneider P, Seed B, Tschopp J. Fas triggers an alternative, caspase-8-independent cell death pathway using the kinase RIP as effector molecule. *Nat Immunol* 2000;1:489-95.

Horiuchi T, Sakata N, Narumi Y, Kimura T, Hayashi T, Nagano K, Liu K, Nishibori M, Tsukita S, Yamada T, Katagiri H, Shirakawa R, Horiuchi H. Metformin directly binds the alarmin HMGB1 and inhibits its proinflammatory activity. *J Biol Chem* 2017;292:8436-46.

Horton JD, Shimano H, Hamilton RL, Brown MS, Goldstein JL. Disruption of LDL receptor gene in transgenic SREBP-1a mice unmasks hyperlipidemia resulting from production of lipid-rich VLDL. *J Clin Invest* 1999;103:1067-76.

Hosoda H, Kojima M, Matsuo H, Kangawa K. Ghrelin and des-acyl ghrelin: two major forms of rat ghrelin peptide in gastrointestinal tissue. *Biochem Biophys Res Commun* 2000;279:909-13.

Hotamisligil GS, Shargill NS, Spiegelman BM. Adipose expression of tumor necrosis factor-alpha: direct role in obesity-linked insulin resistance. *Science* 1993;259:87-91.

Howard AD, Feighner SD, Cully DF, Arena JP, Liberator PA, Rosenblum CI, Hamelin M, Hreniuk DL, Palyha OC, Anderson J, Paress PS, Diaz C, Chou M, Liu KK, McKee KK, Pong SS, Chaung LY, Elbrecht A, Dashkevicz M, Heavens R, Rigby M, Sirinathsinghji DJ, Dean DC, Melillo DG, Patchett AA, Nargund R, Griffin PR, DeMartino JA, Gupta SK, Schaeffer JM, Smith RG, Van der Ploeg LH. A receptor in pituitary and hypothalamus that functions in growth hormone release. *Science* 1996;273:974-7.

Illan-Gómez F, Gonzálvez-Ortega M, Orea-Soler I, Alcaraz-Tafalla MS, Aragón-Alonso A, Pascual-Díaz M, Pérez-Paredes M, Lozano-Almela ML. Obesity and inflammation: change in adiponectin, C-reactive protein, tumour necrosis factor-alpha and interleukin-6 after bariatric surgery. *Obes Surg* 2012;22:950-5.

Ipsen DH, Lykkesfeldt J, Tveden-Nyborg P. Molecular mechanisms of hepatic lipid accumulation in non-alcoholic fatty liver disease. *Cell Mol Life Sci* 2018;75:3313-27.

Jiang D, Niwa M, Koong AC. Targeting the IRE1alpha-XBP1 branch of the unfolded protein response in human diseases. *Semin Cancer Biol* 2015;33:48-56.

Jiang D, Wan F. Exendin-4 protects INS-1 cells against palmitate-induced apoptosis through the IRE1alpha-Xbp1 signaling pathway. *Exp Ther Med* 2018;16:1029-35.

Johansson HE, Haenni A, Zethelius B. Platelet counts and liver enzymes after bariatric surgery. *J Obes* 2013;2013:567984.

Joseph AE, Saverymuttu SH, al-Sam S, Cook MG, Maxwell JD. Comparison of liver histology with ultrasonography in assessing diffuse parenchymal liver disease. *Clin Radiol* 1991;43:26-31.

Kahn BB, Alquier T, Carling D, Hardie DG. AMP-activated protein kinase: ancient energy gauge provides clues to modern understanding of metabolism. *Cell Metab* 2005;1:15-25.

Kamegai J, Tamura H, Shimizu T, Ishii S, Sugihara H, Wakabayashi I. Central effect of ghrelin, an endogenous growth hormone secretagogue, on hypothalamic peptide gene expression. *Endocrinology* 2000;141:4797-800.

Kammoun HL, Chabanon H, Hainault I, Luquet S, Magnan C, Koike T, Ferre P, Foufelle F. GRP78 expression inhibits insulin and ER stress-induced SREBP-1c activation and reduces hepatic steatosis in mice. *J Clin Invest* 2009;119:1201-15.

Kashyap SR, Bhatt DL, Wolski K, Watanabe RM, Abdul-Ghani M, Abood B, Pothier CE, Brethauer S, Nissen S, Gupta M, Kirwan JP, Schauer PR. Metabolic effects of bariatric surgery in patients with moderate obesity and type 2 diabetes: analysis of a randomized control trial comparing surgery with intensive medical treatment. *Diabetes Care* 2013;36:2175-82.

Kasimay O, Iseri SO, Barlas A, Bangir D, Yegen C, Arbak S, Yegen BC. Ghrelin ameliorates pancreaticobiliary inflammation and associated remote organ injury in rats. *Hepatol Res* 2006;36:11-9.

Katsuma S, Hirasawa A, Tsujimoto G. Bile acids promote glucagon-like peptide-1 secretion through TGR5 in a murine enteroendocrine cell line STC-1. *Biochem Biophys Res Commun* 2005;329:386-90.

Katsuragi Y, Ichimura Y, Komatsu M. p62/SQSTM1 functions as a signaling hub and an autophagy adaptor. *FEBS J* 2015;282:4672-8.

Katz DP, Lee SR, Nachiappan AC, Willis MH, Bray CD, Farinas CA, Whigham CJ, Spiegel F. Laparoscopic sleeve gastrectomy: a guide to postoperative anatomy and complications. *Abdom Imaging* 2011;36:363-71.

Kawano Y, Cohen DE. Mechanisms of hepatic triglyceride accumulation in non-alcoholic fatty liver disease. *J Gastroenterol* 2013;48:434-41.

Khaleel EF, Abdel-Aleem GA. Obestatin protects and reverses nonalcoholic fatty liver disease and its associated insulin resistance in rats via inhibition of food intake, enhancing hepatic adiponectin signaling, and blocking ghrelin acylation. *Arch Physiol Biochem* 2019;125:64-78.

Kim MS, Yoon CY, Jang PG, Park YJ, Shin CS, Park HS, Ryu JW, Pak YK, Park JY, Lee KU, Kim SY, Lee HK, Kim YB, Park KS. The mitogenic and antiapoptotic actions of ghrelin in 3T3-L1 adipocytes. *Mol Endocrinol* 2004;18:2291-301.

Kinner S, Reeder SB, Yokoo T. Quantitative imaging biomarkers of NAFLD. *Dig Dis Sci* 2016;61:1337-47.

Kleiner DE, Brunt EM, Van Natta M, Behling C, Contos MJ, Cummings OW, Ferrell LD, Liu YC, Torbenson MS, Unalp-Arida A, Yeh M, McCullough AJ, Sanyal AJ. Design and validation of a histological scoring system for nonalcoholic fatty liver disease. *Hepatology* 2005;41:1313-21.

Kleiner DE, Brunt EM. Nonalcoholic fatty liver disease: pathologic patterns and biopsy evaluation in clinical research. *Semin Liver Dis* 2012;32:3-13.

Kleiner DE, Makhlouf HR. Histology of nonalcoholic fatty liver disease and nonalcoholic steatohepatitis in adults and children. *Clin Liver Dis* 2016;20:293-312.

Kojima M, Hosoda H, Date Y, Nakazato M, Matsuo H, Kangawa K. Ghrelin is a growth-hormone-releasing acylated peptide from stomach. *Nature* 1999;402:656-60.

Koliaki C, Szendroedi J, Kaul K, Jelenik T, Nowotny P, Jankowiak F, Herder C, Carstensen M, Krausch M, Knoefel WT, Schlensak M, Roden M. Adaptation of hepatic mitochondrial function in humans with non-alcoholic fatty liver is lost in steatohepatitis. *Cell Metab* 2015;21:739-46.

Koo SH. Nonalcoholic fatty liver disease: molecular mechanisms for the hepatic steatosis. *Clin Mol Hepatol* 2013;19:210-5.

Kopelman PG. Obesity as a medical problem. *Nature* 2000;404:635-43.

Kotronen A, Seppala-Lindroos A, Vehkavaara S, Bergholm R, Frayn KN, Fielding BA, Yki-Jarvinen H. Liver fat and lipid oxidation in humans. *Liver Int* 2009;29:1439-46.

Kowdley KV. The role of iron in nonalcoholic fatty liver disease: the story continues. *Gastroenterology* 2010;138:817-9.

Lăpădat AM, Jianu IR, Ungureanu BS, Florescu LM, Gheonea DI, Sovaila S, Gheonea IA. Non-invasive imaging techniques in assessing non-alcoholic fatty liver disease: a current status of available methods. *J Med Life* 2017;10:19-26.

Lassailly G, Caiazzo R, Pattou F, Mathurin P. Bariatric surgery for curing NASH in the morbidly obese? *J Hepatol* 2013;58:1249-51.

Lauwers E, Landuyt B, Arckens L, Schoofs L, Luyten W. Obestatin does not activate orphan G protein-coupled receptor GPR39. *Biochem Biophys Res Commun* 2006;351:21-5.

Lavallard VJ, Gual P. Autophagy and non-alcoholic fatty liver disease. *Biomed Res Int* 2014;2014:120179.

Lawrence CB, Snape AC, Baudoin FM, Luckman SM. Acute central ghrelin and GH secretagogues induce feeding and activate brain appetite centers. *Endocrinology* 2002;143:155-62.

Lee AH, Scapa EF, Cohen DE, Glimcher LH. Regulation of hepatic lipogenesis by the transcription factor XBP1. *Science* 2008;320:1492-6.

Lee HJ, Cui R, Choi SE, Jeon JY, Kim HJ, Kim TH, Kang Y, Lee KW. Bitter melon extract ameliorates palmitate-induced apoptosis via inhibition of endoplasmic reticulum stress in HepG2 cells and high-fat/high-fructose-diet-induced fatty liver. *Food Nutr Res* 2018;62:

Lee SS, Park SH. Radiologic evaluation of nonalcoholic fatty liver disease. *World J Gastroenterol* 2014;20:7392-402.

Lee SW, Park SH, Kim KW, Choi EK, Shin YM, Kim PN, Lee KH, Yu ES, Hwang S, Lee SG. Unenhanced CT for assessment of macrovesicular hepatic steatosis in living liver donors: comparison of visual grading with liver attenuation index. *Radiology* 2007;244:479-85.

Lemarie A, Grimm S. Mitochondrial respiratory chain complexes: apoptosis sensors mutated in cancer? *Oncogene* 2011;30:3985-4003.

Leung C, Rivera L, Furness JB, Angus PW. The role of the gut microbiota in NAFLD. *Nat Rev Gastroenterol Hepatol* 2016;13:412-25.

Leung PK, Chow KB, Lau PN, Chu KM, Chan CB, Cheng CH, Wise H. The truncated ghrelin receptor polypeptide (GHS-R1b) acts as a dominant-negative mutant of the ghrelin receptor. *Cell Signal* 2007;19:1011-22.

Li JV, Ashrafian H, Bueter M, Kinross J, Sands C, le Roux CW, Bloom SR, Darzi A, Athanasiou T, Marchesi JR, Nicholson JK, Holmes E. Metabolic surgery profoundly influences gut microbial-host metabolic cross-talk. *Gut* 2011;60:1214-23.

Li Q, Dhyani M, Grajo JR, Sirlin C, Samir AE. Current status of imaging in nonalcoholic fatty liver disease. *World J Hepatol* 2018;10:530-42.

Li S, Shin HJ, Ding EL, van Dam RM. Adiponectin levels and risk of type 2 diabetes: a systematic review and meta-analysis. *JAMA* 2009;302:179-88.

Li Z, Xu G, Qin Y, Zhang C, Tang H, Yin Y, Xiang X, Li Y, Zhao J, Mulholland M, Zhang W. Ghrelin promotes hepatic lipogenesis by activation of mTOR-PPARgamma signaling pathway. *Proc Natl Acad Sci USA* 2014;111:13163-8.

Lim CT, Kola B, Grossman A, Korbonits M. The expression of ghrelin O-acyltransferase (GOAT) in human tissues. *Endocr J* 2011a;58:707-10.

Lim CT, Kola B, Korbonits M. The ghrelin/GOAT/GHS-R system and energy metabolism. *Rev Endocr Metab Disord* 2011b;12:173-86.

Lin L, Saha PK, Ma X, Henshaw IO, Shao L, Chang BH, Buras ED, Tong Q, Chan L, McGuinness OP, Sun Y. Ablation of ghrelin receptor reduces adiposity and improves insulin sensitivity during aging by regulating fat metabolism in white and brown adipose tissues. *Aging Cell* 2011;10:996-1010.

Lin L, Lee JH, Bongmba OY, Ma X, Zhu X, Sheikh-Hamad D, Sun Y. The suppression of ghrelin signaling mitigates age-associated thermogenic impairment. *Aging* 2014;6:1019-32.

Liu HY, Han J, Cao SY, Hong T, Zhuo D, Shi J, Liu Z, Cao W. Hepatic autophagy is suppressed in the presence of insulin resistance and hyperinsulinemia: inhibition of FoxO1-dependent expression of key autophagy genes by insulin. *J Biol Chem* 2009;284:31484-92.

Lonardo A, Nascimbeni F, Maurantonio M, Marrazzo A, Rinaldi L, Adinolfi LE. Nonalcoholic fatty liver disease: Evolving paradigms. *World J Gastroenterol* 2017;23:6571-92.

Long YC, Zierath JR. AMP-activated protein kinase signaling in metabolic regulation. *J Clin Invest* 2006;116:1776-83.

López M, Lage R, Saha AK, Pérez-Tilve D, Vázquez MJ, Varela L, Sangiao-Alvarellos S, Tovar S, Raghay K, Rodríguez-Cuenca S, Deoliveira RM, Castaneda T, Datta R, Dong JZ, Culler M, Sleeman MW, Álvarez CV, Gallego R, Lelliott CJ, Carling D, Tschöp MH,

Diéguez C, Vidal-Puig A. Hypothalamic fatty acid metabolism mediates the orexigenic action of ghrelin. *Cell Metab* 2008;7:389-99.

Machado M, Marques-Vidal P, Cortez-Pinto H. Hepatic histology in obese patients undergoing bariatric surgery. *J Hepatol* 2006;45:600-6.

Madrigal-Matute J, Cuervo AM. Regulation of liver metabolism by autophagy. *Gastroenterology* 2016;150:328-39.

Malhi H, Kaufman RJ. Endoplasmic reticulum stress in liver disease. *J Hepatol* 2011;54:795-809.

Malhotra JD, Kaufman RJ. Endoplasmic reticulum stress and oxidative stress: a vicious cycle or a double-edged sword? *Antioxid Redox Signal* 2007;9:2277-93.

Malin SK, Samat A, Wolski K, Abood B, Pothier CE, Bhatt DL, Nissen S, Brethauer SA, Schauer PR, Kirwan JP, Kashyap SR. Improved acylated ghrelin suppression at 2 years in obese patients with type 2 diabetes: effects of bariatric surgery vs standard medical therapy. *Int J Obes* 2014;38:364-70.

Mano-Otagiri A, Ohata H, Iwasaki-Sekino A, Nemoto T, Shibasaki T. Ghrelin suppresses noradrenaline release in the brown adipose tissue of rats. *J Endocrinol* 2009;201:341-9.

Mano-Otagiri A, Iwasaki-Sekino A, Nemoto T, Ohata H, Shuto Y, Nakabayashi H, Sugihara H, Oikawa S, Shibasaki T. Genetic suppression of ghrelin receptors activates brown adipocyte function and decreases fat storage in rats. *Regul Pept* 2010;160:81-90.

Mao Y, Cheng J, Yu F, Li H, Guo C, Fan X. Ghrelin attenuated lipotoxicity via autophagy induction and nuclear factor-κB inhibition. *Cell Physiol Biochem* 2015a;37:563-76.

Mao Y, Zhang S, Yu F, Li H, Guo C, Fan X. Ghrelin attenuates liver fibrosis through regulation of TGF-beta1 expression and autophagy. *Int J Mol Sci* 2015b;16:21911-30.

Mao Y, Wang J, Yu F, Li Z, Li H, Guo C, Fan X. Ghrelin protects against palmitic acid or lipopolysaccharide-induced hepatocyte apoptosis through inhibition of MAPKs/iNOS and restoration of Akt/eNOS pathways. *Biomed Pharmacother* 2016;84:305-13.

Mao Z, Yang Q, Yin W, Su W, Lin H, Feng M, Pan K, Yin Y, Zhang W. ETV5 regulates GOAT/ghrelin system in an mTORC1-dependent manner. *Mol Cell Endocrinol* 2019;485:72-80.

Marchesini G, Pagotto U, Bugianesi E, De Iasio R, Manini R, Vanni E, Pasquali R, Melchionda N, Rizzetto M. Low ghrelin concentrations in nonalcoholic fatty liver disease are related to insulin resistance. *J Clin Endocrinol Metab* 2003;88:5674-9.

Marra F, Svegliati-Baroni G. Lipotoxicity and the gut-liver axis in NASH pathogenesis. *J Hepatol* 2018;68:280-95.

Martínez-López N, Singh R. Autophagy and lipid droplets in liver. *Annu Rev Nutr* 2015;35:215-37.

Martínez SM, Crespo G, Navasa M, Forns X. Noninvasive assessment of liver fibrosis. *Hepatology* 2011;53:325-35.

Martinou JC, Youle RJ. Mitochondria in apoptosis: Bcl-2 family members and mitochondrial dynamics. *Dev Cell* 2011;21:92-101.

Martins L, Fernández-Mallo D, Novelle MG, Vázquez MJ, Tena-Sempere M, Nogueiras R, López M, Diéguez C. Hypothalamic mTOR signaling mediates the orexigenic action of ghrelin. *PLoS One* 2012;7:e46923.

Mathurin P, Hollebecque A, Arnalsteen L, Buob D, Leteurtre E, Caiazzo R, Pigeyre M, Verkindt H, Dharancy S, Louvet A, Romon M, Pattou F. Prospective study of the long-term effects of bariatric surgery on liver injury in patients without advanced disease. *Gastroenterology* 2009;137:532-40.

Mattar SG, Velcu LM, Rabinovitz M, Demetris AJ, Krasinskas AM, Barinas-Mitchell E, Eid GM, Ramanathan R, Taylor DS, Schauer PR. Surgically-induced weight loss significantly improves nonalcoholic fatty liver disease and the metabolic syndrome. *Ann Surg* 2005;242:610-7; discussion 18-20.

McCowen KC, Maykel JA, Bistrian BR, Ling PR. Circulating ghrelin concentrations are lowered by intravenous glucose or hyperinsulinemic euglycemic conditions in rodents. *J Endocrinol* 2002;175:R7-11.

Mencin A, Kluwe J, Schwabe RF. Toll-like receptors as targets in chronic liver diseases. *Gut* 2009;58:704-20.

Méndez-Giménez L, Rodríguez A, Balaguer I, Frühbeck G. Role of aquaglyceroporins and caveolins in energy and metabolic homeostasis. *Mol Cell Endocrinol* 2014;397: 78–92.

Méndez-Giménez L, Becerril S, Moncada R, Valentí V, Ramírez B, Lancha A, Gurbindo J, Balaguer I, Cienfuegos JA, Catalán V, Fernández S, Gómez-Ambrosi J, Rodríguez A, Frühbeck G. Sleeve gastrectomy reduces hepatic steatosis by improving the coordinated regulation of aquaglyceroporins in adipose tissue and liver in obese rats. *Obes Surg* 2015;25:1723-34.

Méndez-Giménez L, Becerril S, Camões SP, da Silva IV, Rodrigues C, Moncada R, Valentí V, Catalán V, Gómez-Ambrosi J, Miranda JP, Soveral G, Frühbeck G, Rodríguez A. Role of aquaporin-7 in ghrelin- and GLP-1-induced improvement of pancreatic beta-cell function after sleeve gastrectomy in obese rats. *Int J Obes* 2017;41:1394-402.

Miegueu P, St Pierre D, Broglio F, Cianflone K. Effect of desacyl ghrelin, obestatin and related peptides on triglyceride storage, metabolism and GHSR signaling in 3T3-L1 adipocytes. *J Cell Biochem* 2011;112:704-14.

Miras AD, le Roux CW. Mechanisms underlying weight loss after bariatric surgery. *Nat Rev Gastroenterol Hepatol* 2013;10:575-84.

Moncada R, Landecho MF, Frühbeck G. Metabolic surgery enters the T2DM treatment algorithm. *Trends Endocrinol Metab* 2016a;27:678-80.

Moncada R, Rodríguez A, Becerril S, Méndez-Giménez L, Valentí V, Ramírez B, Cienfuegos JA, Fernández S, Catalán V, Gómez-Ambrosi J, Frühbeck G. Sleeve gastrectomy decreases body weight, whole-body adiposity, and blood pressure even in aged diet-induced obese rats. *Obes Surg* 2016b;26:1549-58.

Moreno M, Chaves JF, Sancho-Bru P, Ramalho F, Ramalho LN, Mansego ML, Ivorra C, Domínguez M, Conde L, Millán C, Mari M, Colmenero J, Lozano JJ, Jares P, Vidal J, Forns X, Arroyo V, Caballería J, Gines P, Bataller R. Ghrelin attenuates hepatocellular injury and liver fibrogenesis in rodents and influences fibrosis progression in humans. *Hepatology* 2010;51:974-85.

Mortensen K, Petersen LL, Ørskov C. Colocalization of GLP-1 and GIP in human and porcine intestine. *Ann N Y Acad Sci* 2000;921:469-72.

Mosinski JD, Pagadala MR, Mulya A, Huang H, Dan O, Shimizu H, Batayyah E, Pai RK, Schauer PR, Brethauer SA, Kirwan JP. Gastric bypass surgery is protective from high-fat

diet-induced non-alcoholic fatty liver disease and hepatic endoplasmic reticulum stress. *Acta Physiol* 2016;217:141-51.

Mottin CC, Moretto M, Padoin AV, Swarowsky AM, Toneto MG, Glock L, Repetto G. The role of ultrasound in the diagnosis of hepatic steatosis in morbidly obese patients. *Obes Surg* 2004;14:635-7.

Müller TD, Müller A, Yi CX, Habegger KM, Meyer CW, Gaylinn BD, Finan B, Heppner K, Trivedi C, Bielohuby M, Abplanalp W, Meyer F, Piechowski CL, Pratzka J, Stemmer K, Holland J, Hembree J, Bhardwaj N, Raver C, Ottaway N, Krishna R, Sah R, Sallee FR, Woods SC, Perez-Tilve D, Bidlingmaier M, Thorner MO, Krude H, Smiley D, DiMarchi R, Hofmann S, Pfluger PT, Kleinau G, Biebermann H, Tschöp MH. The orphan receptor Gpr83 regulates systemic energy metabolism via ghrelin-dependent and ghrelin-independent mechanisms. *Nat Commun* 2013;4:1968.

Müller TD, Nogueiras R, Andermann ML, Andrews ZB, Anker SD, Argente J, Batterham RL, Benoit SC, Bowers CY, Broglio F, Casanueva FF, D'Alessio D, Depoortere I, Geliebter A, Ghigo E, Cole PA, Cowley M, Cummings DE, Dagher A, Diano S, Dickson SL, Dieguez C, Granata R, Grill HJ, Grove K, Habegger KM, Heppner K, Heiman ML, Holsen L, Holst B, Inui A, Jansson JO, Kirchner H, Korbonits M, Laferrere B, LeRoux CW, López M, Morin S, Nakazato M, Nass R, Perez-Tilve D, Pfluger PT, Schwartz TW, Seeley RJ, Sleeman M, Sun Y, Sussel L, Tong J, Thorner MO, van der Lely AJ, van der Ploeg LH, Zigman JM, Kojima M, Kangawa K, Smith RG, Horvath T, Tschöp MH. Ghrelin. *Mol Metab* 2015;4:437-60.

Munday MR. Regulation of mammalian acetyl-CoA carboxylase. *Biochem Soc Trans* 2002;30:1059-64.

Musso G, Gambino R, Cassader M, Pagano G. Meta-analysis: natural history of non-alcoholic fatty liver disease (NAFLD) and diagnostic accuracy of non-invasive tests for liver disease severity. *Ann Med* 2011;43:617-49.

Mykhalchyshyn G, Kobyliak N, Bodnar P. Diagnostic accuracy of acyl-ghrelin and it association with non-alcoholic fatty liver disease in type 2 diabetic patients. *J Diabetes Metab Disord* 2015;14:44.

Myronovych A, Kirby M, Ryan KK, Zhang W, Jha P, Setchell KD, Dexheimer PJ, Aronow B, Seeley RJ, Kohli R. Vertical sleeve gastrectomy reduces hepatic steatosis while increasing serum bile acids in a weight-loss-independent manner. *Obesity* 2014;22:390-400.

Naleid AM, Grace MK, Cummings DE, Levine AS. Ghrelin induces feeding in the mesolimbic reward pathway between the ventral tegmental area and the nucleus accumbens. *Peptides* 2005;26:2274-9.

NCD Risk Factor Collaboration (NCD-RisC). Worldwide trends in body-mass index, underweight, overweight, and obesity from 1975 to 2016: a pooled analysis of 2416 population-based measurement studies in 128.9 million children, adolescents, and adults. *Lancet* 2017;390:2627-42.

Neff KJ, Olbers T, le Roux CW. Bariatric surgery: the challenges with candidate selection, individualizing treatment and clinical outcomes. *BMC Med* 2013;11:8.

Neish AS. Microbes in gastrointestinal health and disease. *Gastroenterology* 2009;136:65-80.

Ng M, Fleming T, Robinson M, Thomson B, Graetz N, Margono C, Mullany EC, Biryukov S, Abbafati C, Abera SF, Abraham JP, Abu-Rmeileh NM, Achoki T, AlBuhairan FS, Alemu ZA, Alfonso R, Ali MK, Ali R, Guzman NA, Ammar W, Anwari P, Banerjee A, Barquera S, Basu S, Bennett DA, Bhutta Z, Blore J, Cabral N, Nonato IC, Chang JC, Chowdhury R, Courville KJ, Criqui MH, Cundiff DK, Dabhadkar KC, Dandona L, Davis A, Dayama A, Dharmaratne SD, Ding EL, Durrani AM, Esteghamati A, Farzadfar F, Fay DF, Feigin VL, Flaxman A, Forouzanfar MH, Goto A, Green MA, Gupta R, Hafezi-Nejad N, Hankey GJ, Harewood HC, Havmoeller R, Hay S, Hernández L, Husseini A, Idrisov BT, Ikeda N, Islami F, Jahangir E, Jassal SK, Jee SH, Jeffreys M, Jonas JB, Kabagambe EK, Khalifa SE, Kengne AP, Khader YS, Khang YH, Kim D, Kimokoti RW, Kinge JM, Kokubo Y, Kosen S, Kwan G, Lai T, Leinsalu M, Li Y, Liang X, Liu S, Logroscino G, Lotufo PA, Lu Y, Ma J, Mainoo NK, Mensah GA, Merriman TR, Mokdad AH, Moschandreas J, Naghavi M, Naheed A, Nand D, Narayan KM, Nelson EL, Neuhouser ML, Nisar MI, Ohkubo T, Oti SO, Pedroza A, Prabhakaran D, Roy N, Sampson U, Seo H, Sepanlou SG, Shibuya K, Shiri R, Shiue I, Singh GM, Singh JA, Skirbekk V, Stapelberg NJ, Sturua L, Sykes BL, Tobias M, Tran BX, Trasande L, Toyoshima H, van de Vijver S, Vasankari TJ, Veerman JL, Velasquez-Melendez G, Vlassov VV, Vollset SE, Vos T, Wang C, Wang X, Weiderpass E, Werdecker A, Wright JL, Yang YC, Yatsuya H, Yoon J, Yoon SJ, Zhao Y, Zhou M, Zhu S, López AD, Murray CJ, Gakidou E. Global, regional, and national prevalence of overweight and obesity in children and adults during 1980-2013: a systematic analysis for the Global Burden of Disease Study 2013. *Lancet* 2014;384:766-81.

Nishi Y, Hiejima H, Hosoda H, Kaiya H, Mori K, Fukue Y, Yanase T, Nawata H, Kangawa K, Kojima M. Ingested medium-chain fatty acids are directly utilized for the acyl modification of ghrelin. *Endocrinology* 2005;146:2255-64.

Nogueiras R, Tovar S, Mitchell SE, Rayner DV, Archer ZA, Diéguez C, Williams LM. Regulation of growth hormone secretagogue receptor gene expression in the arcuate nuclei of the rat by leptin and ghrelin. *Diabetes* 2004;53:2552-8.

Nogueiras R, Pfluger P, Tovar S, Arnold M, Mitchell S, Morris A, Pérez-Tilve D, Vázquez MJ, Wiedmer P, Castaneda TR, DiMarchi R, Tschöp M, Schurmann A, Joost HG, Williams LM, Langhans W, Diéguez C. Effects of obestatin on energy balance and growth hormone secretion in rodents. *Endocrinology* 2007;148:21-6.

Obay BD, Tasdemir E, Tumer C, Bilgin H, Atmaca M. Dose dependent effects of ghrelin on pentylenetetrazole-induced oxidative stress in a rat seizure model. *Peptides* 2008;29:448-55.

Ouchi N, Parker JL, Lugus JJ, Walsh K. Adipokines in inflammation and metabolic disease. *Nat Rev Immunol* 2011;11:85-97.

Ozcan U, Yilmaz E, Ozcan L, Furuhashi M, Vaillancourt E, Smith RO, Gorgun CZ, Hotamisligil GS. Chemical chaperones reduce ER stress and restore glucose homeostasis in a mouse model of type 2 diabetes. *Science* 2006;313:1137-40.

Pacifico L, Poggiogalle E, Costantino F, Anania C, Ferraro F, Chiarelli F, Chiesa C. Acylated and nonacylated ghrelin levels and their associations with insulin resistance in obese and normal weight children with metabolic syndrome. *Eur J Endocrinol* 2009;161:861-70.

Pankiv S, Clausen TH, Lamark T, Brech A, Bruun JA, Outzen H, Øvervatn A, Bjørkøy G, Johansen T. p62/SQSTM1 binds directly to Atg8/LC3 to facilitate degradation of ubiquitinated protein aggregates by autophagy. *J Biol Chem* 2007;282:24131-45.

Paradies G, Paradies V, Ruggiero FM, Petrosillo G. Oxidative stress, cardiolipin and mitochondrial dysfunction in nonalcoholic fatty liver disease. *World J Gastroenterol* 2014;20:14205-18.

Park JM, Jung CH, Seo M, Otto NM, Grunwald D, Kim KH, Moriarity B, Kim YM, Starker C, Nho RS, Voytas D, Kim DH. The ULK1 complex mediates MTORC1 signaling to the autophagy initiation machinery via binding and phosphorylating ATG14. *Autophagy* 2016;12:547-64.

Park S, Jiang H, Zhang H, Smith RG. Modification of ghrelin receptor signaling by somatostatin receptor-5 regulates insulin release. *Proc Natl Acad Sci USA* 2012;109:19003-8.

Park YS, Park SH, Lee SS, Kim DY, Shin YM, Lee W, Lee SG, Yu ES. Biopsy-proven nonsteatotic liver in adults: estimation of reference range for difference in attenuation between the liver and the spleen at nonenhanced CT. *Radiology* 2011;258:760-6.

Patrikakos P, Toutouzas KG, Gazouli M, Perrea D, Menenakos E, Papadopoulos S, Zografos G. Long-term plasma ghrelin and leptin modulation after sleeve gastrectomy in Wistar rats in comparison with gastric tissue ghrelin expression. *Obes Surg* 2011;21:1432-7.

Pei XM, Yung BY, Yip SP, Chan LW, Wong CS, Ying M, Siu PM. Protective effects of desacyl ghrelin on diabetic cardiomyopathy. *Acta Diabetol* 2015;52:293-306.

Peng KY, Watt MJ, Rensen S, Greve JW, Huynh K, Jayawardana KS, Meikle PJ, Meex RCR. Mitochondrial dysfunction-related lipid changes occur in nonalcoholic fatty liver disease progression. *J Lipid Res* 2018;59:1977-86.

Peng Y, Rideout DA, Rakita SS, Gower WR, Jr., You M, Murr MM. Does LKB1 mediate activation of hepatic AMP-protein kinase (AMPK) and sirtuin1 (SIRT1) after Roux-en-Y gastric bypass in obese rats? *J Gastrointest Surg* 2010;14:221-8.

Peng Y, Murr MM. Roux-en-Y gastric bypass improves hepatic mitochondrial function in obese rats. *Surg Obes Relat Dis* 2013;9:429-35.

Pereira K, Salsamendi J, Casillas J. The global nonalcoholic fatty liver disease epidemic: What a radiologist needs to know. *J Clin Imaging Sci* 2015;5:32.

Perfield JW, 2nd, Ortinau LC, Pickering RT, Ruebel ML, Meers GM, Rector RS. Altered hepatic lipid metabolism contributes to nonalcoholic fatty liver disease in leptin-deficient Ob/Ob mice. *J Obes* 2013;2013:296537.

Perks KL, Ferreira N, Richman TR, Ermer JA, Kuznetsova I, Shearwood AJ, Lee RG, Viola HM, Johnstone VPA, Matthews V, Hool LC, Rackham O, Filipovska A. Adult-onset obesity is triggered by impaired mitochondrial gene expression. *Sci Adv* 2017;3:e1700677.

Peterli R, Steinert RE, Woelnerhanssen B, Peters T, Christoffel-Courtin C, Gass M, Kern B, von Fluee M, Beglinger C. Metabolic and hormonal changes after laparoscopic Roux-en-Y gastric bypass and sleeve gastrectomy: a randomized, prospective trial. *Obes Surg* 2012;22:740-8.

Polyzos SA, Kountouras J, Zavos C. Nonalcoholic fatty liver disease: the pathogenetic roles of insulin resistance and adipocytokines. *Curr Mol Med* 2009;9:299-314.

Pories WJ, Swanson MS, MacDonald KG, Long SB, Morris PG, Brown BM, Barakat HA, deRamon RA, Israel G, Dolezal JM, et al. Who would have thought it? An operation

proves to be the most effective therapy for adult-onset diabetes mellitus. *Ann Surg* 1995;222:339-50; discussion 50-2.

Porteiro B, Díaz-Ruiz A, Martínez G, Senra A, Vidal A, Serrano M, Gualillo O, López M, Malagón MM, Diéguez C, Nogueiras R. Ghrelin requires p53 to stimulate lipid storage in fat and liver. *Endocrinology* 2013;154:3671-9.

Pöykkö SM, Ukkola O, Kauma H, Kellokoski E, Hörkkö S, Kesäniemi YA. The negative association between plasma ghrelin and IGF-I is modified by obesity, insulin resistance and type 2 diabetes. *Diabetologia* 2005;48:309-16.

Preitner F, Ibberson M, Franklin I, Binnert C, Pende M, Gjinovci A, Hansotia T, Drucker DJ, Wollheim C, Burcelin R, Thorens B. Gluco-incretins control insulin secretion at multiple levels as revealed in mice lacking GLP-1 and GIP receptors. *J Clin Invest* 2004;113:635-45.

Puri P, Mirshahi F, Cheung O, Natarajan R, Maher JW, Kellum JM, Sanyal AJ. Activation and dysregulation of the unfolded protein response in nonalcoholic fatty liver disease. *Gastroenterology* 2008;134:568-76.

Qayyum A, Goh JS, Kakar S, Yeh BM, Merriman RB, Coakley FV. Accuracy of liver fat quantification at MR imaging: comparison of out-of-phase gradient-echo and fat-saturated fast spin-echo techniques--initial experience. *Radiology* 2005;237:507-11.

Rector RS, Thyfault JP, Morris RT, Laye MJ, Borengasser SJ, Booth FW, Ibdah JA. Daily exercise increases hepatic fatty acid oxidation and prevents steatosis in Otsuka Long-Evans Tokushima Fatty rats. *Am J Physiol Gastrointest Liver Physiol* 2008;294:G619-26.

Reeder SB, Cruite I, Hamilton G, Sirlin CB. Quantitative assessment of liver fat with magnetic resonance imaging and spectroscopy. *J Magn Reson Imaging* 2011;34:729-49.

Ribaric G, Buchwald JN, McGlennon TW. Diabetes and weight in comparative studies of bariatric surgery vs conventional medical therapy: a systematic review and meta-analysis. *Obes Surg* 2014;24:437-55.

Riedl SJ, Shi Y. Molecular mechanisms of caspase regulation during apoptosis. *Nat Rev Mol Cell Biol* 2004;5:897-907.

Rinella ME. Nonalcoholic fatty liver disease: a systematic review. *JAMA* 2015;313:2263-73.

Ring A, Le Lay S, Pohl J, Verkade P, Stremmel W. Caveolin-1 is required for fatty acid translocase (FAT/CD36) localization and function at the plasma membrane of mouse embryonic fibroblasts. *Biochim Biophys Acta* 2006;1761:416-23.

Rodríguez A, Catalán V, Gómez-Ambrosi J, Frühbeck G. Visceral and subcutaneous adiposity: are both potential therapeutic targets for tackling the metabolic syndrome? *Curr Pharm Des* 2007;13:2169-75.

Rodríguez A, Catalán V, Becerril S, Gil MJ, Mugueta C, Gómez-Ambrosi J, Frühbeck G. Impaired adiponectin-AMPK signalling in insulin-sensitive tissues of hypertensive rats. *Life Sci* 2008;83:540-9.

Rodríguez A, Gómez-Ambrosi J, Catalán V, Gil MJ, Becerril S, Sainz N, Silva C, Salvador J, Colina I, Frühbeck G. Acylated and desacyl ghrelin stimulate lipid accumulation in human visceral adipocytes. *Int J Obes* 2009;33:541-52.

Rodríguez A, Gómez-Ambrosi J, Catalán V, Becerril S, Sainz N, Gil MJ, Silva C, Salvador J, Barba J, Colina I, Frühbeck G. Association of plasma acylated ghrelin with blood pressure and left ventricular mass in patients with metabolic syndrome. *J Hypertens* 2010;28:560-7.

Rodríguez A, Becerril S, Valentí V, Moncada R, Méndez-Giménez L, Ramérez B, Lancha A, Martín M, Burrell MA, Catalán V, Gómez-Ambrosi J, Frühbeck G. Short-term effects of sleeve gastrectomy and caloric restriction on blood pressure in diet-induced obese rats. *Obes Surg* 2012a;22:1481-90.

Rodríguez A, Becerril S, Valentí V, Ramírez B, Martin M, Méndez-Giménez L, Lancha A, del Sol Calderón P, Catalán V, Burrell MA, Gómez-Ambrosi J, Frühbeck G. Sleeve gastrectomy reduces blood pressure in obese (*fa/fa*) Zucker rats. *Obes Surg* 2012b;22:309-15.

Rodríguez A, Gómez-Ambrosi J, Catalán V, Rotellar F, ValentI V, Silva C, Mugueta C, Pulido MR, Vázquez R, Salvador J, Malagón MM, Colina I, Frühbeck G. The ghrelin *O*-acyltransferase-ghrelin system reduces TNF-alpha-induced apoptosis and autophagy in human visceral adipocytes. *Diabetologia* 2012c;55:3038-50.

Rodríguez A, Catalán V, Frühbeck G. Metabolism and satiety. In: Blundell J, Bellisle F, editors. Satiation, Satiety and the Control of Food Intake: Woodhead Publishing 2013. p. 75-111.

Rodríguez A. Novel molecular aspects of ghrelin and leptin in the control of adipobiology and the cardiovascular system. *Obes Facts* 2014;7:82-95.

Rodríguez A, Ezquerro S, Méndez-Giménez L, Becerril S, Frühbeck G. Revisiting the adipocyte: a model for integration of cytokine signaling in the regulation of energy metabolism. *Am J Physiol Endocrinol Metab* 2015;309:E691-714.

Romeo S, Kozlitina J, Xing C, Pertsemlidis A, Cox D, Pennacchio LA, Boerwinkle E, Cohen JC, Hobbs HH. Genetic variation in PNPLA3 confers susceptibility to nonalcoholic fatty liver disease. *Nat Genet* 2008;40:1461-5.

Romero A, Kirchner H, Heppner K, Pfluger PT, Tschöp MH, Nogueiras R. GOAT: the master switch for the ghrelin system? *Eur J Endocrinol* 2010;163:1-8.

Rossetti A, Togliatto G, Rolo AP, Teodoro JS, Granata R, Ghigo E, Columbano A, Palmeira CM, Brizzi MF. Unacylated ghrelin prevents mitochondrial dysfunction in a model of ischemia/reperfusion liver injury. *Cell Death Discov* 2017;3:17077.

Rubino F, Nathan DM, Eckel RH, Schauer PR, Alberti KG, Zimmet PZ, Del Prato S, Ji L, Sadikot SM, Herman WH, Amiel SA, Kaplan LM, Taroncher-Oldenburg G, Cummings DE. Metabolic surgery in the treatment algorithm for type 2 diabetes: A joint statement by international diabetes organizations. *Diabetes Care* 2016;39:861-77.

Ryan KK, Tremaroli V, Clemmensen C, Kovatcheva-Datchary P, Myronovych A, Karns R, Wilson-Pérez HE, Sandoval DA, Kohli R, Backhed F, Seeley RJ. FXR is a molecular target for the effects of vertical sleeve gastrectomy. *Nature* 2014;509:183-8.

Saadeh S, Younossi ZM, Remer EM, Gramlich T, Ong JP, Hurley M, Mullen KD, Cooper JN, Sheridan MJ. The utility of radiological imaging in nonalcoholic fatty liver disease. *Gastroenterology* 2002;123:745-50.

Sacks J, Mulya A, Fealy CE, Huang H, Mosinski JD, Pagadala MR, Shimizu H, Batayyah E, Schauer PR, Brethauer SA, Kirwan JP. Effect of Roux-en-Y gastric bypass on liver mitochondrial dynamics in a rat model of obesity. *Physiol Rep* 2018;6:

Salehi M, Prigeon RL, D'Alessio DA. Gastric bypass surgery enhances glucagon-like peptide 1-stimulated postprandial insulin secretion in humans. *Diabetes* 2011;60:2308-14.

Sangiao-Alvarellos S, Vázquez MJ, Varela L, Nogueiras R, Saha AK, Cordido F, López M, Diéguez C. Central ghrelin regulates peripheral lipid metabolism in a growth hormone-independent fashion. *Endocrinology* 2009;150:4562-74.

Sanyal AJ, Campbell-Sargent C, Mirshahi F, Rizzo WB, Contos MJ, Sterling RK, Luketic VA, Shiffman ML, Clore JN. Nonalcoholic steatohepatitis: association of insulin resistance and mitochondrial abnormalities. *Gastroenterology* 2001;120:1183-92.

Sato T, Nakamura Y, Shiimura Y, Ohgusu H, Kangawa K, Kojima M. Structure, regulation and function of ghrelin. *J Biochem* 2012;151:119-28.

Scully T. Public health: Society at large. *Nature* 2014;508:S50-1.

Schauer PR, Bhatt DL, Kirwan JP, Wolski K, Brethauer SA, Navaneethan SD, Aminian A, Pothier CE, Kim ES, Nissen SE, Kashyap SR. Bariatric surgery versus intensive medical therapy for diabetes--3-year outcomes. *N Engl J Med* 2014;370:2002-13.

Schellekens H, Dinan TG, Cryan JF. Taking two to tango: a role for ghrelin receptor heterodimerization in stress and reward. *Front Neurosci* 2013;7:148.

Schneider JL, Cuervo AM. Liver autophagy: much more than just taking out the trash. *Nat Rev Gastroenterol Hepatol* 2014;11:187-200.

Schon EA, Bonilla E, DiMauro S. Mitochondrial DNA mutations and pathogenesis. *J Bioenerg Biomembr* 1997;29:131-49.

Schroder M, Kaufman RJ. The mammalian unfolded protein response. *Annu Rev Biochem* 2005;74:739-89.

Seeras K, López PP. Roux-en-Y gastric bypass, chronic complications. StatPearls. Treasure Island 2019.

Seim I, Herington AC, Chopin LK. New insights into the molecular complexity of the ghrelin gene locus. *Cytokine Growth Factor Rev* 2009;20:297-304.

Senties-G´0mez MD, Gálvez-Gastelum FJ, Meza-García E, Armendáriz-Borunda J. Hepatic fibrosis: role of matrix metalloproteases and TGFbeta. *Gac Med Mex* 2005;141:315-22.

Seoane LM, Al-Massadi O, Pazos Y, Pagotto U, Casanueva FF. Central obestatin administration does not modify either spontaneous or ghrelin-induced food intake in rats. *J Endocrinol Invest* 2006;29:RC13-5.

Sha H, He Y, Yang L, Qi L. Stressed out about obesity: IRE1alpha-XBP1 in metabolic disorders. *Trends Endocrinol Metab* 2011;22:374-81.

Simões ICM, Fontes A, Pinton P, Zischka H, Wieckowski MR. Mitochondria in non-alcoholic fatty liver disease. *Int J Biochem Cell Biol* 2018;95:93-99.

Singh R, Kaushik S, Wang Y, Xiang Y, Novak I, Komatsu M, Tanaka K, Cuervo AM, Czaja MJ. Autophagy regulates lipid metabolism. *Nature* 2009;458:1131-5.

Singh R, Cuervo AM. Autophagy in the cellular energetic balance. *Cell Metab* 2011;13:495-504.

Singh R, Cuervo AM. Lipophagy: connecting autophagy and lipid metabolism. *Int J Cell Biol* 2012;2012:282041.

Sjöström L, Lindroos AK, Peltonen M, Torgerson J, Bouchard C, Carlsson B, Dahlgren S, Larsson B, Narbro K, Sjöström CD, Sullivan M, Wedel H. Lifestyle, diabetes, and cardiovascular risk factors 10 years after bariatric surgery. *N Engl J Med* 2004;351:2683-93.

Sjöström L, Narbro K, Sjöström CD, Karason K, Larsson B, Wedel H, Lystig T, Sullivan M, Bouchard C, Carlsson B, Bengtsson C, Dahlgren S, Gummesson A, Jacobson P, Karlsson J, Lindroos AK, Lonroth H, Naslund I, Olbers T, Stenlof K, Torgerson J, Agren G, Carlsson LM. Effects of bariatric surgery on mortality in Swedish obese subjects. *N Engl J Med* 2007;357:741-52.

Sjöström L. Bariatric surgery and reduction in morbidity and mortality: experiences from the SOS study. *Int J Obes* 2008;32 Suppl 7:S93-7.

Sjöström L. Review of the key results from the Swedish Obese Subjects (SOS) trial - a prospective controlled intervention study of bariatric surgery. *J Intern Med* 2013;273:219-34.

Skibicka KP, Hansson C, Alvarez-Crespo M, Friberg PA, Dickson SL. Ghrelin directly targets the ventral tegmental area to increase food motivation. *Neuroscience* 2011;180:129-37.

Sloth B, Holst JJ, Flint A, Gregersen NT, Astrup A. Effects of PYY1-36 and PYY3-36 on appetite, energy intake, energy expenditure, glucose and fat metabolism in obese and lean subjects. *Am J Physiol Endocrinol Metab* 2007;292:E1062-8.

Slupecka M, Wolinski J, Pierzynowski SG. The effects of enteral ghrelin administration on the remodeling of the small intestinal mucosa in neonatal piglets. *Regul Pept* 2012;174:38-45.

Small BC, Quiniou SMA, Kaiya H, Bledsoe JW, Musungu B. Characterization of a third ghrelin receptor, GHS-R3a, in channel catfish reveals novel expression patterns and a high affinity for homologous ligand. *Comp Biochem Physiol A Mol Integr Physiol* 2019;229:1-9.

Softic S, Cohen DE, Kahn CR. Role of dietary fructose and hepatic de novo lipogenesis in fatty liver disease. *Dig Dis Sci* 2016;61:1282-93.

Song YM, Lee YH, Kim JW, Ham DS, Kang ES, Cha BS, Lee HC, Lee BW. Metformin alleviates hepatosteatosis by restoring SIRT1-mediated autophagy induction via an AMP-activated protein kinase-independent pathway. *Autophagy* 2015;11:46-59.

Steinert RE, Peterli R, Keller S, Meyer-Gerspach AC, Drewe J, Peters T, Beglinger C. Bile acids and gut peptide secretion after bariatric surgery: a 1-year prospective randomized pilot trial. *Obesity* 2013;21:E660-8.

Strader AD, Vahl TP, Jandacek RJ, Woods SC, D'Alessio DA, Seeley RJ. Weight loss through ileal transposition is accompanied by increased ileal hormone secretion and synthesis in rats. *Am J Physiol Endocrinol Metab* 2005;288:E447-53.

Sun N, Wang H, Wang L. Protective effects of ghrelin against oxidative stress, inducible nitric oxide synthase and inflammation in a mouse model of myocardial ischemia/reperfusion injury via the HMGB1 and TLR4/NF-kappaB pathway. *Mol Med Rep* 2016;14:2764-70.

Sun Y, Asnicar M, Saha PK, Chan L, Smith RG. Ablation of ghrelin improves the diabetic but not obese phenotype of ob/ob mice. *Cell Metab* 2006;3:379-86.

Sweeney TE, Morton JM. The human gut microbiome: a review of the effect of obesity and surgically induced weight loss. *JAMA Surg* 2013;148:563-9.

Tack J, Deloose E. Complications of bariatric surgery: dumping syndrome, reflux and vitamin deficiencies. *Best Pract Res Clin Gastroenterol* 2014;28:741-9.

Taitano AA, Markow M, Finan JE, Wheeler DE, Gonzalvo JP, Murr MM. Bariatric surgery improves histological features of nonalcoholic fatty liver disease and liver fibrosis. *J Gastrointest Surg* 2015;19:429-36; discussion 36-7.

Tan SH, Shui G, Zhou J, Li JJ, Bay BH, Wenk MR, Shen HM. Induction of autophagy by palmitic acid via protein kinase C-mediated signaling pathway independent of mTOR (mammalian target of rapamycin). *J Biol Chem* 2012;287:14364-76.

Tapper EB, Loomba R. Noninvasive imaging biomarker assessment of liver fibrosis by elastography in NAFLD. *Nat Rev Gastroenterol Hepatol* 2018;15:274-82.

Targher G, Byrne CD. Obesity: Metabolically healthy obesity and NAFLD. *Nat Rev Gastroenterol Hepatol* 2016;13:442-4.

Teodoro JS, Rolo AP, Duarte FV, Simões AM, Palmeira CM. Differential alterations in mitochondrial function induced by a choline-deficient diet: understanding fatty liver disease progression. *Mitochondrion* 2008;8:367-76.

Theander-Carrillo C, Wiedmer P, Cettour-Rose P, Nogueiras R, Pérez-Tilve D, Pfluger P, Castañeda TR, Muzzin P, Schurmann A, Szanto I, Tschöp MH, Rohner-Jeanrenaud F. Ghrelin action in the brain controls adipocyte metabolism. *J Clin Invest* 2006;116:1983-93.

Tian X, Liu Z, Yu T, Yang H, Feng L. Ghrelin ameliorates acute lung injury induced by oleic acid via inhibition of endoplasmic reticulum stress. *Life Sci* 2018;196:1-8.

Tong Q, Ye CP, Jones JE, Elmquist JK, Lowell BB. Synaptic release of GABA by AgRP neurons is required for normal regulation of energy balance. *Nat Neurosci* 2008;11:998-1000.

Toplak H, Woodward E, Yumuk V, Oppert JM, Halford JC, Frühbeck G. 2014 EASO position statement on the use of anti-obesity drugs. *Obes Facts* 2015;8:166-74.

Tschöp M, Smiley DL, Heiman ML. Ghrelin induces adiposity in rodents. *Nature* 2000;407:908-13.

Tschöp M, Weyer C, Tataranni PA, Devanarayan V, Ravussin E, Heiman ML. Circulating ghrelin levels are decreased in human obesity. *Diabetes* 2001;50:707-9.

Tsubone T, Masaki T, Katsuragi I, Tanaka K, Kakuma T, Yoshimatsu H. Ghrelin regulates adiposity in white adipose tissue and UCP1 mRNA expression in brown adipose tissue in mice. *Regul Pept* 2005;130:97-103.

Ukkola O, Ravussin E, Jacobson P, Snyder EE, Chagnon M, Sjostrom L, Bouchard C. Mutations in the preproghrelin/ghrelin gene associated with obesity in humans. *J Clin Endocrinol Metab* 2001;86:3996-9.

Ukkola O, Kesaniemi YA. Preproghrelin Leu72Met polymorphism in patients with type 2 diabetes mellitus. *J Intern Med* 2003;254:391-4.

Unamuno X, Gómez-Ambrosi J, Rodríguez A, Becerril S, Frühbeck G, Catalán V. Adipokine dysregulation and adipose tissue inflammation in human obesity. *Eur J Clin Invest* 2018;48:e12997.

Uribe M, Zamora-Valdés D, Moreno-Portillo M, Bermejo-Martínez L, Pichardo-Bahena R, Baptista-González HA, Ponciano-Rodríguez G, Uribe MH, Medina-Santillán R, Méndez-Sánchez N. Hepatic expression of ghrelin and adiponectin and their receptors in patients with nonalcoholic fatty liver disease. *Ann Hepatol* 2008;7:67-71.

Valentí V, Martín M, Ramírez B, Gómez-Ambrosi J, Rodríguez A, Catalán V, Becerril S, Lancha A, Fernández S, Cienfuegos JA, Burrell MA, Frühbeck G. Sleeve gastrectomy induces weight loss in diet-induced obese rats even if high-fat feeding is continued. *Obes Surg* 2011;21:1438-43.

van Marken Lichtenbelt WD, Vanhommerig JW, Smulders NM, Drossaerts JM, Kemerink GJ, Bouvy ND, Schrauwen P, Teule GJ. Cold-activated brown adipose tissue in healthy men. *N Engl J Med* 2009;360:1500-8.

Van Remmen H, Hamilton ML, Richardson A. Oxidative damage to DNA and aging. *Exerc Sport Sci Rev* 2003;31:149-53.

Velásquez DA, Martínez G, Romero A, Vázquez MJ, Boit KD, Dopeso-Reyes IG, López M, Vidal A, Nogueiras R, Diéguez C. The central Sirtuin 1/p53 pathway is essential for the orexigenic action of ghrelin. *Diabetes* 2011;60:1177-85.

Virtanen KA, Lidell ME, Orava J, Heglind M, Westergren R, Niemi T, Taittonen M, Laine J, Savisto NJ, Enerback S, Nuutila P. Functional brown adipose tissue in healthy adults. *N Engl J Med* 2009;360:1518-25.

Wang D, Wei Y, Pagliassotti MJ. Saturated fatty acids promote endoplasmic reticulum stress and liver injury in rats with hepatic steatosis. *Endocrinology* 2006;147:943-51.

Wang L, Saint-Pierre DH, Tache Y. Peripheral ghrelin selectively increases Fos expression in neuropeptide Y - synthesizing neurons in mouse hypothalamic arcuate nucleus. *Neurosci Lett* 2002;325:47-51.

Wang Y, Liu J. Sleeve gastrectomy relieves steatohepatitis in high-fat-diet-induced obese rats. *Obes Surg* 2009;19:921-5.

Waseem T, Duxbury M, Ito H, Ashley SW, Robinson MK. Exogenous ghrelin modulates release of pro-inflammatory and anti-inflammatory cytokines in LPS-stimulated macrophages through distinct signaling pathways. *Surgery* 2008;143:334-42.

Wei JL, Leung JC, Loong TC, Wong GL, Yeung DK, Chan RS, Chan HL, Chim AM, Woo J, Chu WC, Wong VW. Prevalence and severity of nonalcoholic fatty liver disease in non-obese patients: a population study using proton-magnetic resonance spectroscopy. *Am J Gastroenterol* 2015;110:1306-14; quiz 15.

Wei Y, Wang D, Topczewski F, Pagliassotti MJ. Saturated fatty acids induce endoplasmic reticulum stress and apoptosis independently of ceramide in liver cells. *Am J Physiol Endocrinol Metab* 2006;291:E275-81.

Weisberg SP, McCann D, Desai M, Rosenbaum M, Leibel RL, Ferrante AW, Jr. Obesity is associated with macrophage accumulation in adipose tissue. *J Clin Invest* 2003;112:1796-808.

Wojciechowicz T, Skrzypski M, Kolodziejski PA, Szczepankiewicz D, Pruszynska-Oszmalek E, Kaczmarek P, Strowski MZ, Nowak KW. Obestatin stimulates

differentiation and regulates lipolysis and leptin secretion in rat preadipocytes. *Mol Med Rep* 2015;12:8169-75.

Wong VW, Chan RS, Wong GL, Cheung BH, Chu WC, Yeung DK, Chim AM, Lai JW, Li LS, Sea MM, Chan FK, Sung JJ, Woo J, Chan HL. Community-based lifestyle modification programme for non-alcoholic fatty liver disease: a randomized controlled trial. *J Hepatol* 2013;59:536-42.

Wree A, Eguchi A, McGeough MD, Pena CA, Johnson CD, Canbay A, Hoffman HM, Feldstein AE. NLRP3 inflammasome activation results in hepatocyte pyroptosis, liver inflammation, and fibrosis in mice. *Hepatology* 2014;59:898-910.

Wu CS, Bongmba OYN, Yue J, Lee JH, Lin L, Saito K, Pradhan G, Li DP, Pan HL, Xu A, Guo S, Xu Y, Sun Y. Suppression of GHS-R in AgRP neurons mitigates diet-induced obesity by activating thermogenesis. *Int J Mol Sci* 2017;18:

Yan H, Gao Y, Zhang Y. Inhibition of JNK suppresses autophagy and attenuates insulin resistance in a rat model of nonalcoholic fatty liver disease. *Mol Med Rep* 2017;15:180-86.

Yang H, Wang H, Wang Y, Addorisio M, Li J, Postiglione MJ, Chavan SS, Al-Abed Y, Antoine DJ, Andersson U, Tracey KJ. The haptoglobin beta subunit sequesters HMGB1 toxicity in sterile and infectious inflammation. *J Intern Med* 2017;282:76-93.

Yang J, Brown MS, Liang G, Grishin NV, Goldstein JL. Identification of the acyltransferase that octanoylates ghrelin, an appetite-stimulating peptide hormone. *Cell* 2008;132:387-96.

Yang L, Li P, Fu S, Calay ES, Hotamisligil GS. Defective hepatic autophagy in obesity promotes ER stress and causes insulin resistance. *Cell Metab* 2010;11:467-78.

Ye J, Rawson RB, Komuro R, Chen X, Dave UP, Prywes R, Brown MS, Goldstein JL. ER stress induces cleavage of membrane-bound ATF6 by the same proteases that process SREBPs. *Mol Cell* 2000;6:1355-64.

Yeh AH, Jeffery PL, Duncan RP, Herington AC, Chopin LK. Ghrelin and a novel preproghrelin isoform are highly expressed in prostate cancer and ghrelin activates mitogen-activated protein kinase in prostate cancer. *Clin Cancer Res* 2005;11:8295-303.

Yin X, Li Y, Xu G, An W, Zhang W. Ghrelin fluctuation, what determines its production? *Acta Biochim Biophys Sin* 2009;41:188-97.

Yoshida H, Matsui T, Yamamoto A, Okada T, Mori K. XBP1 mRNA is induced by ATF6 and spliced by IRE1 in response to ER stress to produce a highly active transcription factor. *Cell* 2001;107:881-91.

Younossi Z, Anstee QM, Marietti M, Hardy T, Henry L, Eslam M, George J, Bugianesi E. Global burden of NAFLD and NASH: trends, predictions, risk factors and prevention. *Nat Rev Gastroenterol Hepatol* 2018;15:11-20.

Younossi ZM, Stepanova M, Negro F, Hallaji S, Younossi Y, Lam B, Srishord M. Nonalcoholic fatty liver disease in lean individuals in the United States. *Medicine* 2012;91:319-27.

Younossi ZM, Koenig AB, Abdelatif D, Fazel Y, Henry L, Wymer M. Global epidemiology of nonalcoholic fatty liver disease-Meta-analytic assessment of prevalence, incidence, and outcomes. *Hepatology* 2016;64:73-84.

Younossi ZM. Non-alcoholic fatty liver disease - A global public health perspective. *J Hepatol* 2018a;

Younossi ZM. The epidemiology of nonalcoholic steatohepatitis. *Clin Liver Dis* 2018b;11:92-94.

Yu AP, Pei XM, Sin TK, Yip SP, Yung BY, Chan LW, Wong CS, Siu PM. Acylated and unacylated ghrelin inhibit doxorubicin-induced apoptosis in skeletal muscle. *Acta Physiol* 2014;211:201-13.

Yu EL, Golshan S, Harlow KE, Angeles JE, Durelle J, Goyal NP, Newton KP, Sawh MC, Hooker J, Sy EZ, Middleton MS, Sirlin CB, Schwimmer JB. Prevalence of nonalcoholic fatty liver disease in children with obesity. *J Pediatr* 2018;

Yuan MJ, Kong B, Wang T, Wang X, Huang H, Maghsoudi T. Ghrelin protects infarcted myocardium by induction of autophagy and AMP-activated protein kinase pathway. *Biochem Biophys Res Commun* 2016;

Zhang J, Zhao Y, Xu C, Hong Y, Lu H, Wu J, Chen Y. Association between serum free fatty acid levels and nonalcoholic fatty liver disease: a cross-sectional study. *Sci Rep* 2014;4:5832.

Zhang JV, Ren PG, Avsian-Kretchmer O, Luo CW, Rauch R, Klein C, Hsueh AJ. Obestatin, a peptide encoded by the ghrelin gene, opposes ghrelin's effects on food intake. *Science* 2005;310:996-9.

Zhang SR, Fan XM. Ghrelin-ghrelin O-acyltransferase system in the pathogenesis of nonalcoholic fatty liver disease. *World J Gastroenterol* 2015;21:3214-22.

Zhang Y, Proenca R, Maffei M, Barone M, Leopold L, Friedman JM. Positional cloning of the mouse obese gene and its human homologue. *Nature* 1994;372:425-32.

Zhang Y, Fang F, Goldstein JL, Brown MS, Zhao TJ. Reduced autophagy in livers of fasted, fat-depleted, ghrelin-deficient mice: reversal by growth hormone. *Proc Natl Acad Sci USA* 2015;112:1226-31.

Zhu J, Gupta R, Safwa M. The mechanism of metabolic surgery: gastric center hypothesis. *Obes Surg* 2016;26:1639-41.

Zhu X, Cao Y, Voogd K, Steiner DF. On the processing of proghrelin to ghrelin. *J Biol Chem* 2006;281:38867-70.

# Other related publications

# 1. Effects of diets on adipose tissue

## Article

**Ezquerro S**, Rodríguez A, Portincasa P, Frühbeck G.
Effects of diets on adipose tissue.
*Curr Med Chem* 2018; doi: 10.2174/0929867324666170518102340.

## Main objective

Overview of the body composition changes, impact on cardiometabolism and potential adverse effects of very-low calorie diets, low-carbohydrate, high-protein or low fat diets.

## Specific objectives

- To describe the main characteristics of obesity and its management.
- To review the regulation of carbohydrate, protein and lipid metabolism in the adipose tissue.
- To identify the influence of the different types of diets including very-low calorie diets, low-carbohydrate, high-protein or low fat diets on adipose tissue.
- To characterize the changes on body composition and weight maintenance achieved with the different types of diets.

Ezquerro S, Rodríguez A, Portincasa P, Frühbeck G. Effects of diets on adipose tissue. Current Medicinal Chemistry 2018;
http://doi.org/10.2174/0929867324666170518102340

## 2. Revisiting the adipocyte: a model for integration of cytokine signaling in the regulation of energy metabolism

### Article

Rodríguez A, **Ezquerro S**, Méndez-Giménez L, Becerril S, Frühbeck G.

Revisiting the adipocyte: a model for integration of cytokine signaling in the regulation of energy metabolism.

*Am J Physiol Endocrinol Metab* 2015;309(8):E691-714.

### Hypothesis

The review focuses on the morphological and functional changes in white adipose tissue during obesity, with special emphasis on its endocrine role in inflammatory processes, insulin sensitivity and the potential involvement of brown and beige adipose tissue in the onset of obesity.

### Objectives

- To characterize the ontogeny and function of white, brown and beige adipose tissue.
- To describe the adipose tissue expansion, adipocyte cell death and the crosstalk between adipose tissue and immune cells in the inflammatory process as well as the altered secretion of adipokines in obesity.
- To evaluate the impact of brown and beige fat depots as thermogenic and energy-dissipating tissues.

Rodríguez A, Ezquerro S, Méndez-Giménez L, Becerril S, Frühbeck G.
Revisiting the adipocyte: a model for integration of cytokine signaling in the regulation of energy metabolism. Am J Physiol Endocrinol Metab 2015;309(8):E691-714.

# 3. Guanylin and uroguanylin stimulate lipolysis in human visceral adipocytes

## Article

Guanylin and uroguanylin stimulate lipolysis in human visceral adipocytes.

Rodríguez A, Gómez-Ambrosi J, Catalán V, **Ezquerro S**, Méndez-Giménez L, Becerril S, Ibáñez P, Vila N, Margall MA, Moncada R, Valentí V, Silva C, Salvador J, Frühbeck G.

*Int J Obes* 2016;40(9):1405-15.

## Hypothesis

Guanylin and uroguanylin levels are altered in obesity and stimulate lipolysis in human visceral adipocytes.

## Objectives

- To explore the potential differences in circulating guanylin and uroguanylin concentrations in normal weight, obesity and obesity-associated T2D as well as in weight loss achieved by bariatric surgery or lifestyle intervention.
- To characterize the expression of guanylin and uroguanylin in human stomach and small intestine and their receptors GUCY2C and GUCY2D in human visceral adipose tissue.
- To study the effects of the guanylin system on lipolysis through protein kinase A (PKA) and/or G (PKG)-dependent mechanisms in human visceral adipocytes.

Guanylin and uroguanylin stimulate lipolysis in human visceral adipocytes.
Rodríguez A, Gómez-Ambrosi J, Catalán V, Ezquerro S, Méndez-Giménez L, Becerril S, Ibáñez P, Vila N, Margall MA, Moncada R, Valentí V, Silva C, Salvador J, Frühbeck G. Int J Obes 2016;40(9):1405-15.

## SUPPLEMENTAL MATERIAL AND METHODS

### Patients

To analyze the effect of obesity and obesity-associated T2D on plasma proguanylin and prouroguanylin concentrations, 134 Caucasian subjects (30 lean and 104 obese) were recruited from healthy volunteers and patients attending the Department of Endocrinology & Nutrition of the Clínica Universidad de Navarra (Pamplona, Spain). Body mass index (BMI) was calculated as weight in kilograms divided by the square of height in meters. Obesity was defined as a BMI≥30 kg/m$^2$, and normal weight as a BMI<25 kg/m$^2$. Obese patients were sub-classified into three groups [normoglycaemia (NG), impaired glucose tolerance (IGT) or T2D] following the criteria of the Expert Committee on the Diagnosis and Classification of Diabetes.[1] T2D subjects were not on insulin therapy or medication likely to influence endogenous insulin levels. It has to be stressed that the patients included in our obese T2D group did not have a long diabetes history (less than 2-3 years or even *de novo* diagnosis as evidenced from their anamnesis and biochemical determinations). Patients with signs of acute inflammation or taking any drug potentially influencing insulin production were excluded.

In addition, the expression of proguanylin and prouroguanylin as well as their functional receptors, GUCY2C and GUCY2D, was assessed in paired samples of gut, small intestine and omental adipose tissue obtained from patients undergoing laparoscopic Roux-en-Y gastric bypass (RYGB) (n=43). Reported investigations were carried out in accordance with the principles of the Declaration of Helsinki that was revised in 2013. The experimental design was approved, from an ethical and scientific standpoint, by the Hospital's Ethical Committee responsible for the research (Clínica Universidad de Navarra), and volunteers gave their informed consent for participating in the studies.

### Interventional studies

A group of 39 obese female patients was selected to investigate the effect of weight loss on circulating proguanylin and prouroguanylin concentrations. The weight loss was achieved either by RYGB (n=24) (evaluated 12 months after surgery) or by prescription of a conventional diet treatment (n=15) (evaluated after 6 months) providing a daily energy deficit of 500-1000 kcal/d as calculated from the determination

of the resting energy expenditure through indirect calorimetry (Vmax29, SensorMedics Corporation, Yorba Linda, CA, USA) and multiplication by the physical activity level factor to obtain the individual's total energy expenditure. This hypocaloric regime allows a safe and steady weight loss of 0.5-1.0 kg/week.

**Analytical procedures**

Blood samples were collected after an overnight fast. Glucose, uric acid, alanine aminotransferase (ALT), aspartate aminotransferase (AST), alkaline phosphatase and γ-glutamyltransferase (γ-GT) were measured by enzymatic tests (Hitachi Modular P800, Roche, Basel, Switzerland). Free fatty acids (FFA) (Wako Pure Chemical Ind., Osaka, Japan), total cholesterol, high-density lipoprotein (HDL)-cholesterol, (LDL)-cholesterol and TG concentrations (Roche) were calculated as previously described.[2,3] Low-density lipoprotein (LDL)-cholesterol was calculated by the Friedewald formula. High sensitivity C-reactive protein (CRP) concentrations were determined as previously reported.[4] Insulin was measured by means of an enzyme-amplified chemiluminiscence assay (IMMULITE 2500; Diagnostics Products Corp., Los Angeles, CA, USA); intra- and inter-assay coefficients of variation were 4.2 and 5.7%, respectively. Insulin resistance and sensitivity were calculated using the homeostasis model of assessment (HOMA) and quantitative insulin sensitivity check index (QUICKI) indices, respectively.[5,6] The adipocyte insulin resistance (Adipo-IR) index, as a surrogate of adipocyte dysfunction, was calculated as fasting NEFA (mmol/L) x fasting insulin (pmol/L).[7] Leptin was quantified by a double-antibody RIA method (Linco Research, Inc., St. Charles, MO, USA); intra- and inter-assay coefficients of variation were 6.7 and 7.8%, respectively.[8] Proguanylin (RD191046100CS, BioVendor Laboratory Medicine, Inc., Modrice, Czech Republic), prouroguanylin (SEG292Hu, USCN Life Science Inc., Wuhan, China) and total ghrelin (EZGRT-89K, Linco Research) were determined by commercially available ELISA kits following the manufacturer's guidelines, with intra- and interassay coefficients of variation being 6.8 and 8.0%, <10% and <12% and 1.9% and 6.5%, respectively.

**RNA extraction and real-time PCR**

RNA isolation was performed by homogenization with an Ultra-Turrax® T25 basic (IKA® Werke Gmbh, Staugen, Germany) using QIAzol® Reagent (Qiagen, Maryland, USA) for adipose tissue and adipocytes, and TRIzol® Reagent (Invitrogen,

Carlsbad, CA, USA) for stroma-vascular fraction cells (SVFC), stomach and small intestine. RNA purification was performed using the RNeasy Mini Lipid Kit (Qiagen) in adipose tissue and adipocytes, and the RNeasy Mini kit (Qiagen) in SVFC, stomach and small intestine. All samples were treated with DNase I (RNase Free DNase set, Qiagen). For first strand cDNA synthesis equal amounts (2 μg) of total RNA were reverse-transcribed using 400 units of M-MLV reverse-transcriptase (Invitrogen) and random primers (Roche Molecular Biochemicals, Mannheim, Germany), as described earlier.[9] Transcript levels for guanylin (*GUCA2A*), uroguanylin (*GUCA2B*), guanylate cyclase 2C (*GUCY2C*) and 2D (*GUCY2D*), aquaporin 7 (*AQP7*), aquaporin 3 (*AQP3*), fatty acid transport protein 1 (*FATP1*) and fatty acid translocase (*CD36*) were quantified by real-time PCR (7300 Real-Time PCR System, Applied Biosystems, Foster City, CA, USA). Primers and probes (**Supplemental Table 1**) were designed using the software Primer Express 2.0 (Applied Biosystems). Primers or TaqMan® probes encompassing fragments of the areas from the extremes of two exons were designed to ensure the detection of the corresponding transcript avoiding genomic DNA amplification. The cDNA was amplified at the following conditions: 95 ºC for 10 min, followed by 45 cycles of 15 s at 95 ºC and 1 min at 59 ºC, using the TaqMan® Universal PCR Master Mix (Applied Biosystems). All results were normalized for the expression of *18S* rRNA (Applied Biosystems), and relative quantification was calculated using the ΔΔCT formula.[10] All samples were run in triplicate and the average values were calculated.

**Western-blot studies**

Samples (30 μg) were run out in Any kD™ Mini-Protean® TGX™ precast polyacrylamide gels (Bio-Rad Laboratories, Inc., Hercules, CA, USA), subsequently transferred to nitrocellulose membranes and blocked in Tris-buffered saline (TBS) with 0.05% Tween 20 containing 5% non-fat dry milk for 1 h at room temperature (RT). Blots were then incubated overnight at 4 ºC with rabbit polyclonal anti-human GUCA2A, anti-human GUCA2B (PAB21024 and H00002981-D01P, Abnova, Taipei, Taiwan), anti-GUCY2C (HPA037655, Sigma) and anti-GUCY2D (SAB1412142, Sigma), anti-hormone sensitive lipase (HSL), anti-phospho-HSL (Ser563) (4107 and 4139, Cell Signaling Technology, Inc., Danvers, MA, USA) antibodies or murine monoclonal anti-β-actin (diluted 1:1,000 [GUCA2A, GUCA2B, HSL and phospho-HSL] or 1:5,000 [β-actin] in blocking solution). The antigen-antibody complexes were visualized using horseradish peroxidase (HRP)-conjugated secondary antibodies

(1:5,000) for 1 h at RT diluted in blocking solution and the enhanced chemiluminescence Pierce ECL Plus Western Blotting Substrate (Thermo Scientific, Rockford, IL, USA). The intensity of the bands was determined by densitometric analysis with the Gel Doc™ gel documentation system and Quantity One 4.5.0 software (Bio-Rad) and normalized with β-actin density values. All assays were performed in duplicate.

**Immunohistochemistry of the guanylin system**

The immunodetection of proguanylin and prouroguanylin in histological sections of stomach and small intestine as well as their receptor GUCY2C and GUCY2D in sections of omental adipose tissue was performed by the indirect immunoperoxidase method. Sections of formalin-fixed paraffin-embedded stomach and small intestine (4 μm) were dewaxed in xylene, rehydrated in decreasing concentrations of ethanol and treated with 3% $H_2O_2$ (Sigma) in absolute methanol for 10 min at RT to quench endogenous peroxidase activity. Slides were blocked during 30 min with 1% murine serum (Sigma, St. Louis, MO, USA) diluted in TBS (50 mmol/l Tris, 0.5 mol/l NaCl; pH 7.36) to prevent non-specific adsorption. Sections were incubated overnight at 4 ºC with anti-human GUCA2A, GUCA2B (Abnova) and GUCY2C (Sigma) polyclonal antibodies or anti-human GUCY2D monoclonal antibody diluted 1:200 (GUCA2A and GUCA2B) or 1:100 (GUCY2C and GUCY2D) in TBS. After washing with TBS, slides were incubated with Dako Real™ EnVision™ HRP-conjugated anti-rabbit/mouse (Dako, Glostrup, Denmark) for 1 h at RT. After washing in TBS, peroxidase reaction was visualized with a 3,3'-diaminobenzidine (DAB, Amersham Biosciences, Buckinghamshire, UK)/$H_2O_2$ solution (0.5 mg/ml DAB, 0.03% H2O2 diluted in 50 mmol/l Tris-HCl, pH 7.36), as chromogen and Harris haematoxylin solution (Sigma) as counterstaining. Sections were dehydrated, coverslipped and observed under a Zeiss Axiovert 40 CFL optic microscope (Zeiss, Göttingen, Germany). Negative control slides without primary antibody were included to assess non-specific staining.

**Cell cultures**

Human SVFC were isolated from omental adipose tissue from obese NG subjects as previously described.[9] SVFC were seeded at 2 x $10^5$ cell/$cm^2$ and grown in adipocyte medium (DMEM/F-12 [1:1] (Invitrogen), 17.5 mmol/l glucose, 16 μmol/l biotin, 18 μmol/l panthotenate, 100 μmol/l ascorbate and antibiotic-antimycotic)

supplemented with 10% newborn calf serum (NCS). After 4 days, the medium was changed to adipocyte medium supplemented with 3% NCS, 0.5 mmol/l 3-isobutyl-1-methylxanthine (IBMX), 0.1 μmol/l dexamethasone, 1 μmol/l BRL49653 and 10 μg/ml insulin. After a 3-day induction period, cells were fed every 2 days with the same medium but without IBMX and BRL49653 supplementation for the remaining 7 days of adipocyte differentiation. Differentiated human omental adipocytes were serum-starved for 24 h and then treated with increasing concentrations of guanylin and uroguanylin (1, 10 and 100 nmol/l) (9800001 and 1039146, Bachem, Bubendorf, Switzerland), isoproterenol (10 μmol/l) (I6504, Sigma) or atrial natriuretic peptide (ANP) (0.1 μmol/l) (4011941.1000, Bachem) for 24 h. One sample per experiment was used to obtain control responses in the presence of the solvent.

**Lipolysis assays**

Differentiated human omental adipocytes were washed twice with phosphate-buffered saline (PBS) without $Ca^{2+}$ and $Mg^{2+}$ ions, and incubated with DMEM containing 2% BSA supplemented with uroguanylin (1, 10 and 100 nmol/l) or guanylin (1, 10 and 100 nmol/l) for 24 h at 37 ºC. In order to gain insight into the likely mechanisms implicated in the lipolytic process, cells were stimulated for 24 h with isoproterenol (10 μmol/l) (Sigma) or ANP (0.1 μmol/l), which stimulate PKA- and PKG-dependent lipolysis, respectively.[11,12] In a second set of experiments, cell were pretreated for 30 min with 10 μg/ml PKA inhibitor fragment (6-22) amide (specific inhibitor of PKA) or with 10 μg/ml KT 5823 (specific inhibitor of PKG) (Tocris, Ellisville, MO, USA). Quantitative enzymatic determination assays were used to measure the glycerol (Free Glycerol Reagent, Sigma) and FFA (Wako Chemicals, GmbH, Neuss, Germany) release in culture media of stimulated cells, as previously described.[4]

**cAMP and cGMP assays**

The intracellular contents of cAMP and cGMP were assayed by using commercially available competitive enzyme immunoassay (EIA) kits (#581001 and #581021, Cayman Chemical, Ann Harbor, MI, USA), according to the manufacturer's protocol instructions.

**Statistical analysis**

Data are expressed as mean ± SD or SEM. Statistical differences between mean values were determined using Student's t test, $\chi^2$ test, and one-way ANOVA followed by Scheffé's or Dunnet's tests, where appropriate. A $P$ value<0.05 was considered statistically significant. In the analysis of Pearson's correlation coefficients ($r$), Bonferroni's correction was applied when multiple comparisons were performed simultaneously, establishing the significance level at $P$=0.003. The statistical analyses were carried out by the SPSS/Windows version 15.0 software (SPSS Inc., Chicago, IL, USA).

## References


1. American Diabetes Association. (2) Classification and diagnosis of diabetes. *Diabetes Care* **38 Suppl**, S8-S16 (2015).
2. Rodríguez A et al. Acylated and desacyl ghrelin stimulate lipid accumulation in human visceral adipocytes. *Int J Obes (Lond)* **33**, 541-552 (2009).
3. Rodríguez, A. et al. Association of plasma acylated ghrelin with blood pressure and left ventricular mass in patients with metabolic syndrome. *J Hypertens* **28**, 560-7 (2010).
4. Rodríguez, A. et al. Insulin- and leptin-mediated control of aquaglyceroporins in human adipocytes and hepatocytes is mediated via the PI3K/Akt/mTOR signaling cascade. *J Clin Endocrinol Metab* **96**, E586-97 (2011).
5. Matthews, D. R. et al. Homeostasis model assessment: insulin resistance and beta-cell function from fasting plasma glucose and insulin concentrations in man. *Diabetologia* **28**, 412-9 (1985).
6. Katz, A. et al. Quantitative insulin sensitivity check index: a simple, accurate method for assessing insulin sensitivity in humans. *J Clin Endocrinol Metab* **85**, 2402-10 (2000).
7. Bell, L. N. et al. Relationship between adipose tissue insulin resistance and liver histology in nonalcoholic steatohepatitis: a pioglitazone versus vitamin E versus placebo for the treatment of nondiabetic patients with nonalcoholic steatohepatitis trial follow-up study. *Hepatology* **56**, 1311-8 (2012).
8. Muruzabal, F. J., Frühbeck, G., Gómez-Ambrosi, J., Archanco, M. & Burrell, M. A. Immunocytochemical detection of leptin in non-mammalian vertebrate stomach. *Gen Comp Endocrinol* **128**, 149-52 (2002).
9. Rodríguez, A. et al. Acylated and desacyl ghrelin stimulate lipid accumulation in human visceral adipocytes. *Int J Obes* **33**, 541-52 (2009).
10. Catalán, V. et al. Validation of endogenous control genes in human adipose tissue: relevance to obesity and obesity-associated type 2 diabetes mellitus. *Horm Metab Res* **39**, 495-500 (2007).
11. Xu, X. et al. Postreceptor events involved in the up-regulation of beta-adrenergic receptor mediated lipolysis by testosterone in rat white adipocytes. *Endocrinology* **132**, 1651-7 (1993).
12. Sengenes, C. et al. Involvement of a cGMP-dependent pathway in the natriuretic peptide-mediated hormone-sensitive lipase phosphorylation in human adipocytes. *J Biol Chem* **278**, 48617-26 (2003).

## 4. Crosstalk between adipokines and myokines in fat browning

### Article

Rodríguez A, Becerril S, **Ezquerro S**, Méndez-Giménez L, Frühbeck G.
Crosstalk between adipokines and myokines in fat browning.
*Acta Physiol* 2017;219(2):362-381.

### Main objective

To review the crosstalk of adipokines and myokines in the switch of the phenotype of energy-storing white adipocytes into energy-dissipating beige adipocytes.

### Specific objectives

- To describe the different types of adipose tissue focus on the transcriptional regulation of brown and beige adipogenesis.
- To review the role of skeletal muscle as an endocrine organ and the impact of myokines on metabolic homeostasis.
- To outline the relevance of the different types of myokines as well as the crosstalk between adipokines and myokines in fat browning.

Rodríguez A, Becerril S, Ezquerro S, Méndez-Giménez L, Frühbeck G. Crosstalk between adipokines and myokines in fat browning. Acta Physiol 2017;219(2):362-381.